THE UNIVERSITY
of EDINBURGH

RSSI Based Self-adaptive Algorithms Targeting Indoor Localisation under Complex Non-Line of Sight Environments

Xiaoyue Hou

A thesis submitted for the degree of Doctor of Philosophy

The University of Edinburgh

December 2017

Declaration

I hereby declare that this thesis was composed and originated entirely by myself, that the work contained herein is my own except where explicitly stated otherwise in the text, and that this work has not been submitted for any other degree or professional qualifications.

Xiaoyue Hou

December 2017

Edinburgh, UK.

Acknowledgement

Firstly, I would like to express my sincere gratitude to my supervisor, Prof Tughrul Arslan, who gave me a lot of support of my Ph.D. study for his patience, motivation, and immense knowledge. His continuous guidance helped me in all the time of research and writing of this thesis. Meanwhile, I would like also to give my gratitude to my second supervisor, Dr Brain Flynn, who helped me a lot in different stages of my research work.

I would like to thank all members of the E-Wireless Group at the University of Edinburgh. In particular, my senior colleague Dr. Wei Zhou, who gave me lots of support during my Ph.D. study though his guidance. My sincere thanks also goes to my college Arief Affendi Juri and Yichen Du. Without they precious support it would not be possible to conduct this research.

Last but not least, I would like to express my deepest gratitude and best wishes to all members of my family. Special thanks go to my wife and my parents for their love, encourage and support.

Abstract

Location Based Services (LBS) are a relatively recent multidisciplinary field which brings together many aspects of the fields of hardware design, digital signal processing (DSP), digital image processing (DIP), algorithm design in mathematics, and systematic implementation. LBS provide indirect location information from a variety of sensors and present these in an understandable and intuitive way to users by employing theories of data science and deep learning. Indoor positioning, which is one of the sub-applications of LBS, has become increasingly important with the development of sensor techniques and smart algorithms. The aim of this thesis is to explore the utilisation of indoor positioning algorithms under complex Non-Line of sight (LOS) environments in order to meet the requirements of both commercial and civil indoor localisation services.

This thesis presents specific designs and implementations of solutions for indoor positioning systems from signal processing to positioning algorithms. Recently, with the advent of the protocol for the Bluetooth 4.0 technique, which is also called Bluetooth Low Energy (BLE), researchers have increasingly begun to focus on developing received signal strength (RSS) based indoor localisation systems, as BLE based indoor positioning systems boast the advantages of lower cost and easier deployment condition. At the meantime, information providers of indoor positioning systems are not limited by RSS based sensors. Accelerometer and magnetic field sensors may also being applied for providing positioning

information by referring to the users' motion and orientation. With regards to this, both indoor localisation accuracy and positioning system stability can be increased by using hybrid positioning information sources in which these sensors are utilised in tandem. Whereas both RSS based sensors, such as BLE sensors, and other positioning information providers are limited by the fact that positioning information cannot be observed or acquired directly, which can be summarised into the Hidden Markov Mode (HMM).

This work conducts a basic survey of indoor positioning systems, which include localisation platforms, using different hardware and different positioning algorithms based on these positioning platforms. By comparing the advantages of different hardware platforms and their corresponding algorithms, a Received Signal Strength Indicator (RSSI) based positioning technique using BLE is selected as the main carrier of the proposed positioning systems in this research. The transmission characteristics of BLE signals are then introduced, and the basic theory of indoor transmission modes is detailed. Two filters, the smooth filter and the wavelet filter are utilised to de-noise the RSSI sequence in order to increase localisation accuracy. The theory behind these two filter types is introduced, and a set of experiments are conducted to compare the performance of these filters.

The utilisation of two positioning systems is then introduced. A novel, off-set centroid core localisation algorithm is proposed firstly and the second one is a modified Monte Carlo localisation (MCL) algorithm based system. The first positioning algorithm utilises BLE as a positioning information provider and is implemented with a weighted framework for increasing localisation accuracy and system stability. The MCL algorithm is tailor-made in order to locate users' position

in an indoor environment using BLE and data received by sensors locating user position in an indoor environment.

The key features in these systems are summarised in the following: the capacity of BLE to compute user position and achieve good adaptability in different environmental conditions, and the compatibility of implementing different information sources into these systems is very high. The contributions of this thesis are as follows: Two different filters were tailor-made for de-nosing the RSSI sequence. By applying these two filters, the localisation error caused by small scale fading is reduced significantly. In addition, the implementation for the two proposed are described. By using the proposed centroid core positioning algorithm in combination with a weighted framework, localisation inaccuracy is no greater than 5 metres under most complex indoor environmental conditions. Furthermore, MCL is modified and tailored for use with BLE and other sensor readings in order to compute user positioning in complex indoor environments. By using sensor readings from BLE beacons and other sensors, the stability and accuracy of the MCL based indoor position system is increased further.

Lay Summary

Recently, positioning services have obtained great success in the area of civil and commercial use. For example, smart phone users can locate their positions on a map by using Global Positioning Systems (GPS) and cell phone signals. These techniques have dramatically improved the quality of people's lives and brought increasing convenience to the modern world. However, for indoor positioning, the situation is completely different. Because of interference caused by furniture and building materials, GPS and cell phone signals cannot be accurately received by mobile devices in indoor areas. As a result, traditional outdoor positioning techniques cannot be used for indoor positioning.

In order to solve these problems mentioned above, new systems have been designed to provide positioning services under complex indoor environmental conditions. These novel positioning systems use Bluetooth 4.0 beacons as signal transmitters and utilise the received signal strength to compute users' positions. By employing this technology, smart phone users can locate their indoor position accurately and conveniently just by using the Bluetooth function on their phones. Meanwhile, our positioning system can also use other sensors such as an accelerometer and compass to compute a user's position. By using a smart algorithm called Monte Carlo Localisation, these data can be applied together extremely efficiently and localisation accuracy can be promoted to a high degree. These indoor positioning systems can provide accurate indoor positioning

services for most smart phone users, and localisation inaccuracy is no greater than 5 metres under the most complex of indoor environments.

Contents

List of Figures

List of Tables

List of Abbreviations

Access Point (AP)

Alternating Current (AC)

Angle of Arrival (AOA)

Bluetooth Low Energy (BLE)

Digital Image Processing (DIP)

Digital Signal Processing (DSP)

Discrete Fourier Transform (DFT)

Discrete Wavelet Transform (DWT)

Effective Isotropic Radiated Power (EIRP)

Fast Fourier Transform (FFT)

Free Space Propagation Model (FSPM)

Frequency Hopping Spread Spectrum (FHSS)

Global Position System (GPS)

Identification (ID)

Indoor Location Based Services (ILBS)

Internet of Things (IoT)

K Nearest Neighbour (KNN)

Line Of Sight (LOS)

Location Based Services (LBS)

Micro Electro Mechanical System (MEMs)

Microprogrammed Control Unit (MCU)

Monte Carlo Localisation (MCL)

One Step Secant (OSS)

Radio Frequency Identification Devices (RFID)

Received Signal Strength (RSS)

Received Signal Strength Indicator (RSSI)

Short Time Fourier Transform (STFT)

Signal to Noise Ratio (SNR)

Sum Squared Error (SSE)

Time Difference of Arrival (TDOA)

Time of Arrival (TOA)

Ultra-Wide Bandwidth (UWB)

Windowed Fourier Transform (WTF)

Chapter 1 : Introduction to Indoor Positioning systems

In recent years, GPS and cellular signal-based outdoor positioning systems have attracted the attention of researchers in areas such as car navigation systems and digital maps [1] [2]. Meanwhile, with the development of positioning technologies, operators and manufacturers have begun to pay attention to the design of indoor positioning systems [3]. Indoor Location Based Services (ILBS) have also begun to play an increasingly important role in driving future applications, especially for mega-structure buildings in areas such as ‘healthcare’ and ‘smart living’. Providing accurate indoor positioning systems is of significant practical importance, as people spend a large amount of time in both private and public indoor areas. An indoor positioning and navigation system could, for example, help visitors to locate their destination within a complex and unfamiliar environment.

However, satellite and mobile phone base-station-based localisation techniques require a LOS transmission channel and stop working in a non-LOS environment such as an indoor area [4]. Because of interference caused by furniture and building materials, GPS and cell phone signals cannot be accurately received by mobile devices in indoor areas. As a result, traditional outdoor positioning techniques cannot be used for indoor positioning.

Many solutions and algorithms for indoor localisation have been investigated and proposed during the last decade [5]. Among them, one of the techniques, the RSS based indoor positioning systems have become one of the best choices for researchers and users with the ever growing deployment density of Wi-Fi. Wi-Fi based localisation systems locate the position of a mobile device with reference to Wi-Fi routers in an indoor area. However, RSS based indoor positioning systems using Wi-Fi have certain limitations. A major disadvantage is that the essential function of Wi-Fi is to provide internet access to mobile users. For indoor positioning, localisation accuracy is affected by the signal cover density. An overlapped Wi-Fi signal coverage area will increase the costs of deploying the Wi-Fi network. In addition, most of the current research on RSSI-based indoor positioning algorithms assumes a LOS environment but ideal LOS is practically non-existent in a real environment [5].

With regards to this, researchers and operators are beginning to obtain better hardware platforms for using RSSI techniques. As a result, since the invention of the BLE and smart mobile devices with Bluetooth 4 (Smart Bluetooth) access functions have grown in popularity, the latest Bluetooth based indoor positioning technologies are attracting increasing attention from researchers. BLE based localisation systems locate the position of a mobile device with reference to low-energy Bluetooth beacons in an indoor area.

Compared with Wi-Fi, BLE devices have advantages of lower power consumption, lower costs, and smaller size [6]. Newer BLE beacons do not require an alternating current (AC) power supply, and can last half a year on only a 3V button battery. A lower cost and smaller beacon without AC power supply could reduce the Bluetooth 4 signal transmitter’s deployment limitations, and signal cover density

can also be significantly increased by deploying more beacons than Wi-Fi routers in complex indoor areas. Thus, the latest Bluetooth based localisation techniques could provide a higher level of accuracy than Wi-Fi based techniques because of the deployment cover density, they also do not require significant additional expenditure.

Meanwhile, because BLE have the same centre frequency (2.45GHz), BLE based positioning system can be easily shifted to Wi-Fi based system. In addition, the location information provided by BLE do not have confliction with other location provider, such as Wi-Fi or UWB based positioning systems. Thus, BLE based positioning can be easily developed with most of recent and future positioning technique.

Figure 1. 1 Comparison of different technologies of server-based indoor positioning [7]

However, BLE based indoor positioning techniques have certain limitations. Normally, the functionality of BLE beacons is to transmit radio signals. These signals will be received by signal receivers, such as smart phones. The received signal strength is then utilised to compute the distance between uses' positions and BLE beacons. Ideally, by applying this distance information and the

coordinates of BLE beacon, users' positions are able to be computed through the use of positioning algorithms. However, furniture, building materials, and moving people will influence the accuracy of the RSSI value [8]. Meanwhile, the indoor propagation model of radio signals is also difficult to predict due to the complexity of indoor environments [8]. Under these circumstances, RSSI based indoor positioning systems, which also include BLE based systems, are seriously limited by the quality of RSSI value. In general, proposing a BLE based indoor positioning system with low computation and high accuracy is still a challenge to researchers.

1.1 Thesis Objectives

The main objective of this thesis is to propose and develop RSSI based indoor positioning systems that exploit BLE techniques and other smart sensors to provide accurate location services under complex indoor environmental conditions. Precisely, it aims to exploit BLE and other sensors to develop adaptable, highly efficient, reliable, affordable and developable indoor positioning systems. These aspects are explained in detail in the following paragraphs.

Adaptability

The proposed indoor positioning systems are supposed to be significantly adaptable. The adaptability can be divided into the following aspects:

Firstly, it should enable these positioning systems to be applied under different kinds of indoor environments with significant complexity. Specifically, these proposed systems can be employed under a variety of environmental conditions without any additional auxiliary equipment.

Secondly, the proposed system can be modified by using different sensors, which can be applied to provide more accurate location information.

Thirdly, the proposed system can be applied without internet access.

High efficiency

The proposed systems should be able to provide the users' position in real-time. Specifically, users should receive their current positions without a long time delay. This requirement limits the computation of the proposed positioning algorithms. Meanwhile, a short response time also requires a signal processing module, such as filters, which are able to de-noise the RSSI sequence efficiently in short time period.

Reliable

The proposed systems should be able to be employed with high reliability. This means if any BLE beacons are not operable, such as being out of power or broken, these positioning systems could still work without these unusable beacons. In addition, if any beacons are moved without authorisation, the effect of a BLE beacon's incorrect location information should not increase the inaccuracy of the positioning system significantly.

Affordable

The proposed indoor positioning systems should be significantly affordable. Specifically, the beacon network should be deployed in most of indoor environments without any complex requirements. Meanwhile, based on the demand mentioned above, the signal deployment density should meet the basic

requirement but do not need to spend lots of budget. In other words, the number of beacons deployed should be as less as possible.

Developable

The proposed systems should be developed with different information sources. In specific, with the development of positioning technology, the proposed system should have the ability for adding different location information provider in order to increase the positioning accuracy and system stability.

In general, the aim of developing these proposed positioning systems using different algorithms is to provide a 1-5 metre positioning accuracy under most of complex indoor environments for civil and commercial use. In specific, these proposed systems can be used in big airport, shopping mall and hospitals for providing location and map information accurately and usefully to mobile users.

1.2 Novelty and Contribution

This thesis presents the employment of smoothing filters and wavelet filters. These filters are tailor made for de-noising the RSSI sequence with a high standard of performance and efficiency when reducing noise. By applying these tailor made filters, the standard deviation of the RSSI sequence is reduced by 80% and localisation errors caused by fluctuations are also reduced effectively.

To enable the positioning system to operate in a complex environment, a novel off-set centroid core positioning algorithm is proposed. This algorithm does not have the disadvantages of most of the existing trilateration based positioning algorithms that, at some points, these algorithms cannot compute users' positions

due to inaccurate RSSI values. Meanwhile, a weighted framework is applied to dynamically choose the best signal providers. Specifically, the utilisation of three key parameters of the weighted framework could weigh all of the signal provider groups by referring to the quality of RSSI, shape, and perimeter of the triangle, and providing feedback of the optimum combination of these factors to the proposed algorithm for computing accurate users' positions.

Another positioning system is proposed in this thesis based on the Monte Carlo algorithm which is also called participle filter. Previously, the MCL algorithm was applied in the area of robotic positioning using a gyroscope and laser range finder. In this thesis, MCL is modified and tailor made in order to use BLE beacons and other sensors such as an accelerometer and compass. By using the tailored MCL and the filters mentioned above, this indoor positioning system could provide users' positions accurately under very complex indoor environmental conditions. The average localisation inaccuracy is no less than 5 metres in general.

1.3 Thesis Outline

The remainder of the thesis is organised as follows:

Chapter 2: Literature Review

Chapter 2 presents the fundamentals and characteristics of indoor positioning systems. The constituent parts of different technique-based indoor positioning systems such as RSSI, angle of arrival (AOA), and time of arrival (TOA) are indicated. Furthermore, the indoor positioning utilised by different architectures such as Bluetooth, Wi-Fi and FRID are discussed. Afterwards, different RSSI based indoor positioning algorithms such as trilateration and Monte Carlo Localisation are introduced.

Chapter 3: The Employment of Tailor-made Smooth Filters

Chapter 3 introduces essential background information on the principles of the signal transmission model. Specifically, the methodology of the free space propagation model is analysed. Furthermore, large-scale and small scale fading is presented to indicate the utilisation of smoothing filters and wavelet filters. The methodology of smoothing filters is then presented specifically, follow by its implementation. Finally, this chapter presents a set of experimental results conducted in different indoor environments in order to demonstrate the performance of wavelet filters in de-noising and stabilising the received signal strength sequence.

Chapter 4: The Employment of Tailor-made Wavelet Filters

Chapter 4 introduces essential background information on wavelet filters, which have become very popular in dealing with non-stationary processes recently. A comparison between wavelet transform and Fourier transform with its transformation is demonstrated. Afterwards, the implementation of the wavelet filters with different parameters is presented. At the end of this chapter, a set of experimental results employing wavelet filters is given and a comparison between wavelet filters and smoothing filters is indicated.

Chapter 5: Offset Centroid Core Based Positioning Algorithm Combining with a Weighted Framework

Chapter 5 presents essential background information on RSSI based trilateration based indoor positioning algorithms. The basic trilateration based indoor positioning algorithm is introduced and its disadvantages are discussed in detail. Afterwards, the proposed off-set trilateration algorithm for indoor positioning is

demonstrated. A weighted framework is also created to increase the stability and localisation accuracy of the proposed trilateration algorithm. Following this, the implementation of this system is introduced, before a set of experimental results under different environmental conditions is given.

Chapter 6: Application of Optimised Monte Carlo Localisation Using Bluetooth Low Energy, Accelerometer and Compass

Chapter 6 introduces the essential background regarding Monte-Carlo Localisation, which includes the theory of the HMM and Bayes filter. The mathematical analysis of Monte-Carlo localisation which is based on the theory mentioned above is presented. Afterwards, the implementation of Monte Carlo Localisation algorithm using Bluetooth beacons, accelerometer sensor, and compass is introduced. Finally, a set of comparisons among different indoor positioning algorithms under various kinds of complex environmental conditions is given, which includes the proposed algorithm in chapter 5, the Monte Carlo Localisation algorithm, and positioning algorithms proposed by other researchers.

Chapter 7: Conclusion

Chapter 7 presents general conclusion and discusses potential avenues for future research.

1.4 Publications

Conferences

1. Indoor Localisation for Bluetooth Low Energy Devices Using Weighted Offset Trilateration Algorithm
   X. Hou, T. Arslan, A. Juri, and F. Wang
   In ION-GNSS 2016, pp.2286-2292, 2016
2. A Received Signal Strength based Self-adaptive Algorithm Targeting Indoor Positioning
   X. Hou, T. Arslan and A. Juri
   In 2016 International Navigation Conference (INC), Glasgow, 2016
3. Monte Carlo Localisation Algorithm for Indoor Positioning using Bluetooth Low Energy Devices
   X. Hou, T. Arslan
   In 7th International Conference on Localization and GNSS (ICL-GNSS), Nottingham, 2017, accepted for publication
4. Indoor Localization for Bluetooth Low Energy Devices Using Wavelet and Smoothing Filters
   X.Hou and T. Arslan
   In 7th International Conference on Localization and GNSS (ICL-GNSS), Nottingham, 2017, accepted for publication

Chapter 2 : Literature Review

Recently, indoor positioning has gradually become the focus of 5G network protocol [9]. The key novelty of a 5G network is to combine large-cells and small-cells together to provide higher transmission speed and other smart functions [10]. As a result, implementation of a 5G technique-wide network of civil and commercial indoor positioning services will become more likely. At the same time, Ultra-wide Bandwidth (UWB), caesium atomic clocks and other techniques are also considered as an important part of indoor positioning [11][12]. A variety of corresponding indoor positioning algorithms have been gradually proposed by researchers.

At present, the positioning of the carrier is mainly the following: the use of UWB, determined by calculating the time of arrival to calculate the distance between the access point (AP) and user to calculate users' position of the TOA system and Time Difference of Arrival (TDOA) system [13], by comparing the arrival of angel's AOA algorithm and through RSSI to calculate the RSSI for indoor positioning of the RSS-based system [14]. From the specific algorithm points, the main two branches are: algorithms based on the use of large fingerprint databases [15], and algorithms to calculate distance in order to determine location by means of triangulation [16] and trilateration [17]. At the same time, the hybrid network of multiple information sources usually uses Kalman filters, Markov algorithms and Monte Carlo algorithms.

In order to provide a low-cost indoor positioning system for commercial applications with high adaptability, we introduced and compared different hardware carriers and different algorithms, and chose to use the Bluetooth 4.0 based Hybrid network. In this chapter, first of all, we compared the different hardware based on indoor positioning systems, and arrived at the decision to utilise BLE. Then, we compared the algorithms of Fingerprint, trilateration and probability based in the process of selecting the algorithm, and gave the reason why we selected trilateration and MCL.

2.1 Hardware Platform

If researchers want to propose a new indoor positioning algorithm, firstly they need to select the system used by the carrier. In this section, some of the major carrier's performance, and advantages and disadvantages, such as Wi-Fi, BLE, UWB and Radio Frequency Identification Devices (RFID) [18] will be analysed and introduced separately. In this research, the reason for using BLE as main carrier will also discussed.

2.1.1 Wi-Fi

At present, a large number of indoor positioning algorithms are based on Wi-Fi techniques [14]. This is largely due to the fact that, in the last 10 years, Wi-Fi has been widely deployed in a lots of public environments. At the same time, handheld smart devices are also very popular and widely used in conjunction with Wi-Fi functionality. Therefore, the establishment of a Wii-based RSSI indoor positioning system does not require more additional equipment, so the cost is very low.

Physically, it is possible to use Wi-Fi for indoor positioning alone. From a mathematical point of view, we only need to receive at least three Wi-Fi router

signals and one can achieve real-time positioning of the user. At present, using the 2.45GHz band Wi-Fi transmission channel [19], a total of 13 can be employed, this means that users can simultaneously receive the 13 Wi-Fi router broadcast signals to meet their positioning needs.

At this stage, most Wi-Fi-based indoor positioning systems use offline broadcast modes and online modes at the same time. Using the broadcast mode means that the system can be offline. Assuming that the user is in the ideal LOS environment, in this case, three Wi-Fi routers can theoretically provide a maximum effective area of 40 square meters for the location service.

Another benefit of using Wi-Fi in broadcast mode is to increase the number of users who can use the positioning system at the same time. At present, the main function of Wi-Fi is to provide internet access [20]. Normally, a Wi-Fi router can connect with 255 devices at the same time, but in reality, when a large number of devices at the same time connect to a Wi-Fi router in time division duplex mode, the communication speed will be significantly reduced. When the user does not need internet access, the equipment that operates in broadcast positioning mode does not consume the bandwidth of the transmission channel. As a result, the use of broadcast mode for indoor positioning can reduce the workload of Wi-Fi routers, thereby improving user experience.

Wi-Fi as a potential indoor positioning system carrier has limitations. Among them, the main drawback is that Wi-Fi router deployment density suffers from restrictions, resulting in the positioning system not being able to provide high accuracy (Less than 2 metres). The most straightforward way to improve localization accuracy is to improve the deployment density of AP. As mentioned above, the main function

of Wi-Fi at present is to provide users with internet access, therefore, increasing the deployment density of Wi-Fi routers is not a principal concern of most users [6]. In addition, increasing the deployment density of Wi-Fi routers requires more cost, and this high cost will significantly reduce the practical value of commercial and civilian indoor positioning systems.

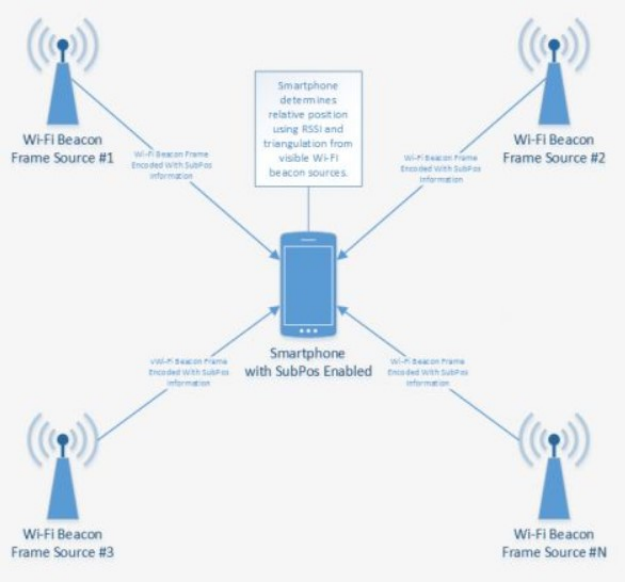

Figure 2. 1 Example of Wi-Fi based indoor positioning system [21]

2.1.2 Ultra-wide Band

UWB technology greatly differs from the traditional communications technology of wireless new technology. It does not need to use a carrier in the traditional communication system sense, but instead sends and receives nanosecond-long pulse signals to carry out data transmission, which has the order of 3.1 ~ 10.6GHz bandwidth [22]. UWB technology's transfer rate is high, reaching more than 1000Mbps, while the transmission power is very low. At the same time, WUB's signal penetration capacity is strong and does not require a carrier. The above features make it possible to provide high accuracy by using UWB in the area of indoor positioning. UWBs typically use the TODA or TOA algorithms to perform

indoor positioning by calculating the time of arrival or time differential of arrival of the signal [23]. The specific algorithm will be described later in this section. At this stage, UWB is mainly used for high-precision indoor positioning systems, according to the use of different systems or algorithms, the indoor positioning is accurate up to 0.1m ~ 0.5m dispersal [24].

At the same time, UWB's working frequency is very high, and its duty ratio is very low. This leads to UWB's signals possessing a very high resolution. Because the pulse signal resolution is very high, it is not susceptible to multi-path impact. In particular, because the pulse signal duration is very short, the multipath component of the signal is easy to filter out. In this case, the energy of the transmission signal can be used fully. According to experimental results, the attenuation of only 5dB is achieved in a multipath environment that can cause normal signals to attenuate between 10-30dB [25].

UWB has a lot of shortcomings. Firstly, UWB requires additional equipment to transmit and receive pulse signals, and the vast majority of mobile phones and other smart devices do not support UWB. Compared to Wi-Fi and BLE, the use of UWB requires additional funding. In addition, UWB usually uses TOA or TDOA algorithms, the main drawback with these is that the positioning system must be strictly synchronized at the nanosecond level, because of the electromagnetic wave transmission speed of $3.0 * 10^8$ / s. Even if only a millisecond system delay occurs, it will produce a few hundred meters of positioning error, resulting in positioning failure. In order to ensure strict synchronization of all measuring devices, high basic input also increases the difficulty of achieving a practical civilian and commercial positioning system.

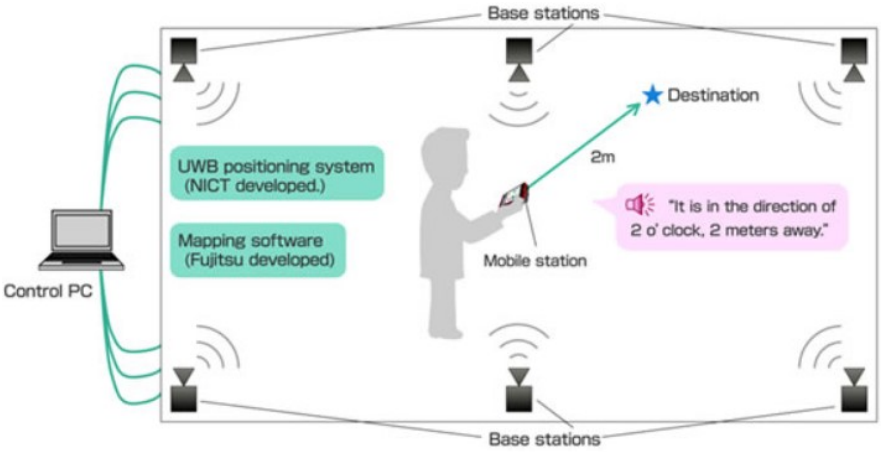

Figure 2. 2 Example of UWB based indoor positioning system [26]

2.1.3 Radio Frequency Identification Devices

RFID is a wireless communication technology that can identify a specific target by wireless signal and read the relevant data without having to establish mechanical or optical contact between the recognition system and the specified target [27]. The main carrier of the system is to record the RFID tags that have entered the corresponding data in advance [28]. These tags do not require power supply, but through an RFID reader are transmitted energy by electromagnetic field. The tag records the electronic pre-entered information, and can be identified within a few meters, and can no longer work in a Non-LOS environment.

An RFID-based indoor positioning system is very easy to implement, and the cost is low [27]. The price of RFID tags is very cheap, the production process is simple, while the RFID reader can also be easily integrated into mobile devices. However, the shortcomings of RFID are also very obvious [29]. In order to ensure the system's longevity, passive RFID would be the best choice. Passive RFID tags can only work reliably in a very small environment (below 3 metres), thus limiting its deployment condition and positioning accuracy.

2.1.4 Bluetooth Low Energy

The central operating frequencies of BLE and Wi-Fi are the same, which is 2.45GHz [30]. Bluetooth 3.0 and below only supports point-to-point transmission [31]. While the latest Bluetooth 4.0 and later versions have made significant improvements [32]. Firstly, Bluetooth 4.0 supports a single beacon for multi-device messaging. Secondly, Bluetooth 4.0 is also known as Bluetooth Low Energy and, compared to Bluetooth 3.0 transmission power, its consumption is significantly reduced [32]. Moreover, newer iterations of Bluetooth are compatible with 3.0 and earlier, so they boast a more powerful compatibility. In addition, Bluetooth 4.1 provides an interface that can intervene in the Internet and supports IPV6 [33]. The Bluetooth 5.0 standard proposed in 2016 further enhanced its capabilities in these areas, which include increased transmission distance, enhanced signal anti-jamming capability, and further optimization for internet of things (IoT) [33].

Bluetooth 4.0 First put forward the concept of BLE through the actual use of the process. A button battery can guarantee BLE beacon life for up to one year. In power saving mode, BLE power consumption is further reduced, potential battery life can reach up to three years [32]. Furthermore, the BLE beacon is small and the cost of production of a single device is relatively cheap. Compared with Wi-Fi, the same cost can provide higher signal and AP deployment density and reduce the AP deployment conditions in complex environments.

Compared to Wi-Fi, BLE uses Frequency Hopping Spread Spectrum (FHSS) to reduce interference [31]. FHSS is a spread spectrum method. FHSS works by making dynamic changes to the frequency of the carrier around the centre

frequency [34]. BLE can dynamically detect the current use of the communication channel, and at any time can adjust the carrier frequency to reduce interference.

With the introduction of BLE beacons and iBeacons, low-power Bluetooth beacons have made it possible to build low-cost BLE networks. Because Bluetooth 4.0 supports multipoint transmission, Bluetooth networks based on star and mesh frameworks can be easily built [33]. Compared with traditional Bluetooth, BLE power consumption is reduced by 50-99% (depending on the situation) [32]. Using the button battery, BLE beacons in low power broadcast mode can last up to 3 years. In addition, the Bluetooth delay rate has dropped from 100 seconds for Bluetooth 3.0 to a delay of 1ms for Bluetooth 4.0. In general, with its small size, low power consumption, low latency, anti-interference ability, etc. BLE beacons have generally become the preferred candidates for many researchers in the area of indoor positioning.

Figure 2. 3 Examples of different types of BLE beacons [35]

2.2 Algorithm

At present, a large number of algorithms for use in indoor positioning have been proposed. Some of these algorithms can only be implemented on a specific hardware platform, such as TOA and TDOA, which can only be used in UWB and similar systems. AOA require special antenna to get Angel information [36]. Some other algorithms have strong adaptability and can be used in many different hardware platforms, such as fingerprint identification and trilateration. The Bayesian filter based on the classification class algorithms, such as the Kalman filter, Markov algorithm, and Monte Carlo algorithm is mostly used for multiple information source based hybrid algorithms. In this section, some of the mainstream indoor positioning algorithms are introduced, and reasons why trilateration and MCL have been used in this research are discussed.

2.2.1 Time of Arrival and Time Difference of Arrival

The TOA technique uses the time of arrival of a signal for measuring the distance between the signal transmitter and signal receiver [37]. The algorithm needs to attach a specific timestamp to the data that is sent. As we know, the propagation speed of electromagnetic waves is roughly equal to the speed of light, close to 3.0 * 10^8 / s. Due to electromagnetic wave propagation speed being known, distance can be calculated by measuring time of arrival [38]. The biggest drawback of the algorithm is that it is very sensitive to the time of the response. Signal receiver and transmitter clocks must operate in very strict synchronization. 1ns error between the two clocks will result in a 300 metre error, which is an unacceptably inaccurate result. In order to achieve errors below 1m, the synchronization time difference

between the primary base stations must be less than 0.3ps. Therefore, this issue limits the TOA algorithm and its supporting facilities are chiefly used for civil and commercial positioning systems.

The TDOA algorithm is similar to the TOA algorithm and calculates the distance between signal transmitter and signal receiver by calculating the difference between time of transmission and time of arrival [37]. Specifically, the TDOA algorithm is an improvement to the TOA algorithm. Instead of using the time of arrival directly, it uses the time difference of the received signal from multiple base stations to determine the user's position. Compared with the TOA algorithm, TDOA does not need to add a special timestamp. Positioning accuracy when compared to TOA is higher. The specific algorithm is shown in Figure 2.4:

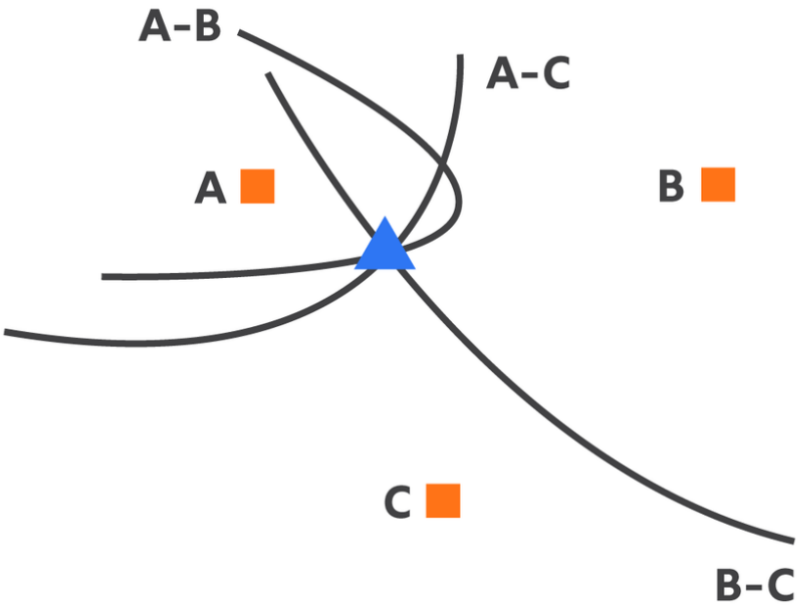

Figure 2. 4 Example of TDOA algorithm [39]

In Figure 2.4, the locations of base stations A, B and C are known. The TDOA of base station A and base station B indicate the time difference between the transmission of the signal from the transmitter to base station A and base station

B. By obtaining the difference of time between A and B, A and C, and B and C, the position of the signal transmitter can be determined. As shown in Figure 2.4, the intersection of two hyperbolic lines is the location of the signal transmitter. As with TOA, TDOA still requires a strict synchronization of the base station time, but when the information channel between the base stations has similar transmission characteristics, the potential for error caused by utilizing multiple stations is significantly reduced.

TOA and TDOA algorithms have certain limitations. First, the algorithm requires all base stations to be strictly synchronized. As mentioned above, minimal latency can lead to significant errors, while ps-level synchronization requires a lot of cost input. In addition, UWB-based TOA and TDOA algorithms use pulse signals for location, and at this stage most mobile phones and other ‘smart’ devices cannot accept and receive pulse signals, which also limits the TOA and TDOA algorithm-based UWB systems in achieving cost effective location services.

2.2.2 Angel of Arrival

The AOA algorithm operates by obtaining information regarding the angle of arrival and the coordinates of the AP [40]. Through a special antenna (usually an antenna array), the difference in angle between a user and the AP can be measured. The position of the user can be calculated by knowing information of three angles, and the coordinates of the three APs. With this, a triangulation algorithm can be used to perform AOA positioning. The specific formula is derived as follows:

The biggest drawback of the AOA algorithm is the need for special antennas to obtain angle information. In order to obtain this angle information, four directive

antennas are used to receive the signal within a range of 90° and use a phase shifter to obtain the time difference once the angle of arrival is obtained. Currently, most mobile phones use omnidirectional antennae, meaning they cannot obtain accurate angle information. Because of this, the AOA algorithm is still unable to be widely used in civil and commercial indoor positioning systems.

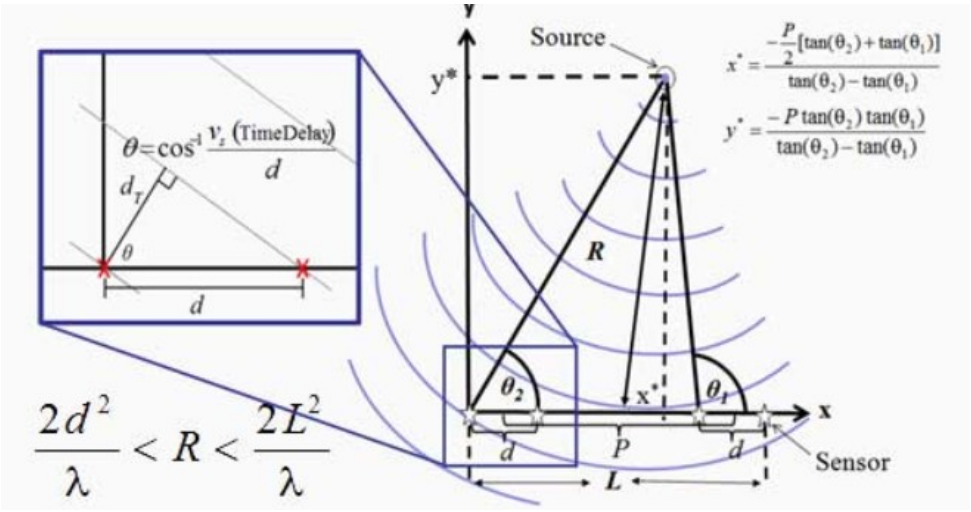

Figure 2. 5 Example of AOA algorithm [41]

2.2.3 Fingerprinting

The Fingerprint algorithm can be widely used in a variety of hardware carriers built for indoor positioning systems. Specifically, the fingerprint algorithm does not need to calculate a user's position [42]. Its core principle involves changing the location information into other information features that are easily accessible directly. The information feature should be geographically related and unique. Ideally, in a limited environment, each coordinate position has an additional information feature, which must be available and unique. In the TDOA-based UWB system, this information feature is the difference in arrival time to each corresponding coordinate. With an indoor positioning system based on the AOA algorithm, this information feature is the angle information between all the APs

corresponding to each coordinate. These system-specific information features are recorded as 'fingerprint' information. The higher the resolution of a fingerprint, the higher the positioning accuracy [43]. An Operator records all the information characteristics of the grid in the environment and enters them into a database. Other users enter a restricted environment, by comparing the received information characteristics and data in the database, a location can be obtained.

Implementing a Fingerprint algorithm requires two stages: a ‘training’ stage and a ‘location’ stage. The specific introduction of them are presented below:

Training stage

A handheld information collection device collects signal strength information from different sources at multiple locations within the target environment. Specifically, in this environment, some locations are marked out, and their coordinates have been obtained by manual measurement. These known positions are set as reference points. At each reference point, the information collection device collects the feature Information from multiple sources, and becomes the fingerprint information for the reference point, the information is then uploaded to a database [44].

Location stage

Initially, a user's particular positioning information is unknown. When the user’s handheld information acquisition device is introduced into the target environment, the information collection device automatically obtains the current location of the feature information, and compares this with the information stored in its database. By matching the algorithm, the user’s uploaded information and the information stored in the database will be compared, and the user's estimated location will be

determined. In the process of comparing the data collected by the user with the data from the training stage, the main methods are as follows: certain classification, probabilistic classification and neural network.

The typical algorithm employed for the method of certain classification is the K Nearest Neighbour (KNN) algorithm [45], which was first proposed by the Microsoft Asia Institute in 2000. This is the first fingerprint-based indoor location algorithm. In the training phase, the system uses Wi-Fi as the characteristic information source, with the average value of the signal strength of multiple Wi-Fi base stations on each reference point acting as a fingerprint, the database formed by the fingerprint is the model of the classifier. In the Location stage, the algorithm estimates the similarity of distance information, and uses the average of the positions corresponding to the k fingerprints with the highest similarity as the estimated position. According to their paper, the average error of the system is 2.94m. However, when the user blocks the signal propagation path, the error potential can increase to 4.9m.

The representative algorithm for probabilistic classification is Naive Bayesian Classifiers (NBC). In the proposed paper [46], Youssef et al., of the University of Maryland proposed the Horus indoor positioning system, the core of the system involves predicting the probability of fingerprint matching. During the training phase, they first sampled the signal strength of each reference point and then use a histogram to record the signal strength probability distribution for each reference point coordinate. In other words, the probability distribution of the signal strength of the known coordinates. During the location phase, according to the Bayesian theorem, the algorithm calculated the probability that the fingerprint information of the user's uploaded signal strength is at each reference point and takes the

coordinates of the probable reference point as the estimated coordinates of the device. The experimental results show that the average positioning error of this algorithm is 1.52 m.

In the neural network based fingerprint localization algorithm [5], Multi-layer perceptual information architecture is used to represent the relationship between signal strength and coordinates [47]. In the training stage, the system sampled fingerprint information as training sample were uploaded to the neural network through one step secant (OSS) [48] to learn the hidden unit coefficient. During the Location stage, the user collected information which was then uploaded to the training system. After this process is complete, the estimated location's current coordinates can be obtained. Test results show that in the training phase, if 5 sample reference points can be obtained, the positioning system can control potential error to less than 3 metres. If the quantity of samples is further increased, the average potential error can reduce to 1.5m or less [48].

Crowd sourcing algorithms are also widely used to enhance the positioning accuracy of the fingerprint algorithm [49]. Unlike traditional methods, crowd sourcing can dynamically change the feature information in a pre-configured database using machine learning by employing all user-uploaded targeting data. The biggest advantage of employing crowd sourcing to optimize the fingerprint algorithm is that the algorithm can increase the degree to which the fingerprint algorithm adapts to environmental changes. The biggest drawback of the traditional fingerprint algorithm is that the database obtained during the training phase is static, and the indoor environment, including the location of the furniture and the number and locations the staff in the environment, are dynamic. Any changes to a large indoor environment will result in invalid database obtained

during the training phase. A crowd sourcing algorithm can dynamically correct the information in the database through user-uploaded location data, thereby increasing the adaptability of the fingerprint to the changing environment [50]. The biggest drawback of crowd sourcing is that the algorithm needs to force all users into an online state; at the same time, this kind of algorithm is very large, and needs to take up more hardware resources.

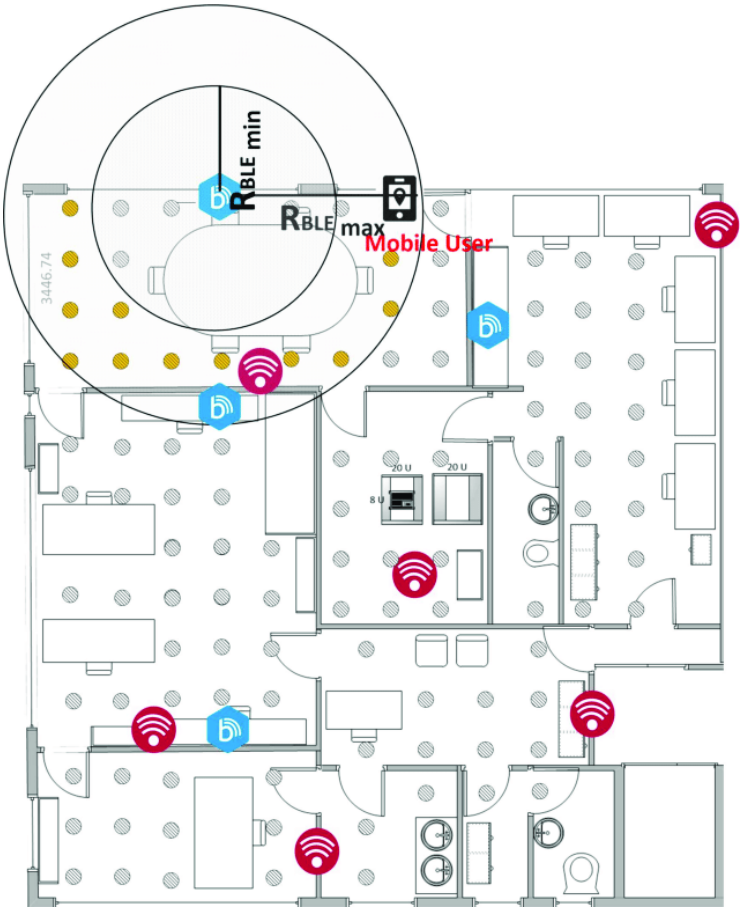

Figure 2. 6 Example of mapping reference points of fingerprinting algorithm [51]

2.2.4 Trilateration

Trilateration is a very common and popular positioning algorithm which can be applied in a variety of platforms such as Wi-Fi and BLE. The main theory of it is to

compute user positions by measurement of distances, using the geometry of circles, spheres or triangles. Based on this, lots of positioning algorithms and systems are proposed by researchers, such as [52], [53] and [54]. In fact, trilateration has become a fundamental theory of many algorithms in the area of indoor localisation. In this paper, trilateration also acts as a rationale theory of the proposed centroid core positioning algorithm which is presented in chapter 5. As the specific introduction of trilateration algorithm is presented in chapter 5, there will be no more discussion of it in this chapter.

2.2.5 Probability Based Positioning Algorithms (Kalman filter, Markov, Monte Carlo)

Recently, Kalman filter [55], Markov and Monte Carlo based positioning systems [56] increasingly attracted the attention of researchers with the development of probabilistic based positioning algorithms. The main theory of them is to compute user's positioning by referring observation and estimation information from multiple sources such are BLE beacon combining multiple information sources together in high efficiency. As the specific introduction of MCL algorithm is presented in chapter 6, there will be no more discussion of it in this chapter.

2.2.6 The strategy of Using BLE, Trilateration and MCL

As mentioned above, the main disadvantage of Wi-Fi is that the deployment of high-density Wi-Fi router nodes will significantly increase cost requirements. Thus, Wi-Fi will not be used as the primary carrier of the positioning system in this thesis. UWB requires additional signal receiving equipment, and currently most mobile phones do not support UWB signal reception, so UWB is not currently considered for use among the proposed systems. Likewise, RFID is not suitable as a primary

carrier for the positioning system due to its short distance. In this case, it was finally decided to use the BLE technique as the primary location information source for positioning. Because of its lower power consumption, lower costs, higher adaptability for different kinds of complex environments and does not require additional hardware facility for mobile users.

BLE based positioning systems use the value of RSSI to calculate distance information, so trilateration, fingerprint, and probabilistic based positioning systems can be selected for use. The biggest drawback with regards to the fingerprint algorithm is that the database cannot be updated in an indoor environment in order to make timely updates, so the algorithm is not considered as the main algorithm among the proposed systems. Because these algorithms do not need to pre-set a database to record location information, they have very good adaptability to environmental changes. Taking into account the advantages and disadvantages of each algorithm, ultimately trilateration and MCL algorithms respectively were selected to design two positioning systems. They are introduced in detail in chapters 5 and 6.

2.3 Conclusion

This chapter gives a survey of indoor positioning systems. The platforms of different indoor positioning systems are introduced. Among them, BLE techniques are selected as the main carrier of the proposed positioning systems by comparing the advantages and disadvantages of these hardware platforms. A variety of positioning algorithms are introduced in detail, including TDOA, AOA, and fingerprint algorithms. Due to the fact that, in this thesis, BLE is selected as the main carrier of the proposed positioning systems, only fingerprint, trilateration, and

MCL can be applied. By considering the disadvantages of fingerprint based algorithms, trilateration and MCL were selected as the main algorithms of the proposed system.

Chapter 3 : The Employment of Tailor-made Smooth Filters

3.1 Introduction

In this chapter, firstly, the introduction of propagation model under indoor environments is introduced as the basic theory of designing the filters in terms of de-noising the received signal strength sequences. Afterwards, the theory of smooth filter is introduced, followed by the implementation with different parameters, which are the window size and multi-stages. Finally, a sets of experimental results are demonstrated under different indoor environments in order to reveal the justification of applying the chosen parameters of smooth filters.

In the area of telecommunications, especially in radio frequency, signal strength refers to the transmitter power output as received by a reference antenna at a distance from the transmitting antenna [57].

High-powered transmissions which are used in broadcasting, are expressed in dB-millivolts per metre (dBmV/m). For very low-power systems, such as mobile phones, signal strength is usually expressed in dB-microvolts per metre (dBμV/m) or in decibels above a reference level of one milliWatt (mW). In this research, dBm, which is an abbreviation for the power ratio in decibels (dB) of the measured power referenced to one mW, is applied to express the received signal strength because the signal strength level in this system is normally less than 1 mW.

The relationship between dBm and mW is shown below:

$$RSSI_{(dBm)} = 10 \cdot log_{10}(\frac{P_{(mW)}}{1_{mW}}) \quad (3.1)$$

Where:

$RSSI_{(dBm)}$ is the received signal strength indicator value in the unit of *dBm*.

$P_{(mW)}$ is the received signal strength in the unit of *mW*.

For example, a power level of 0 *dBm* corresponds to a power of 1*mW* and -10*dBm* corresponds to 0.1 *mW* (100*μW*).

As introduced in chapter 2, in this research RSSI signals are applied to provide the distance information between users and BLE beacons. The Bluetooth version applied in this research is Bluetooth *4.0*.

Bluetooth applies wireless channels to transmit information. Thus, it is significant to have a full understanding of the limitations and performance of the wireless channel. The transmission media between signal receiver and transmitter can be simple, for example LOS, or complicated, such as walls and furniture. In this case, it is difficult to predict the propagation characteristics of wireless channels under real environments. Normally, statistical methods are widely applied in modelling a certain wireless channel with specific transmission frequency.

The transmission channel of Bluetooth in this research can be defined as an indoor transmission channel. The indoor transmission channel is different from the outdoor channel in that the signal coverage area for each transmitter is smaller, meanwhile the transmission environment changes acutely [58]. The major effects

for indoor signal transmission are the layout and the material of the building. In such cases, the path loss model is explained in the following section.

3.2 Free Space Propagation Model and Path Loss Model

The free space propagation model (FSPM) is applied to predict the signal strength between signal receiver and transmitter under LOS environment [59]. The signal attenuation of FSPM is a function of the distance between signal receiver and transmitter: the transmission power is reduced with an increase in distance, which is similar to most of the large-scale radio wave propagation models. The relationship between the distance and received power can be presented with Friis transmission equation [60]:

$$P_r(d) = \frac{P_t G_t G_r \lambda^2}{(4\pi)^2 d^2 L} \tag{3.2}$$

Where:

P_t is the transmission power,

$P_r(d)$ is the function of the distance between signal transmitter and receiver,

G_t is the gain of the antenna in the transmitter end,

G_r is the gain of the antenna in the receiver end,

d is the distance between signal transmitter and receiver,

L is the loss factor which is not related to the propagation process (L >1),

λ is the wave length.

The gain of the antenna G is related with the effective apertureA_e, which is shown below:

$$G = \frac{4\pi A_e}{\lambda^3} \tag{3.3}$$

The effective area of the antenna is justified by the physical dimensions of the antenna and the wave length is related to the frequency of the carrier:

$$\lambda = \frac{c}{f} = \frac{2\pi c}{\omega_c} \tag{3.4}$$

Where:

f is the frequency of the carrier,

ω_c is the angular frequency of the carrier,

c is the velocity of light.

Notice that P_t and P_r must be applied with same unit. G_t and G_r do not have dimension. The power loss caused by system, which is L in Equation 3.2, is consistent with the attenuation of transmission line, filter loss, antenna loss and so on. L =1 means the loss is equal to zero.

According to the Friis transmission equation, the signal power in the receiving end is inversely proportional to the square power of the distance. Assume that the antenna applied is an ideal antenna which is isotropous, the effective isotropic radiated power (EIRP) [61] can be expressed as:

$$EIRP = P_t G_t \tag{3.5}$$

For half wave dipole antenna, the effective radiated power can be utilized instead of the EIRP for expressing the maximum signal transmitting power. Under a real

environment, the gain of the antenna (dB) is normally expressed by dBi for omnidirectional antennae and dBd for half wave dipole antennae.

Path loss is defined by the expression of the difference between effective transmission power and receiving power. For FSPM, by considering the antenna gain, path loss can be shown in Equation 3.6:

$$PL = 10lg\frac{P_t}{P_R} = -10\lg[\frac{\lambda^2 G_t G_r}{(4\pi)^2 d^2}] \ (dB) \tag{3.6}$$

If $G_t G_r$ is equal to 1, this means the gain is ignored, the path loss can be derived to:

$$PL = 10lg\frac{P_t}{P_R} = -10\lg[\frac{\lambda^2}{(4\pi)^2 d^2}] \ (dB) \tag{3.7}$$

The Friis transmission equation is only applied in the case that a signal is transmitted outside the near-zone field of the antenna [60]. The far-field region, which is also called the Fraunhofer region, is the area outside the d_f. d_f is related to the antenna cross sectional area and the wave length of the carrier signal:

$$d_f = \frac{2D^2}{\lambda} \tag{3.8}$$

Where:

D is the maximum size of the antenna cross sectional area.

The value of d_f should also be much larger than D and λ.

In such cases, D should not equal to zero. Normally, d_0 which is the reference distance is applied for referring to the received power. When the distance d is larger than d_0, the received signal power at distance d is related to the reference

power at distance d_0. $P(d_0)$ can be obtained by experimentation. Notice that d_0 should much larger than d_f.

As a result, the received signal strength can be presented according to the signal strength at the reference distance and the actual distance d:

$$P_r(d) = P_t(d_0)\left(\frac{d_0}{d}\right)^2 \quad (d \geq d_0 \geq d_f) \tag{3.9}$$

For indoor areas, the reference distance d_0 is normally equal to 1 while for outdoor areas, the reference distance can be 100 or 1000, which are powers of 10.

3.2.1 Reflection, Diffraction and Scattering

Reflection, diffraction and scattering are the key mechanisms of transmission when transmitting signals [62]. In large-scale transmission models, these factors can be utilized to measure the received signal strength. For small-scaling, fading, and multi-path models, an explanation of their transmission mechanisms could also be given by these factors.

Reflection

When a signal is transmitted to a junction between two different propagation mediums, a part of the electromagnetic wave will go through the transmission medium while a part of the signal will be reflected [63]. If the second propagation medium is perfect dielectric, the reflection and refraction is equal to zero. If the signal goes into an ideal reflector, all of the energy will be reflected without power loss. The electric field intensity of the reflected signal and refracted signal is justified by the Fresnel reflection coefficient inverse L. The reflection coefficient is a function of material property, which is also effected by signal frequency, incident angle and direction of polarization.

Diffraction

The phenomenon of diffraction can explain the situation where signals can transmit beyond obstacles, even if the field intensity decreases dramatically when the receiver moves into the shadow field of obstacles. The principle of diffraction can be explained by Huygens' law [64]. According Huygens' law, all of the obstacle points act as the generator of the secondary wave. These secondary waves combining together result in a new direction of the signal transmission.

Scattering

Normally, the received signal strength is stronger than the expected result. This is because the scattering factor increases the signal strength. When signals transmit through rough surfaces, the energy of reflection will be dispersed to different directions due to the impact of scattering [65]. These obstacles could increase the received energy at the receiving end, which is larger than the expected result.

3.2.2 Introduction of Indoor Transmission Model

BLE is a near field communication transmission system, which means the major range of application is indoor areas. Indoor wireless channels are different from traditional outdoor wireless channels: the coverage range is lower and the environmental change is higher. Specifically, the major interference in indoor areas is caused by architectural composition, building materials, and the location of furniture. In this chapter, the path loss model for indoor transmission will be introduced.

The principle of the indoor path loss model is extended from FSPM. However, more influential factors need to be considered specific to indoor environments. For instance, the state of the door, which means the door is switched on or off, will dramatically affect the power level of the received signal. Antennae at the transmitting end deployed either on the celling or floor of the building will also result in a different RSSI value. In the next section, the indoor path loss model is introduced.

3.2.3 Indoor Path Loss Model

According to the FSPM, the Equation 3.9 gives a relationship between received signal power and the transmitting signal power [66]. As introduced, FSPM

assumes an ideal LOS environment without any additional antenna gain. Under a real environment, noise and interference such as multi-path will affect the accuracy of this equation, however, the relationship between receiver and transmitter signal strength is still extant:

$$\overline{PL}(d) \propto \left(\frac{d}{d_0}\right)^n \tag{3.10}$$

This equation demonstrates that the average signal power loss caused by the propagation path is inversely proportional to the nth-power of the distance. This equation can be transferred to dB, which is:

$$\overline{PL}(dB) = \overline{PL}(d_0) + 10n \times lg\left(\frac{d}{d_0}\right) + X\sigma \quad (dB) \tag{3.11}$$

Where:

$\overline{PL}$ is the RSSI of the unknown position at the distance r between the receiver and transmitter.

$\overline{PL}(d_0)$ is the received signal power of the position at the distance d_0 between the receiver and transmitter. Normally, d_0 is one metre.

$X\sigma$ is a Gaussian random variable caused by shadow fading.

n is the path loss coefficient with a range between 2-6.

Normally n is no less than two as the discussion above. However, sometimes it is possible that the value of n is less than 2 [5].

Assuming that the signal passes through a long corridor, in this case the corridor can be considered as a wave guide tube; the signal will travel in a particular

direction. As a result, the signal energy will be collected more effectively and the value of n will be less than 3.

One thing to note is that the path loss of the signal is a random variable under certain distance. This is because the interference caused by obstacles is unpredictable and changes with changes in the environment. Normally this phenomenon is described in statistics. Normally, this power loss is expressed in Gaussian distribution, which is the $X\sigma$ in Equation 3.11.

Table 3. 1 Path loss coefficient under different environmental conditions [67]

Environment	n coefficient
LOS outdoor	2
Populated regions	2.7 to 3.5
populated regions with large size obstacles	3 to 5
Indoor LOS environment	1.6 to 1.8
Indoor Non-LOS environment	4 to 6

3.2.4 Separation Loss Model

Buildings have multiple building separations and obstacles. For civil architecture, the material of separation between each room can be lime or wood, and the material of floor separation is normally wood and concrete. Buildings for commercial use normally have larger empty areas, these areas are separated by removable walls which are normally made of plastic. The electrical characteristics for different separation materials have a large variation. The path loss model could not apply to these conditions without optimisation. Researchers have done a lot of experiments to build the electrical characteristics database for different materials, which is shown below:

Table 3. 2 Power loss caused by building materials [68]

Material	Power loss/dB	Frequency/MHz
5m file cabinet	6	1300
5m metal cabinet	20	1300
Machine	8 to 10	1300
plate metals (12 sq inch)	4 to 7	1300
0.6m concrete column	12 to 14	1300
stainless steel tube	15	1300
concrete wall	8 to 15	1300
cement floor	10	1300
metal	26	815
one layer floor	20 to 30	1300
corner of the corridor	10 to 15	1300
Dry plywood (0.75 inch)	1	9600
Dry plywood (0.75 inch)	4	28800
Dry plywood (0.75 inch)	8	57600
Dry plywood (1.5 inch)	4	9600
Dry plywood (1.5 inch)	6	28800

3.2.5 Small-Scale Fading and Multi-path

Small-scale fading is normally called fading, which is utilized to describe the phenomenon that wireless signals fluctuate dramatically when transmitted over short periods or short distances [69]. Because this fluctuation is very dramatic, the large-scale fading becomes inconspicuous. For small-scale fading, the change in signal power can be 10dB within several milliseconds. In short, large-scaling fading is utilized to describe the average signal change over long periods, while small-scaling fading is applied to explain the transient variation of the signal power due to the effect of the channel variance.

The major impact of small-scale fading is caused by multi-path and Doppler principles. The Multi-path principle [70] will result in time, amplitude, and phase delay of the signal at the receiving end, which will generate a time dispersion effect and frequency selective attenuation of the received signal. The Doppler principle will result in a frequency dispersion effect and time-selective fading of the received signal. For BLE signals in an indoor environment, the major effect of the fluctuated interference is caused by multi-path. Because the movement speed for most humans in an indoor area is around one meter per second, the effect of the Doppler principle does not play a major role in this assumption. In this case, the multi-path principle is introduced in this chapter only.

In real indoor environments, lots of static obstacles, such as walls and tables, and dynamic obstacles, for example moving people, are deployed randomly. The effect of these interferences are difficult to predict; each obstacle will generate reflection, diffraction, and scattering effects and these obstacles do not have ideal electrical characteristics. In addition, the relative position between the receiver

and each obstacle changes constantly. In this situation, each signal component caused by reflection, diffraction, and scattering is impossible to predict and quantify. These obstacles build an environment that reduces the signal energy continuously, along with signal changes in phase and amplitude. A sets of example is shown below:

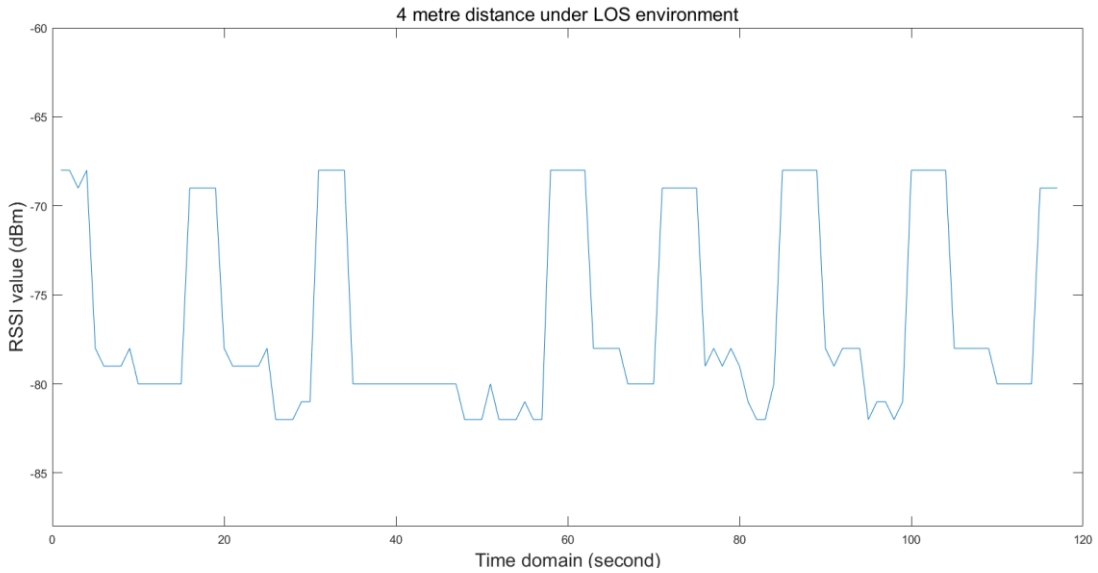

Figure 3. 1 RSSI sequence at four metre distance under LOS environment

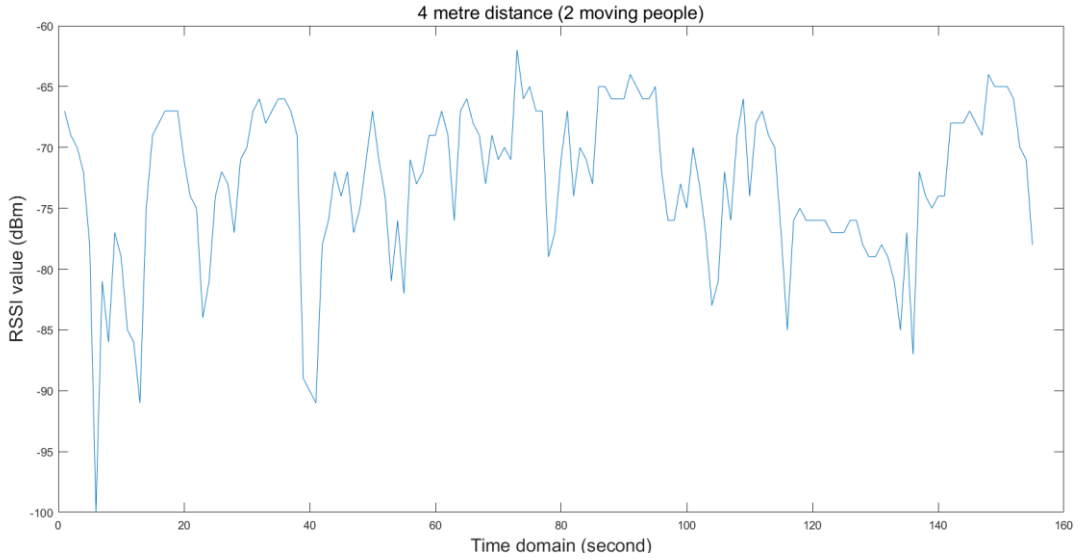

Figure 3. 2 RSSI sequence at four metre distance (two moving people between transmitter and receiver)

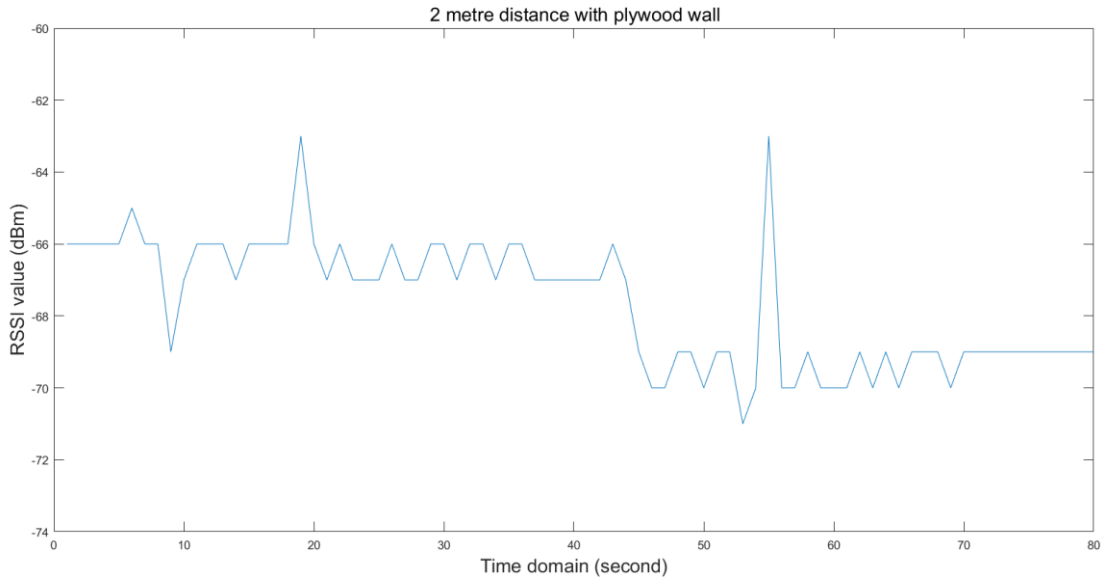

Figure 3. 3 RSSI sequence at two metre distance (0.4 metre plywood as obstacles between transmitter and receiver)

In Figure 3.1, the distance between the BLE signal receiver and transmitter is 4 metres, and the signal transmission environment can be defined as a real LOS environment. In this case, the ideal average RSSI signal value should be -68.63 dBm (n=1.6) to -69.83 dBm (n=1.8) and the feature of the signal curve should be stable without fluctuation. However, as can be seen, the RSSI value fluctuates dramatically between -68 dBm to -81 dBm. In Figure 3.2, the distance between receiver and transmitter is 4 metres, while two people walk randomly between the receiver and transmitter. The signal strength changes fluctuate and the signal curve can be defined as a non-stationary process. In Figure 3.3, a wall was deployed between the receiver and transmitter, and the distance between each other is 2 metres (the thickness of the wall is 0.4 metres). The fluctuation of the signal is weaker compared with the curve in Figure 3.1 and Figure 3.2. This is because most of the energy is reflected to another room which results in a decrease of the effect of reflection.

As shown above, the multi-path principle causes small-scale fading to increase the challenge of accurately estimating the users' position noticeably. In such case, to provide an efficient filter to de-noise the interference caused by small-scale fading is indispensable. As a solution, two filters, the smoothing filter and wavelet filter, are utilized to remove this interference. In this chapter, the methodology and employment of the smoothing filters is introduced. Detail regarding the wavelet filter will be given in the next chapter.

3.3 The Theory and Utilisation of Smooth Filter

During the experiments in an indoor area, a user's position changes rather smoothly as a function of time. However, the RSSI noise has rapid, random changes in amplitude from point to point within the RSSI sequence. Therefore, it may be useful to reduce the noise through a process called smoothing [71].

3.3.1 Methodology of Smooth Filter

In this research, the reason for applying a smoothing filter is to decrease the fluctuation of the sequence of RSSI signal strength. By applying the smoothing filter, the RSSI values are modified and stabilized: RSSI values that are higher than the immediately adjacent points (normally caused by the shadow fading effect and the variations of the environment) are decreased, while the values that are lower than the adjacent points are increased [71]. The shape of the RSSI sequence becomes smoother, and the step response to the value changes is slower. Because the user coordinates cannot change dramatically, as a human cannot teleport from place to place, the sequence of RSSI values can be assumed to be smooth. Therefore, the RSSI signal will not be distorted too much by smoothing, and the noise can be decreased [71]. In this situation, a smoothing filter can be defined as a low-pass filter. The low-frequency components (RSSI sequence) in the spectrum can pass with little change while the high-frequency components (noise) are reduced. The basic three-point rectangular smoothing algorithm can be written as follows [71]:

$$S = \frac{S(i-1)+S(i)+S(i+1)}{3} \tag{3.12}$$

Where:

S is the smoothing result.

$S(i)$ is the current RSSI value.

Overall, more smoothing filters could be built with any necessary window width but normally, the width of window, m, should be an odd number. If the noise added into the data is white noise, meaning the noise is evenly distributed within all frequencies, the standard deviation of the noise within the signal after being processed by a basic smoothing filter will be approximately the value of standard deviation over the square root of m (s/sqrt(m)). In short, smoothing filters are generally an optimum solution to the problem of de-noising the signal, and does not generate too much information drop-off.

Smoothing filters have multiple variants, one is the triangular smoothing filter. The triangular smoothing filter looks like the basic smoothing filter: the rectangular filter, but implements a weighted framework. A 5-point triangular smoothing filter is shown below:

$$S = \frac{S(i-2)+2S(i-1)+3S(i)+2S(i+1)S+S(i+2)}{39} \tag{3.13}$$

Normally, to smooth a smoothing result multiple times is usually a useful way to build a longer and more complicated smoothing filter [71]. Actually, the 5-point weight smoothing filter is equivalent to applying a 3 point rectangular smoothing filter twice. Similarly, applying a 3-point rectangular smoothing filter three times will generate a 7-point “pseudo-Gaussian” smoothing filter, which is also called a haystack smoothing filter. The coefficient ratio of its weight value for each element is 1:3:6:7:6:3:1. The general theory is as follows: for n-passes with w-width smoothing result, the window width for the new combined smoothing filter is

n*w+1-n. For instance, 3 passes of a 13-point smoothing filter is equal to a 37 point smoothing filter. A multi-pass smoothing filter is more efficient than a basic rectangular smoothing filter especially in cases dealing with high frequency noise.

3.3.2 The Effect of Lost Points

The problem of Equation 3.12 above is that the 3-point rectangular smoothing filter is defined for *j = 2* to *n-1*. However, at the very beginning, there is not enough data provided by the signal sequence to achieve a full 3-point smoothing process because the first point and the last point in the signal are not extant. In summary, for an m point smoothing filter, the points before and after the mid-point ((m+1)/2) cannot be calculated at the beginning of the de-noise process.

There are two solution to solve this problem. One is to accept the loss of points and trim off those points or replace them with zeros in the smoothing signal [71].The other solution is to apply progressively smaller smoothing at the ends of the signal, for example to use 2, 3, 5, 7… point smoothing for signal points 1, 2, 3, and 4..., and for points n, n-1, n-2, n-3..., respectively [71].The later approach may be preferable if the edges of the signal contain critical information. This does, however increase execution time [71].

3.3.3 Problems of Smoothing Filters

One important thing which needs to be understood is that smoothing results may be deceptively impressive as the results show a very good performance visually [71]. This is because most of the high frequency components are removed by the smoothing filter. Figure 3.4 and Figure 3.5 bellow show a pair of examples of smoothing an RSSI sequence:

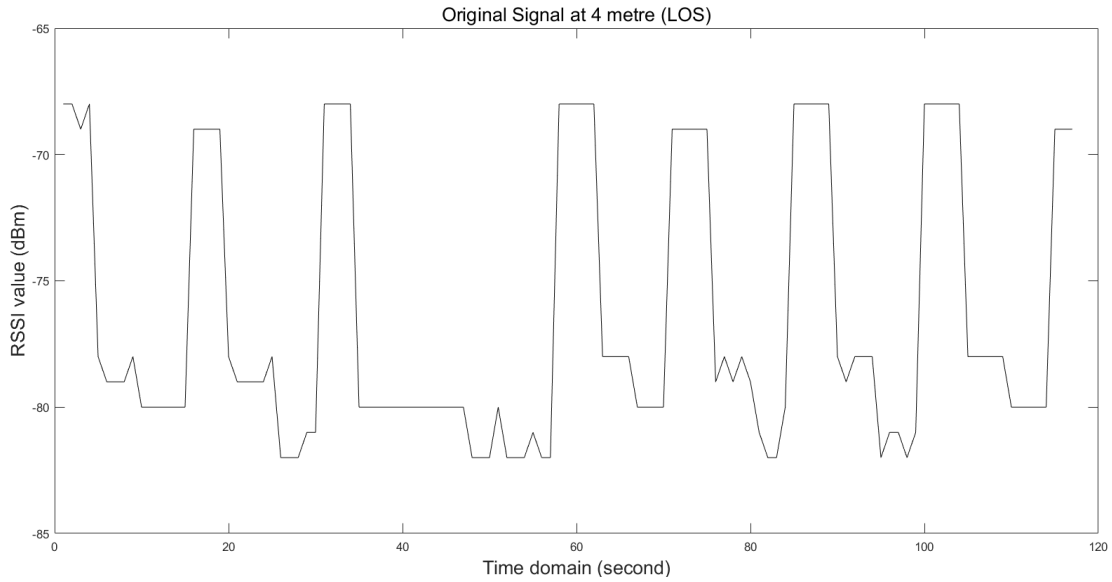

Figure 3. 4 RSSI sequence : Original result at 4 metre (LOS environment)

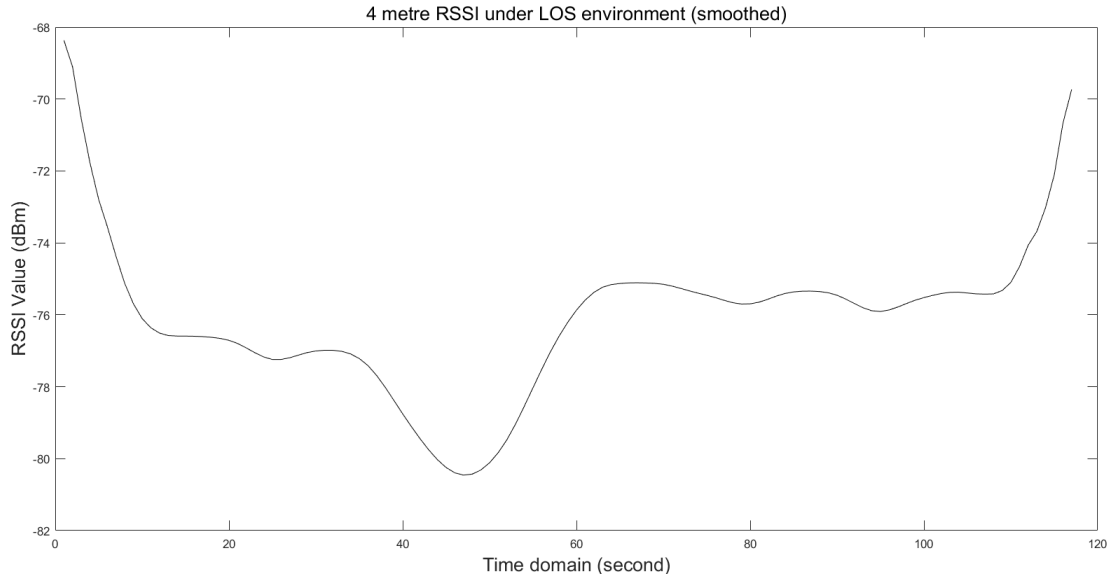

Figure 3. 5 Four metre RSSI value under LOS environment (smoothed result)

As can be seen by comparing Figure 3.4 and 3.5, the smoothed results are seemingly more ‘purified’. However the major interference, a -4dBm noise in low frequency, is still extant and produces a nearly 1.5 metre error in indoor localisation. In general, the signal looks stable and smooth but is not equivalent to being noise free. Low frequency noise components retained in the signals after

smoothing will still disturb the measurement of all of the attributes of signal such as peak value, width, and height. It should be recognised that smoothing filters cannot fully eliminate noise in most cases. The reason for this is that most noise is deployed into the signal at different frequencies, and smoothing cannot remove them.

Time delay is another problem caused by applying smooth filter. For example, a 3 length smooth filter average the point at t-1, t and t+1 as the output result in mathematic. In the real situation, as the t+1 cannot acquired at time t, normally it can be assumed that the result at time t-1 is controlled by the point t-2, t-1 and t. If the weight for each point are the same, it means that the value at time t-1 only affect the 33% of overall result. It seems that this effect will not affect the output result as human activities are normally continuous that the position at time t should have certain relationship with the position at time t-1 and t+1. However, if the length of window is increased to more than 20 points, the situation will be different. When the RSSI value at time t is received, the central point of recent output of smooth filter is controlled by the RSSI value at time t-10, which means the output result at time t is trying to exhibit the result at time t-10. In such case, a 10 point delay is generated. Ideally, the BLE beacon could increase the output package frequency to decrease this time delay physically, but this will also cause an evidently increase of power consumption. According to the experimental result, if the output frequency was set to 1HZ, a standard-size button battery could sustain a TI BLE beacon for 4 weeks at least however the endurance time for 10 HZ output frequency will be decreased to 4 days only. By considering the power consumption and time of endurance, the output frequency for BLE beacon is set to 1HZ and a 21 point smooth filter will generate a 10.5 second system delay.

3.4 Implementation and Experimental Results

3.4.1 Discussion of Signal to Noise Ratio

The aim of using filters is to remove the fluctuated frequency components which are small-scale faded as discussed, but to keep the features of large-scale fading which present distance information. Specifically, small-scale fading results in a fluctuated RSSI sequence, which decrease localization accuracy. Meanwhile, large-scale fading should be kept in the RSSI sequence to present the distance between the users and the beacons.

The major key parameters of smoothing are given follow: window size, stages, and weight value. Increasing the window size could increase the result of the smoothing. However, it should be noted that the results appearing smoother does not mean that the results of signal to noise ratio (SNR) is higher. The relationship between SNR and window width is shown below:

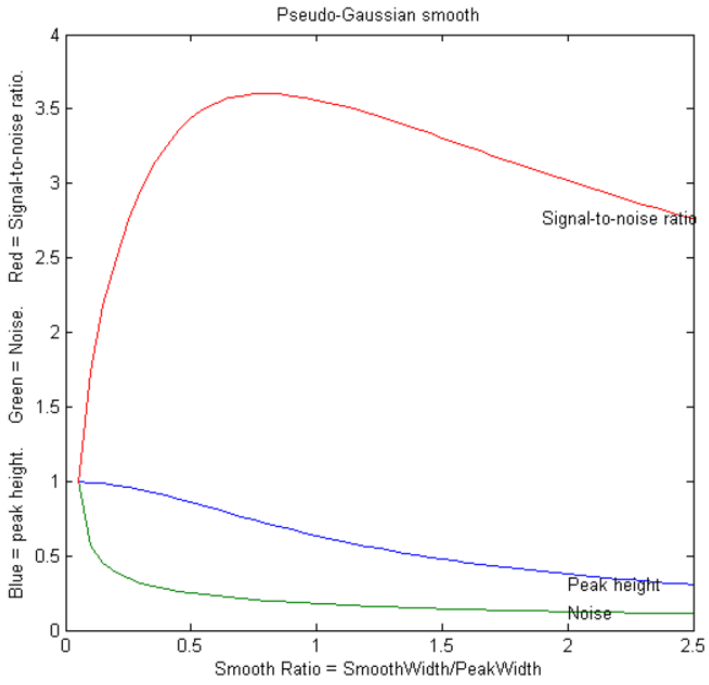

Figure 3. 6 Signal to Noise Ratio of smooth filter [71]

In Figure 3.6, it can be seen that the SNR increases at the beginning with the increase of window width, after the SNR reaches the peak value, the SNR is then inversely proportional to the window width.

Ideally, if researchers can achieve a 'purified' signal strength under real environmental conditions, the optimal width of the window can be computed by comparing the SNR. However, this is practically impossible. According to the FSPM analysis, the path loss coefficient n is set to 2 in an ideal environment, such as a chamber at lab level. However, in a real indoor environment, the coefficient is normally less than 2 (1.6 to 1.8). The reason for this is discussed previously in this chapter. In this case, if researchers want to obtain pure signal strength in a real environment, they must to build a complex environment where n coefficient must be completely equal to 1.6, 1.7 or 1.8 in any place in the room. This is potentially even more difficult than building a 'perfect' chamber. On the other hand, the transmission coefficient is less than 2, meaning that small-scale fading provides a positive impact on signal strength. Thus, an accurate SNR cannot be obtained if researchers only consider the negative impact of small-scale fading.

3.4.2 Key Parameter: Window Width

Increasing the window width could increase the response time of the system, which means the average results are averaged by longer time. This normally results in a higher responding delay but decreases the fluctuation of the RSSI sequence. As introduced in the discussion of the methodology of smoothing filters, the response delay is half of the window width. Assuming that the sampling rate is 1 second each time, a 10 point window will result in a 5 second delay while the response delay is 20 seconds if the window width is 40 points.

In actuality, the final objective is to remove the fluctuations within the RSSI signal curve and retain the sensitivity in detecting the changes to the RSSI sequence average value. At the same time, the response time should not be too long. The window width should be less than 30 points, which means the response time of the system is less than 15 seconds. Based on this assumption, a set of experimental results under different experimental conditions with different window widths from 5 points to 30 points is shown below.

Experiment 1

The first experiment tested for and compared the differences of applying different widths of window. The environment for this experiment was set inside a cabin office, as shown in Figure 3.7. This experimental condition can be assumed to be a real LOS indoor environment. The distance between receiver, a Nexus 6 google phone (as shown in Figure 3.8), and the transmitter, TI BLE beacons (as shown in Figure 3.9), are from 3 metres to 6 metres. Meanwhile, a set of smoothing filters with different window widths of 11, 21 and 31 points are applied to make comparisons.

Figure 3. 7 Experimental environment of cabin office

Figure 3. 8 Nexus 6 smart phone

Figure 3. 9 TI BLE beacons (cc2540 based) [72]

Figure 3.10 shows the experimental result of the 3 metre results, while Figure 3.11 shows the 4 metre results, Figure 3.12 gives the de-noised RSSI curve of the 5 metre results, and the 6 metre results are given in Figure 3.13. All of these RSSI sequences were processed by a smoothing filter with different window widths from 11 points to 31 points separately. The aim of these sets of experiments is to measure the performance of smoothing filters in de-noising the RSSI sequence under a static situation.

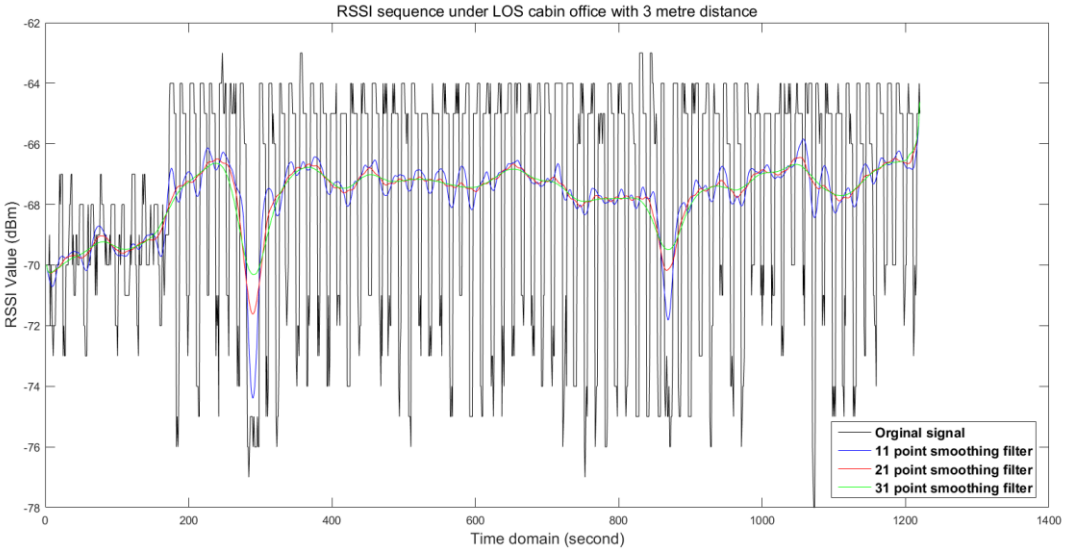

Figure 3. 10 RSSI sequence under LOS cabin office with 3 metre distance: comparison among original sequence, 11, 21 and 31 point smoothing filter results

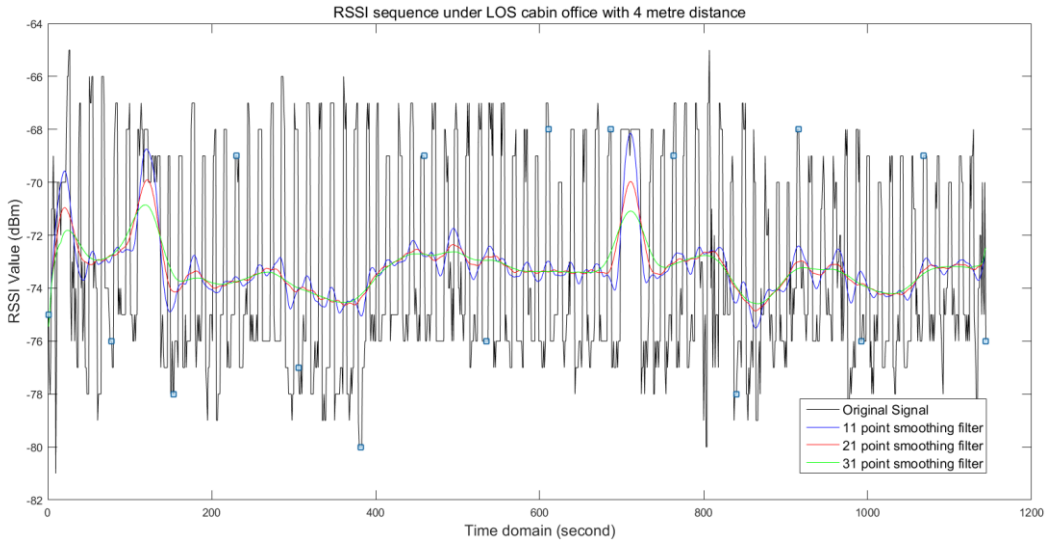

Figure 3. 11 RSSI sequence under LOS cabin office with 4 metre distance: comparison among original sequence, 11, 21 and 31 point smoothing filter results

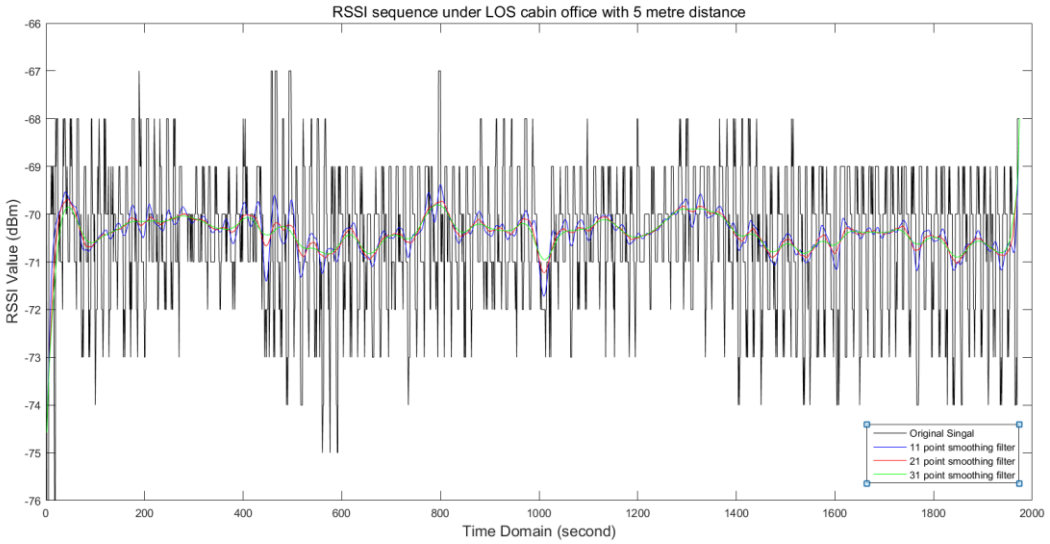

Figure 3. 12 RSSI sequence under LOS cabin office with 5 metre distance: comparison among original sequence, 11, 21 and 31 point smoothing filter results

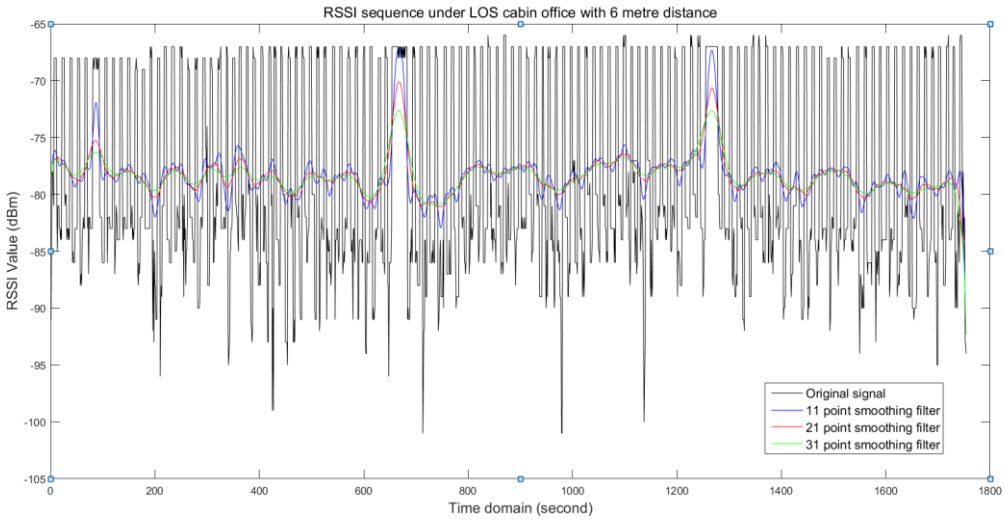

Figure 3. 13 RSSI sequence under LOS cabin office with 6 metre distance: comparison among original sequence, 11, 21 and 31 point smoothing filter results

During each individual experiment, the mobile device was kept stationary by users and there was no obstacle between signal receiver and transmitter. In this case, the RSSI sequence should keep stable if small scale fading was not present. However, the RSSI sequence fluctuated dramatically. For example, a -4 to +11 dBm peak to peak value fluctuation at 3 metres produced a -1.5 to +8.3 metre distance error. The specific distance error and standard deviation for Figure 3.8 to Figure 3.11 are shown in Table 3.3 and Table 3.4 below.

As discussed above, small scale fading causes the phenomenon of an unstable RSSI sequence. As can be seen, the average values do not change after signal sequences are processed by a smoothing filter. Thus, under stationary conditions, the utilization of a smoothing filter does produce additional errors. Meanwhile, the standard deviation is in direct proportion to the distance. In this situation, for weaker RSSI values, a smoothing filter with longer width should be applied for de-noising the RSSI sequence effectively. However, by applying the equation 3.11,

when the path loss coefficient is set to 1.8, it can be seen that a set of fixed errors are still extant and could not be removed by the smoothing filter.

In general, by applying the smoothing filter, the standard deviation decreases sharply, which means that the RSSI sequence was smoothed effectively and the noise caused by fluctuations was removed efficiently. However, the fixed noises which are integrated into the RSSI sequence could not be detected and removed.

Table 3. 3 Average value of RSSI sequence

Average signal strength (RSSI)	Ideal RSSI value	Original signal	11 point filter	21 point filter	31 point filter
3 metre	-67.58	-67.74	-67.73	-67.72	-67.72
4 metre	-69.83	-73.22	-73.22	-73.22	-73.24
5 metre	-71.58	-74.39	-74.39	-74.69	-74.40

Table 3. 4 Standard deviation of RSSI sequence

Standard deviation	Original signal	11 point filter	21 point filter	31 point filter
3 metre	3.86	1.23	1.06	0.99
4 metre	3.67	1.13	0.89	0.76
5 metre	1.34	0.43	0.38	0.37

The limitation of the first experiment is that the sensibility of environmental changes could not be measured. In this situation, another test in same

environment was made to measure the effect of information drop off, which was introduced in the above section.

Experiment 2

The second experiment was applied to measure whether the distance information will drop off when using the smoothing filter. The distance between the user and the BLE beacon was 3-4-5-4-5-6 metres. Experimental results are shown in Figure 3.14 and Figure 3.15.

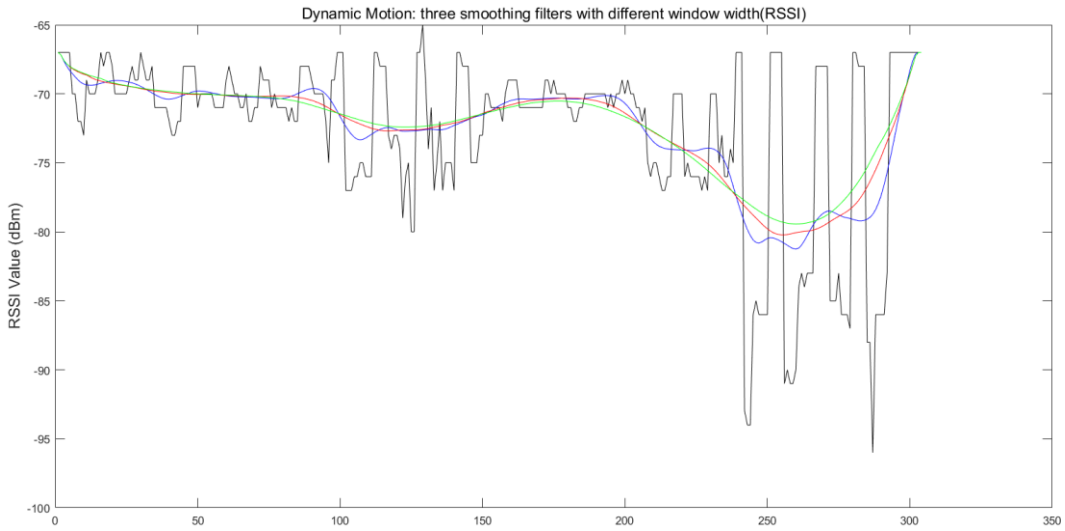

Figure 3. 14 Dynamic motion from 3 metres to 6 metres (RSSI-Time): comparison among original sequence, 11, 21 and 31 point smoothing filter results

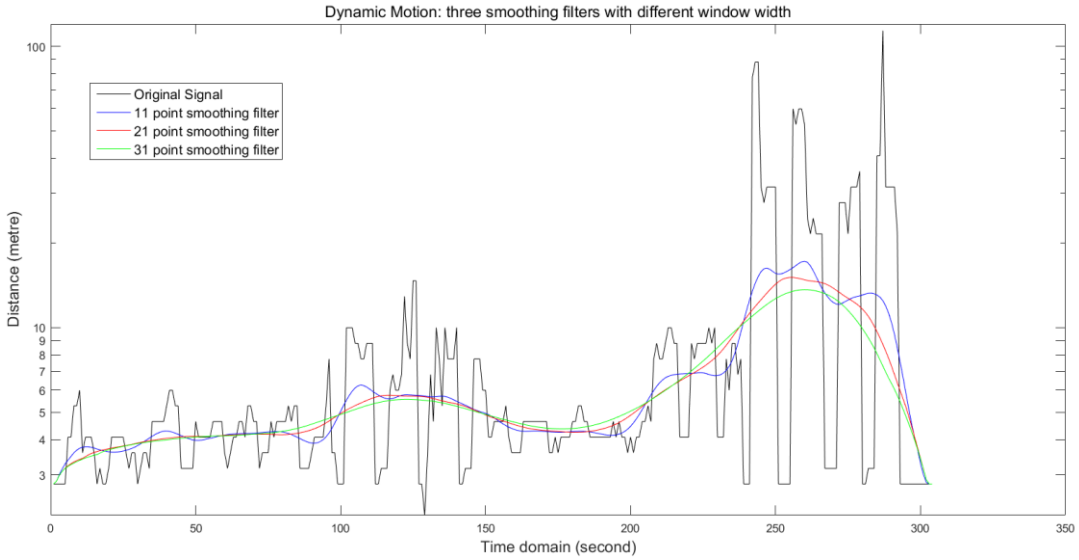

Figure 3. 15 Dynamic motion from 3 metres to 6 metres (computed distance-Time): comparison among original sequence, 11, 21 and 31 point smoothing filter results

Figure 3.14 and Figure 3.15 shows the performance of utilizing smooth filters with different window widths. In Figure 3.15, RSSI values are transferred over distance and the path loss coefficient is 1.8 and 1 metre with reference to the RSSI value, which is -59dBm. According to the previous experiment, a smaller standard deviation normally means that the positioning system is more stable. However, by considering the response time and the effect of information drop off, the window width of smoothing filters should not be selected for as long as possible. As can be seen that only a small amount of distance information was lost when applying the 11-point smoothing filter. In comparison, the user's motion cannot be detected accurately when applying the 31-point smoothing filter. For instance, at the time between 200 seconds to 250 seconds, the user kept a 5 metre distance between the mobile device and BLE beacon. The result of the 11-point smoothing filter showed this state clearly, however the 31-point filter showed that the user was moving slowly between 4 and 6 metres. In this instance, by considering the

response time and the sensitivity of detecting users' motions, the window width should be no larger than 21-points in an LOS environment.

Experiment 3

Sets of similar experiments were conducted in the Kings Building library, third floor. The map view is shown in Figure 3.16. Compared with the small cabin office, the library has more tables, bookshelves and computers, as well as lots of moving people which produced an unpredictable pattern of interference at all times. The first experiment in the library was to test the performance of smoothing filters in complex non-LOS environments with different window widths. The aim of the second experiment was to measure the distance with dynamic motions.

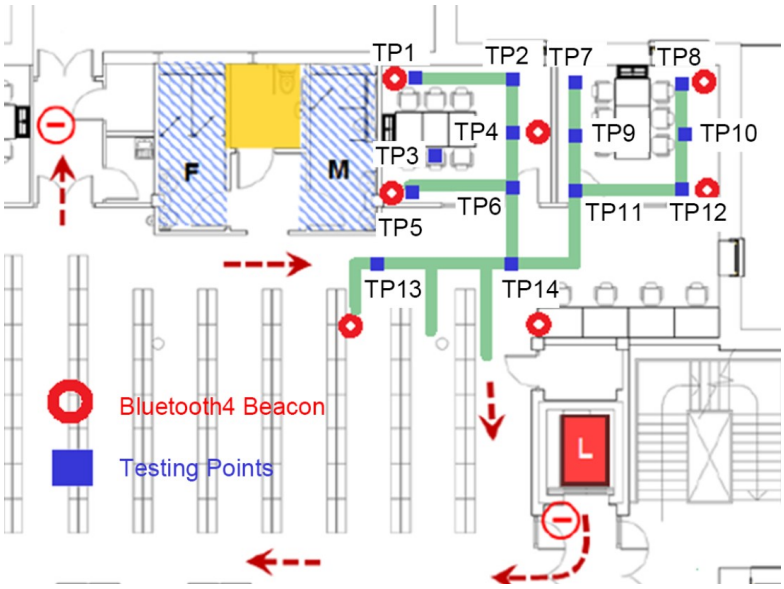

Figure 3. 16 Experimental environment in Kings Building library

For the first experiment in the library, 3 metre results are shown in Figure 3.17, 4 metre results are shown in Figure 3.18 and 5 metre distance results are shown in Figure 3.19. All were separately tested using 11-point, 21-point and 31-point

smoothing filters. Table 3.5 and Table 3.6 gives the average and standard deviations of the RSSI sequences.

Table 3. 5 Average value of RSSI sequence

Average signal strength (RSSI)	Ideal RSSI value	Original signal	11 point filter	21 point filter	31 point filter
3 metre	-67.58	-67.74	-67.73	-67.72	-67.72
4 metre	-69.83	-73.22	-73.22	-73.22	-73.24
5 metre	-71.58	-74.39	-74.39	-74.69	-74.40
6 metre	-73.00	-78.28	-78.31	-78.33	-78.34

Table 3. 6 Standard deviation of RSSI sequence

Standard deviation	Original signal	11 point filter	21 point filter	31 point filter
3 metre	3.86	1.23	1.06	0.99
4 metre	3.67	1.13	0.89	0.76
5 metre	1.34	0.43	0.38	0.37
6 metre	8.52	2.51	1.78	1.56

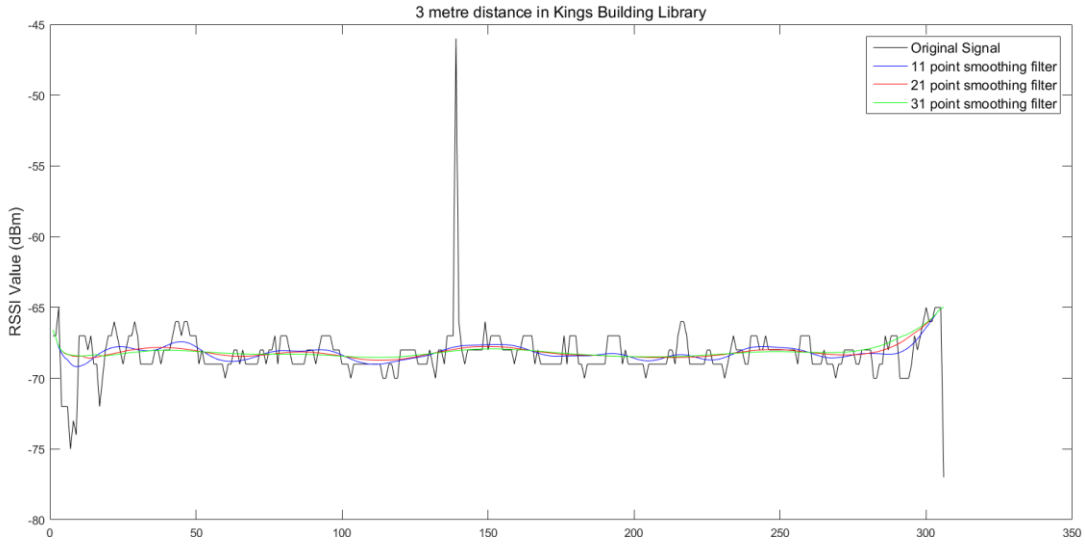

Figure 3. 17 Three metre distance in Kings Building Library: comparison among original sequence, 11, 21 and 31 point smoothing filter results

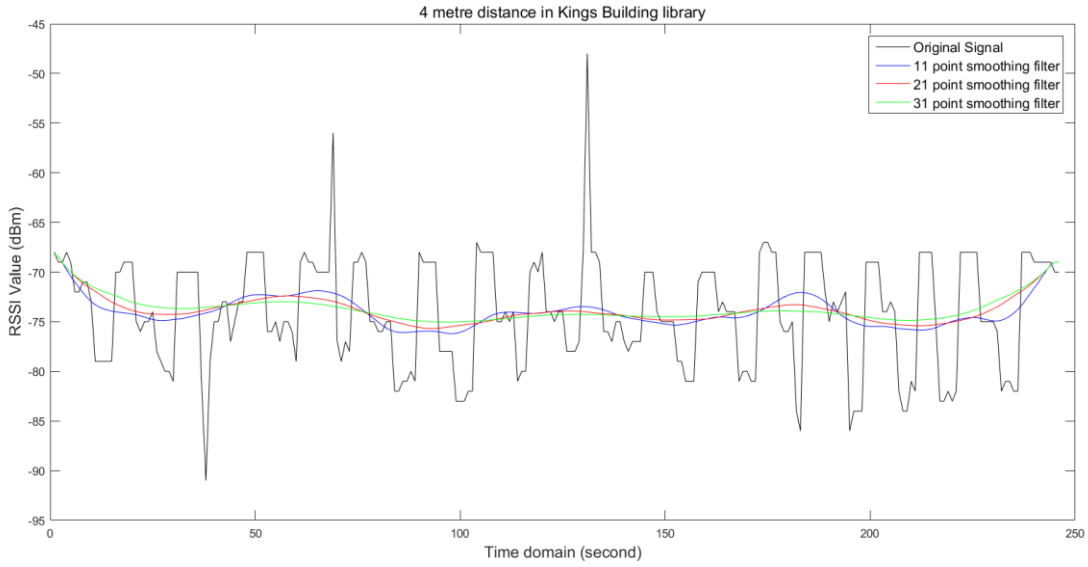

Figure 3. 18 Four metre distance in Kings Building Library: comparison among original sequence, 11, 21 and 31 point smoothing filter results

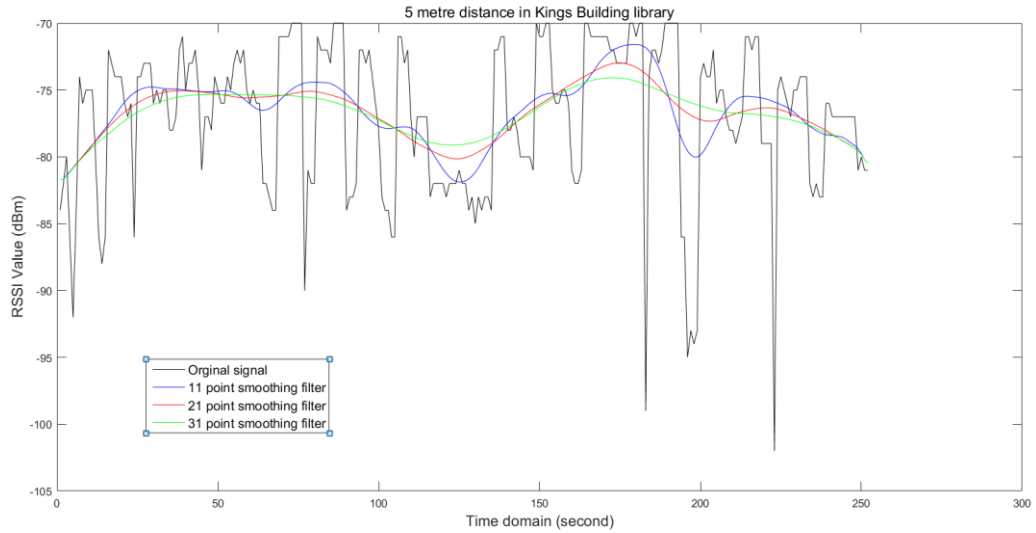

Figure 3. 19 Five metre distance in Kings Building Library: comparison among original sequence, 11, 21 and 31 point smoothing filter results

In the library, smoothing showed similar performance when compared with the experiment in the cabin office. Firstly, RSSI sequences became more stable than the original curve. Secondly, the average values were not changed when using smoothing filters. However, as the library is a more complex environment when compared with the small cabin, more obstacles such as tables and bookshelves made it more difficult to accurately measure the distance between the transmitter and receiver. In addition, moving people can also increase of the uncertainty of the RSSI sequence. As can be seen in Figure 3.17, a -46dBm 'pulse' occurred at the 144 second mark, and in Figure3.19, the average value had a conspicuous fluctuation between -83 to -75 dBm whilst the ideal RSSI average value should be -71 only. Ultimately, the multiplicative noise inside the RSSI sequence could not be removed efficiently by using smoothing filters alone.

Experiment 4

The utilization of smoothing filters under conditions of dynamic user motion was tested in the library in order to make a comparison with the experimental results

tested for in the cabin office. During the progress of the experiment, a user held a mobile device, and walked from a 3 metre distance to a 4 metre and then 5 metre distance away from the deployed BLE beacon. Figure 3.20 gives the measured distance of the original sequence with the results of using 11, 21 and 31 point smoothing filters separately. As can be seen, the original RSSI curve cannot be applied for computing distance, and the maximum distance at the time of 123 seconds was more than 40 metres. In comparison, the distance information can be measured more accurately by using smoothing filters. Specifically, the 11-point smoothing filter showed better performance than the 21 or 31-point smoothing filters. The results of using 21 and 31-point smoothing filters were smoother than the 11-point smoothing filter, however the user's motions are not detected clearly, which was similar to the results of the previous test result conducted in the cabin office.

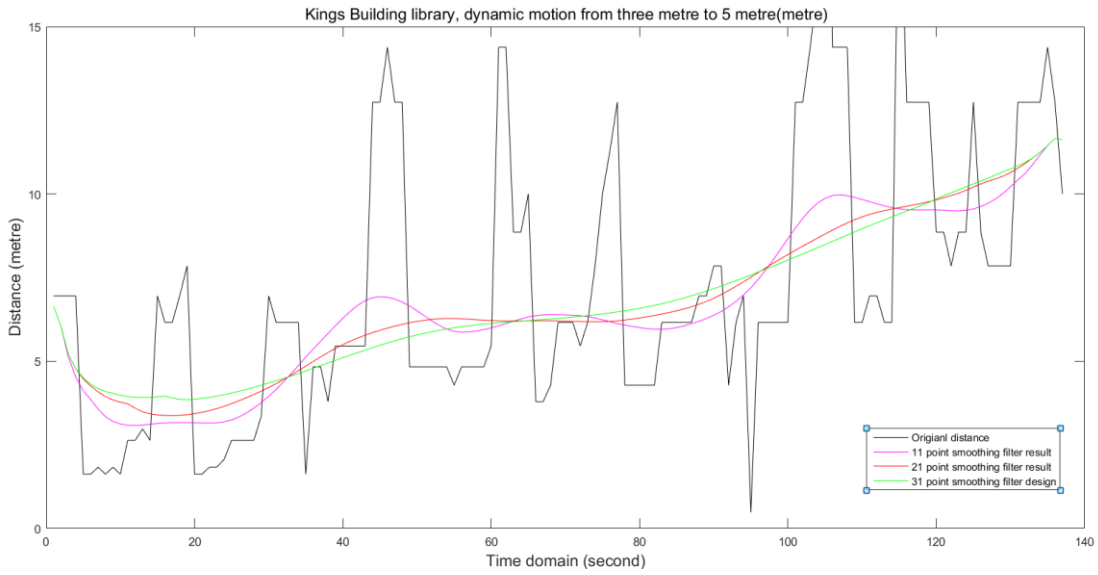

Figure 3. 20 Dynamic motion from 3 metres to 5 metres in the Kings Building library (Distance): comparison among original sequence, 11, 21 and 31 point smoothing filter results

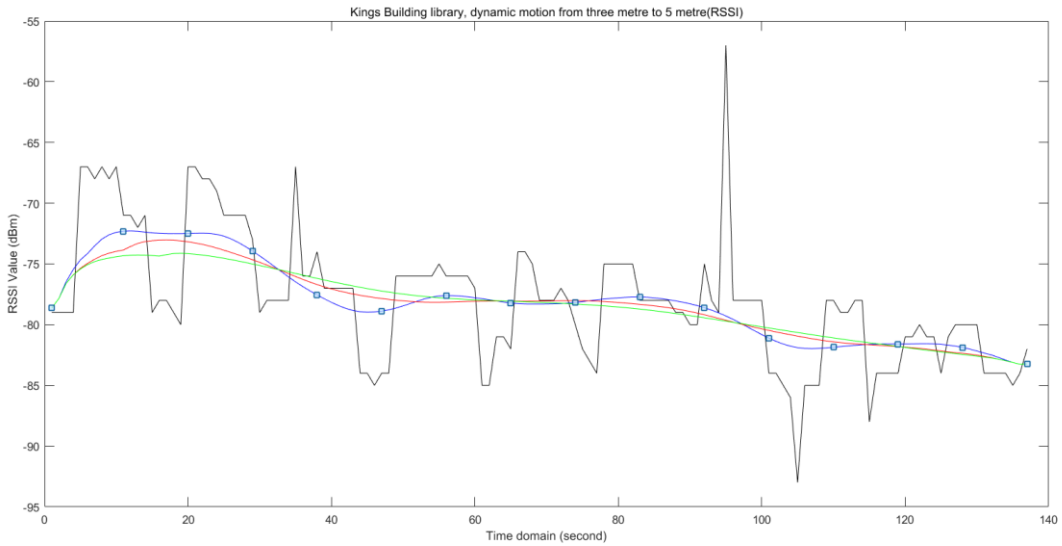

Figure 3. 21 Dynamic motion from 3 metres to 5 metres in the Kings Building library (RSSI): comparison among original sequence, 11, 21 and 31 point smoothing filter results

According to the experimental results above, firstly, longer window width made the RSSI sequence smoother and decreased the standard deviation dramatically. This is due to the fluctuating noise components caused by small-scale fading especially the multipath effect being 'averaged' into the original sequence. As introduced in the previous section, indoor reflection will increase the average signal strength. In order to fix this offset caused by applying smoothing filters, the path loss coefficient should be set a marginally higher. Secondly, the response time of the system was increased when wider smoothing filters were applied, meanwhile the sensitivity of the smoothing filter was also reduced with the increase of the window width. For example, in Figure 3.20, at the 100 second mark, the distance between user and BLE beacon was 4 metres, but the average power level did not respond to the change of distance immediately, especially for the 31-point curve. The average value of the delay was 16 seconds. Meanwhile, when the user remained stationary, the 31-point smoothing filter could not detect the

user's motion accurately. According to the results of these experiments, the optimal window width should be 11-points to 21-points. The response delay caused by window width is between 5 seconds and 10 seconds, whilst the sensitivity delay is between 2 to 5 seconds.

According to the experimental results mentioned above, it can be seen that increasing the window width could decrease the fluctuation of RSSI sequence. The standard deviation of RSSI sequence is decreased dramatically compared with the smoothed and un-smoothed results. In specific, the decrease of standard deviation from 0 to 11 point is remarkable and the results from 11 to 21 point is also visible. In comparison, the standard deviation decreased slightly from 21 to 31 point. Meanwhile, the average value of smoothed RSSI do not have big change from 11 to 31 point. In such situation, smooth filters with more than 21 window points could not provide obviously improvement for the de-noise performance, but increase the information drop off. By considering the responding delay, the overall delay time should no less than 10 second in order to provide good user experience, which means the length of window should no larger than 23 point in most cases. As a result, the value of window width in this research is selected between 11-21 points, which can be changed by different environmental conditions dynamically.

3.4.3 Key Parameter: Multiple Stages

Extending the stages of the smoothing filter is another way to increase the results of smoothing. By using multiple stages, smoothed RSSI sequence could have a higher sensitivity when suffering a dramatic change but do not affect the overall average when RSSI sequences are steady. Specifically, as introduced in the methodology chapter, the purpose of increasing the stages is to smooth the smoothed results. For example, applying a 3-point smoothing filter twice is equal to applying a 5-point triangle filter. Actually, the real way of employing a multi-stage smoothing filter is to build the final equation of the smoothing filter, but not to apply a short smoothing filter multiple times. The minimum width of the smoothing filter is related to the stages of the filter. For one stage of smoothing, the minimum size is 3, for two stages, the minimum size is 5. In this case, increasing the number of stages will also increase the width of the window.

By applying a multiple-stage smoothing filter, the weight of the mid-point will be much larger than the rest of the other points. Meanwhile the weight value of the points at the beginning and the end of the sequence will be very low, which will not affect the smoothing process greatly. Based on this situation, a set of 7-point smoothing filters with different stages was tested under different environmental conditions.

Experiment 1

Firstly, three smoothing filters with 7-point window widths were tested in the cabin office environment shown in Figure 3.7. The aim of this experiment is to test the performance of different stages of smoothing filters within a stationary

environment. Figure 3.22 to Figure 3.25 shows the results of 3 metre to 6 metre distances.

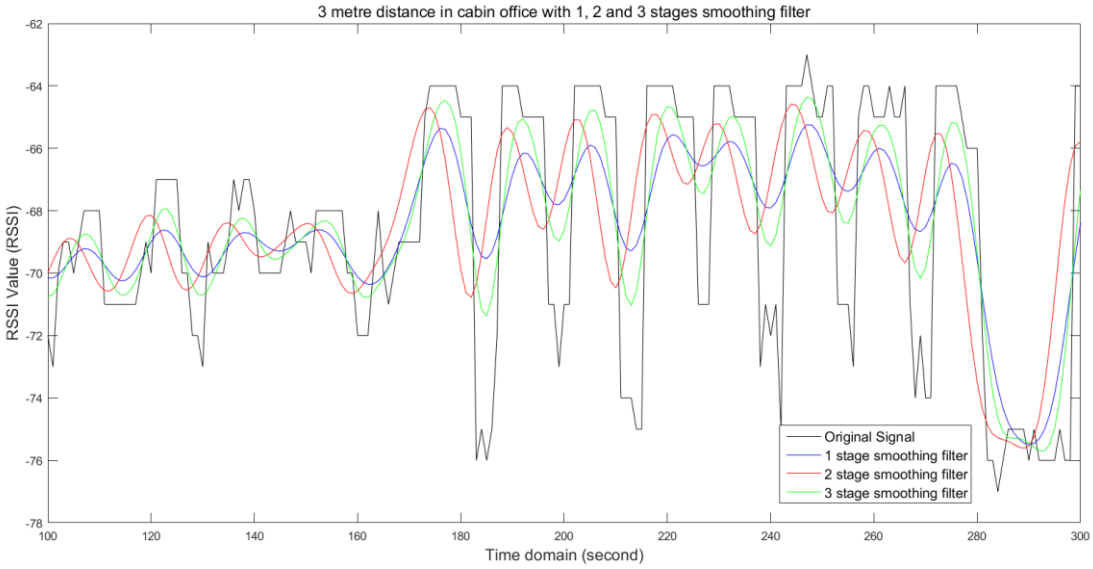

Figure 3. 22 RSSI sequence at three metre distance in cabin office: comparison among original sequence with 1, 2 and 3-stage smooth filter results

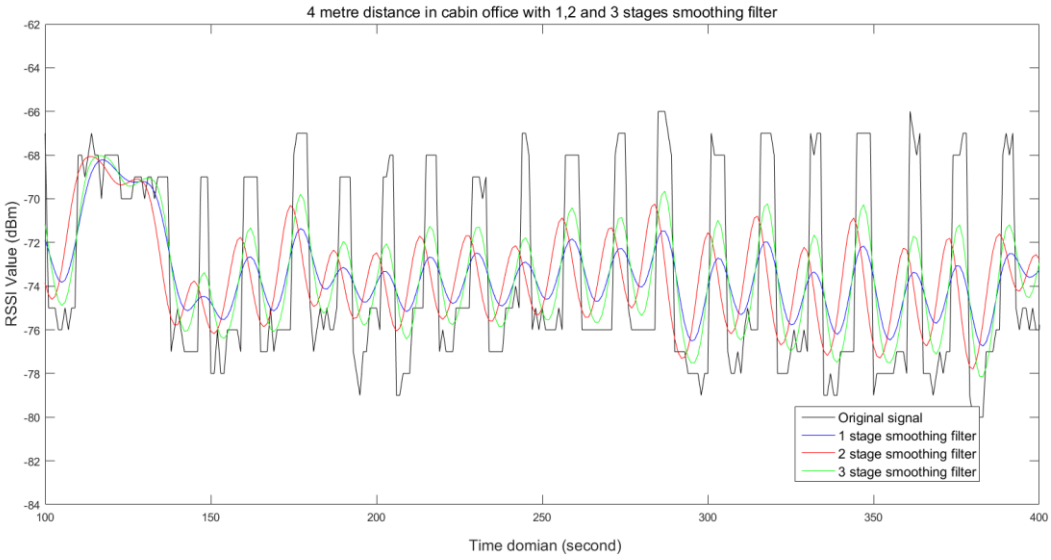

Figure 3. 23 RSSI value at four metre distance in cabin office: comparison among original sequence with 1, 2 and 3-stage smooth filter results

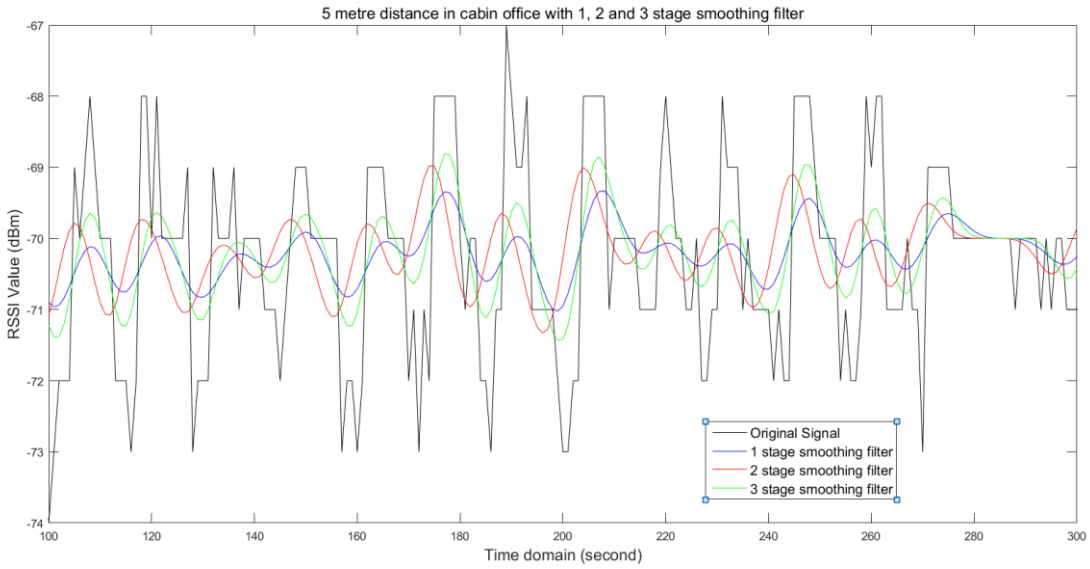

Figure 3. 24 RSSI value at five metre distance in cabin office: comparison among original sequence with 1, 2 and 3-stage smooth filter results

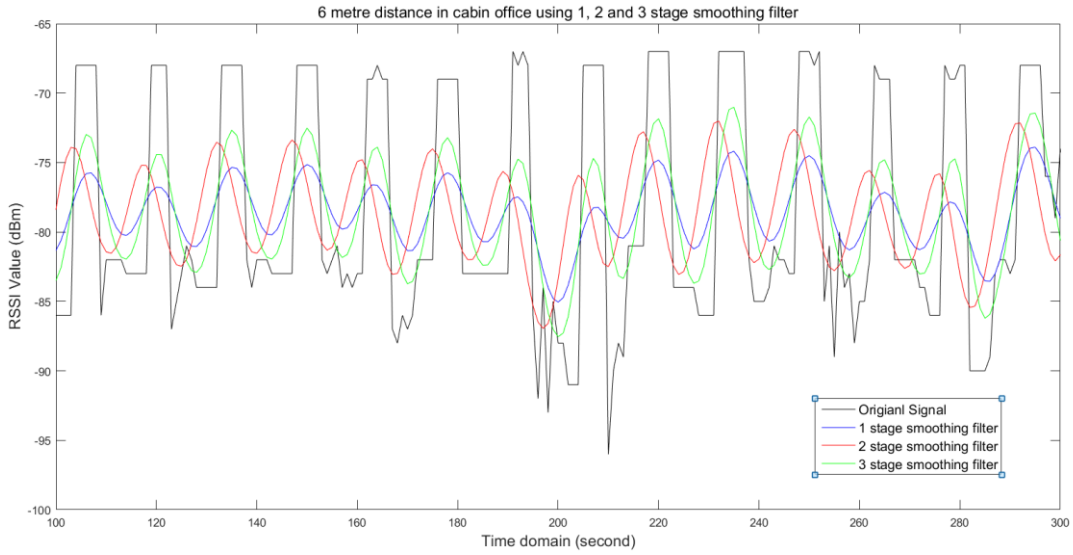

Figure 3. 25 RSSI value at six metre distance in cabin office: comparison among original sequence with 1, 2 and 3-stage smooth filter results

Table 3. 7 Localisation error of RSSI sequence in library

Average signal strength (RSSI)	Ideal RSSI value	Original signal	1 stage	2 stage	3 stage
3 metre	-67.58	-67.74	-67.73	-67.72	-67.74

4 metre	-69.83	-73.22	-73.22	-73.22	-73.24
5 metre	-71.58	-74.39	-74.39	-74.69	-74.40
6 metre	-73.00	-78.28	-78.31	-78.33	-78.34

Table 3. 8 Standard deviation of RSSI sequence in library

Standard deviation	Original signal	1 stage	2 stage	3 stage
3 metre	3.86	1.60	1.99	2.18
4 metre	3.67	1.50	1.87	2.06
5 metre	1.34	0.55	0.67	0.76
6 metre	8.52	3.08	4.11	4.15

According to the results shown in Table 3.7, the average RSSI value did not change after being processed by the smoothing filters, this is the same as the results shown in Table 3.8. Meanwhile, the standard deviation is increased with the increase in the number of stages in the filters. This is because the weight value of the points are not balanced. The result in the middle will be given a higher weight value, which means these points will have more influence on the smoothed result.

In general, under stationary conditions, using a multiple stage smoothing filter will slightly decrease the standard deviation and the fluctuation of the processed RSSI sequence. In this case, it seems that a 1-stage smoothing filter is the best choice.

Experiment 2

Multiple stage smoothing filters are also tested when users' motions are dynamic. Figure 3.27 gives the RSSI sequence results of 3-4-5-4-5-6 metre distances, while

Figure 3.26 shows the distances results using different stages of smoothing filter. The aim of this experiment was to test the performance of multiple stage smoothing filters when users are moving.

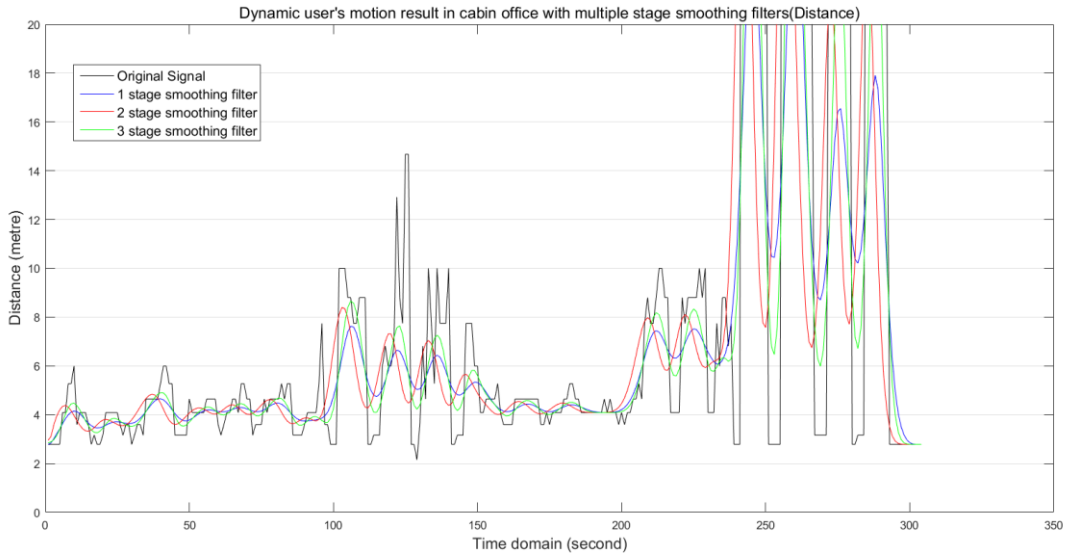

Figure 3. 26 Dynamic users' motion results in cabin office using multiple stage smoothing filters (Distance)

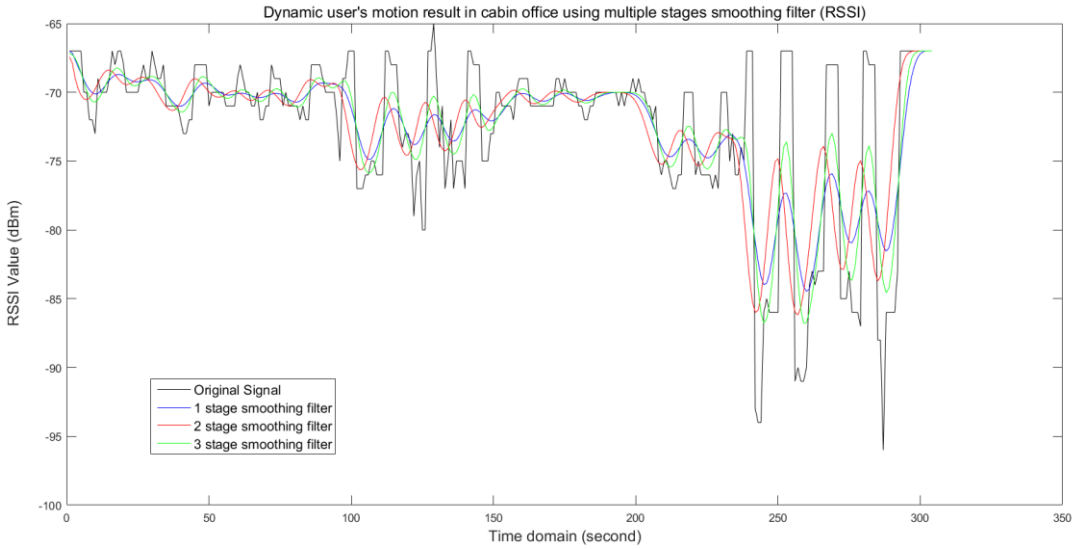

Figure 3. 27 Dynamic users' motion result in cabin office using multiple stage smoothing filters (RSSI)

As shown in Figure 3.26, users' motion can be detected accurately as the window width of these smoothing filters is 7-point. When the RSSI sequence was not dramatically fluctuated, the difference among these three filters cannot be differentiated observably (such as is shown between 0 to 100 seconds and 150 to 200 seconds). However, the difference among these multiple stage smoothing filters are conspicuous: higher stage smoothing filters result in a more sensitive RSSI sequence. Under complex conditions such as Non-LOS environments or the users' motion being dynamic, higher stage smoothing filters could detect the distance faster and more effectively. In summary, by considering the users' motion, in this research multiple stage smoothing filters were utilized in order to detect the distance change efficiently.

Experiment 3

Similarly, two sets of experiments were tested in the Kings Building library to measure the de-noising performance of multiple stage smoothing filters in Non-LOS environments. Firstly, the performance of 1, 2 and 3-stage smoothing filters under stationary distance conditions was tested, afterwards these filters were tested under dynamic distance conditions.

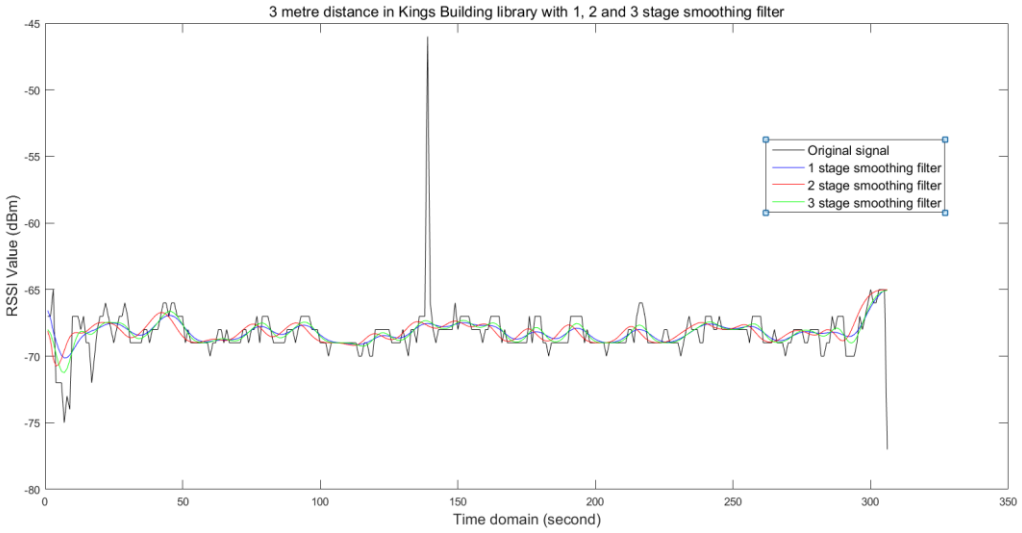

Figure 3. 28 Three metre RSSI results in Kings Building with 1, 2 and 3-stage smoothing filters

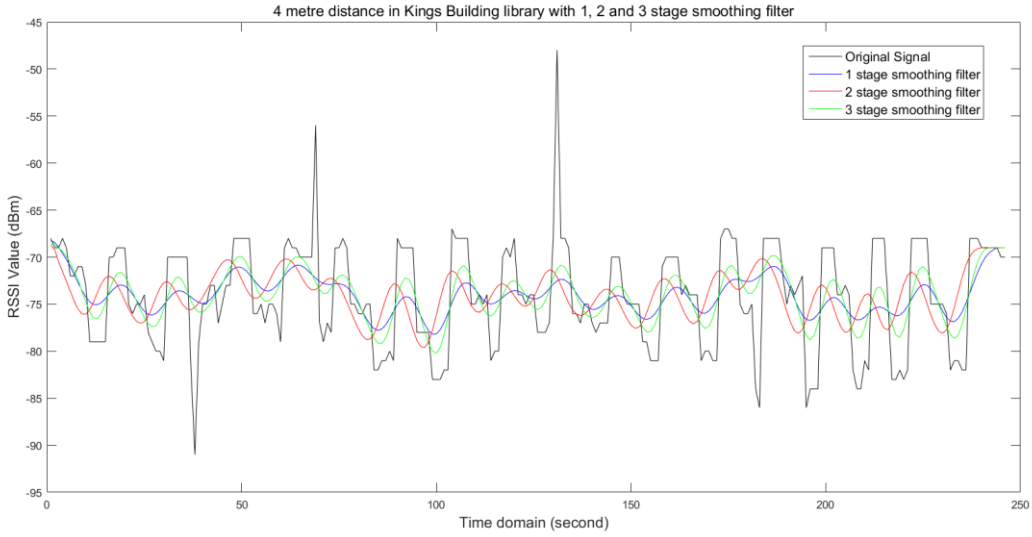

Figure 3. 29 Four metre RSSI results in Kings Building with 1, 2 and 3-stage smoothing filters

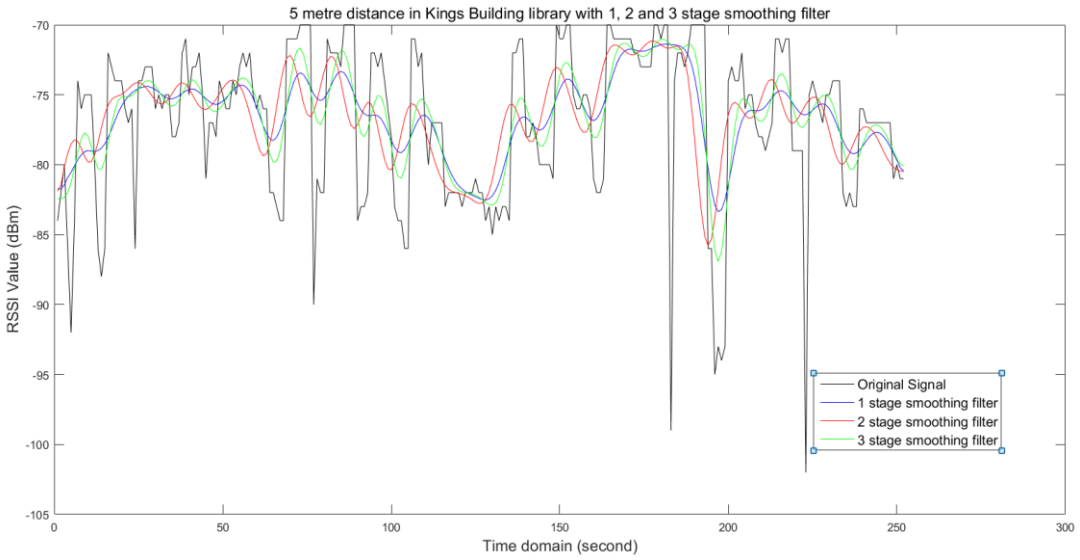

Figure 3. 30 Five metre RSSI results in Kings Building with 1, 2 and 3-stage smoothing filters

Table 3. 9 Average value of RSSI sequence in library

Average signal strength (RSSI)	Ideal RSSI value	Original signal	1 stage	2 stage	3 stage
3 metre	-67.58	-68.21	-68.19	-68.16	-68.21
4 metre	-70.44	-74.02	-74.01	-74.01	-74.02
5 metre	-72.28	-76.56	-76.57	-76.54	-76.56

Table 3. 10 Standard deviation of RSSI sequence in library

Standard deviation	Original signal	1 stage	2 stage	3 stage
3 metre	1.87	0.68	0.79	0.79
4 metre	5.56	1.94	2.40	2.62
5 metre	5.68	2.77	3.05	3.23

As shown in Table 3.9 and Table 3.10, the average value of the RSSI sequence did not have any changes with the employment of multiple stage smoothing filters. Furthermore, the stationary value of the RSSI sequence decreased dramatically after being processed by smoothing filters. Specifically, the standard deviation of the 1-stage smoothing filter was smaller than the 2 and 3-stage filters results, and as shown in Figure 3.28 to Figure 3.30, most of the shape points were removed by the smoothing filters, however the average RSSI values still keep a dynamic noise, from 0.63 dBm for a 3 metre distance, to 4.28 dBm at a 5 metre distance.

Experiment 4

The following experiment was conducted in order to measure the performance of multi-stage smoothing filters when distance changes in complex Non-LOS environments. The distance between the mobile device and BLE beacon was 3 metres in the first instance, then was altered to 4 metres, and finally 5 metres.

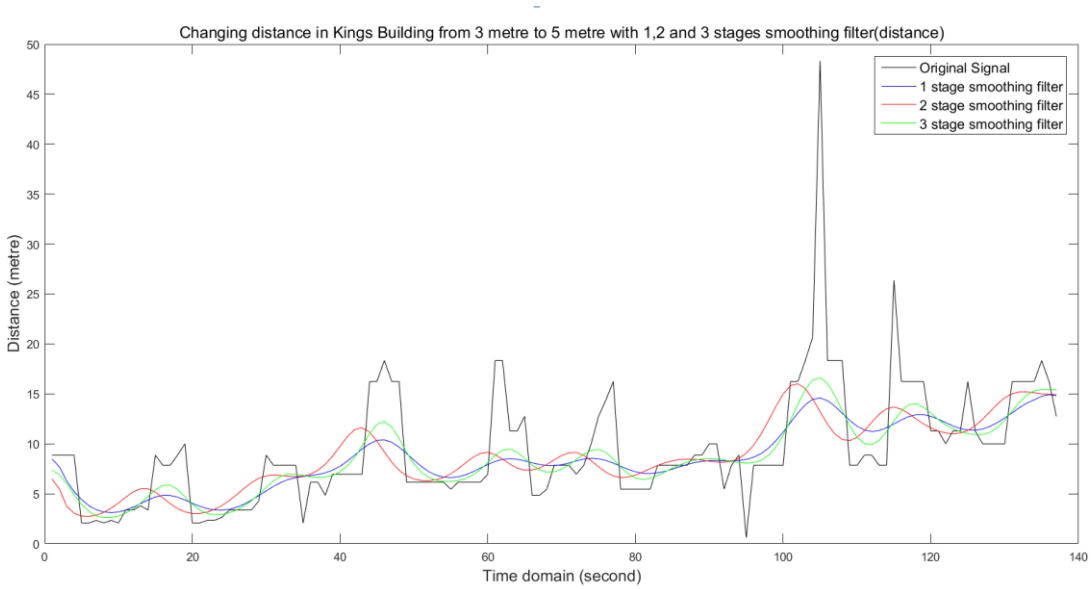

Figure 3. 31 3, 4 and 5 metre distance results in Kings Building with 1, 2 and 3-stage smoothing filters (distance)

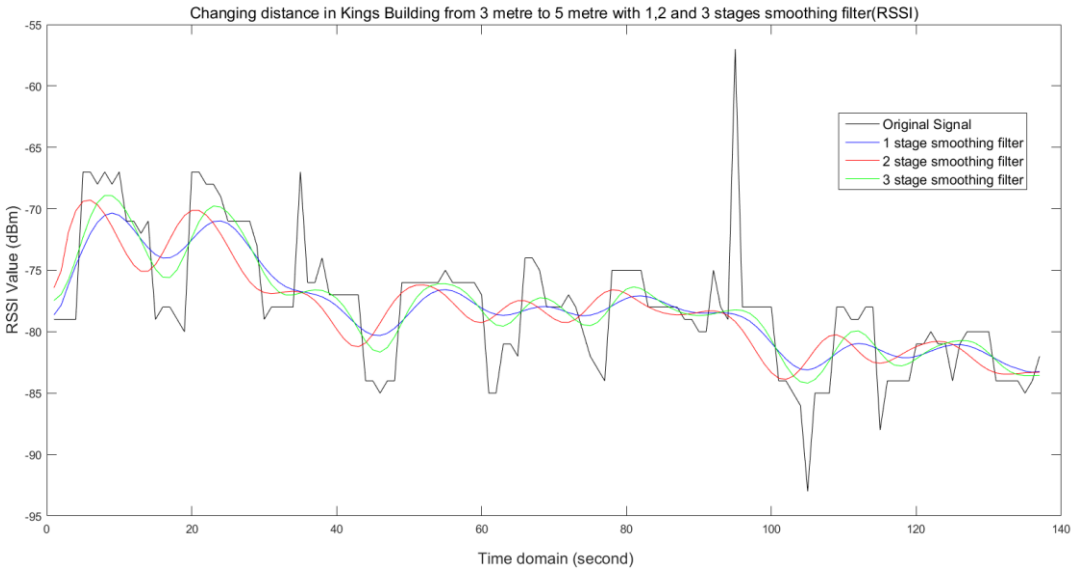

Figure 3. 32 3, 4 and 5 metre RSSI results in Kings Building with 1, 2 and 3-stage smoothing filters (RSSI)

The utilisation of multi-stage smoothing filters with varying distances was tested in the library in order to compare the experimental results tested in the cabin office. Users held a mobile device and walked from 3 to 5 metres away from the deployed BLE beacon. Figure 3.31 and Figure 3.32 gives the measured distance and RSSI value of the original sequence and the processed sequences of using 1, 2 and 3-stage smoothing filters separately. According to the experimental results, firstly, the RSSI sequence became smoother with the decrease of stages applied. Specifically, the furcation of the 1-stage smoothed result is smoother than the results of the 2 and 3-stage smoothing filters. Moreover, at the period when the RSSI sequence was kept stationary (such as can be observed between 0 and 40 seconds), the difference between these three filters was not distinct. However, when the RSSI sequence fluctuated dramatically, higher stage smoothing filters

showed strong sensitivity for detecting the change of distance. In this case, by using higher stage smoothing filters, users' motion can be detected accurately.

Experiment 5

In general, by comparing the experimental results shown above, the window width of smoothing filters should be set between 11 to 21-points and the number of stages should be 2 or 3 stages. The following figures show the performance of a 14-point window width smoothing filter and the stages utilised were 1, 2 and 3-stages. The experimental environments were the cabin office and the Kings Building library.

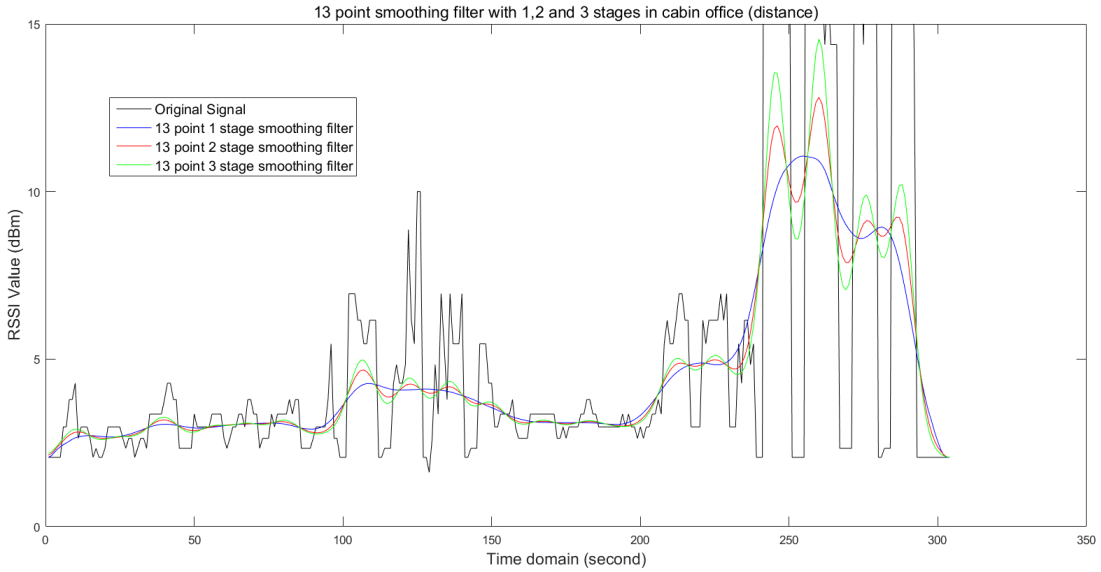

Figure 3. 33 13-point smoothing filter results with 1, 2 and 3 stages in cabin office (distance)

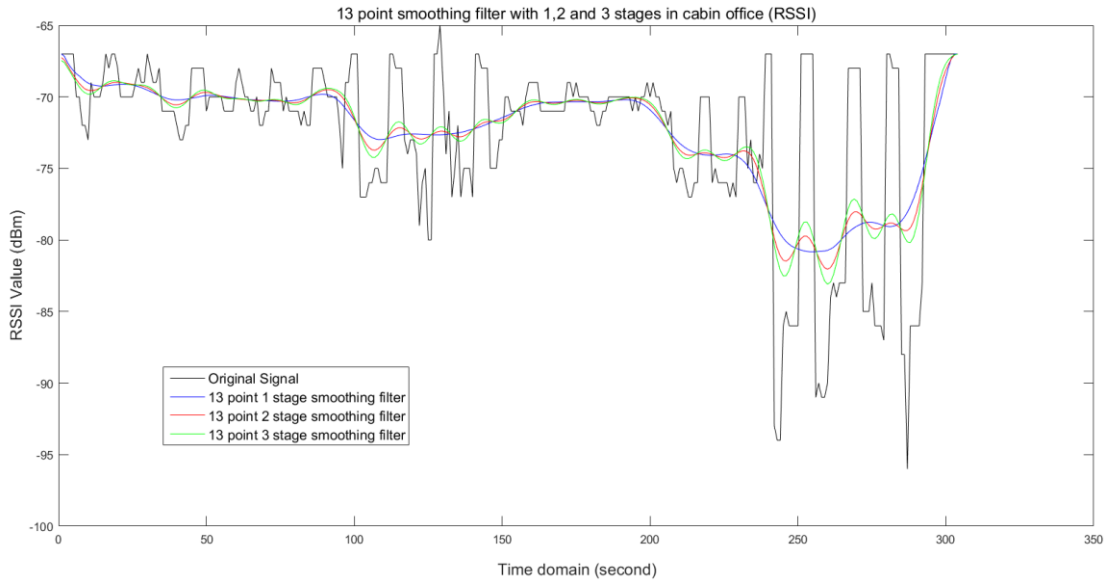

Figure 3. 34 13-point smoothing filter results with 1, 2 and 3 stages in cabin office (RSSI)

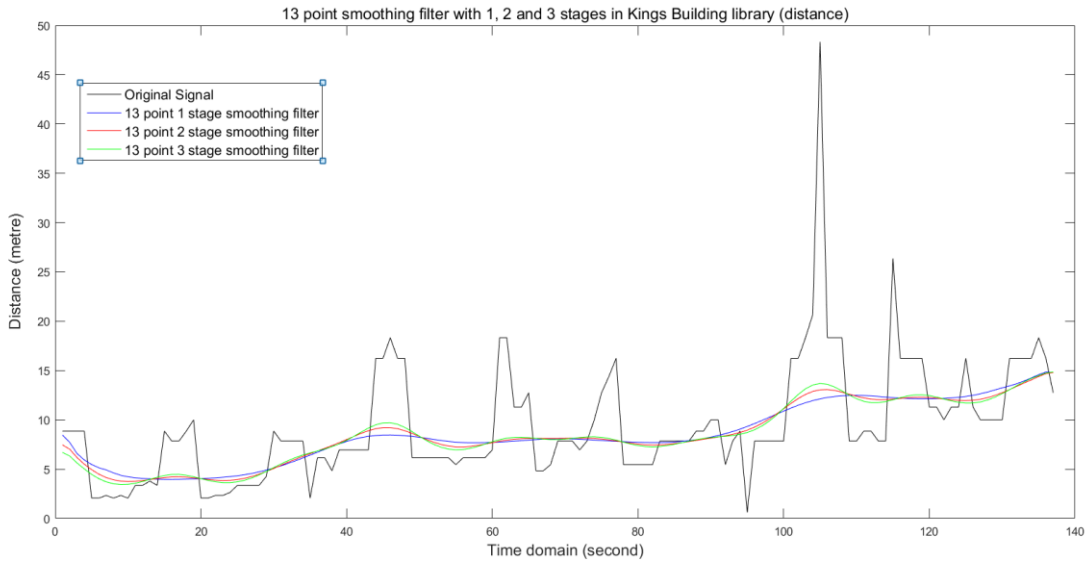

Figure 3. 35 13-point smoothing filter results with 1, 2 and 3 stages in library (distance)

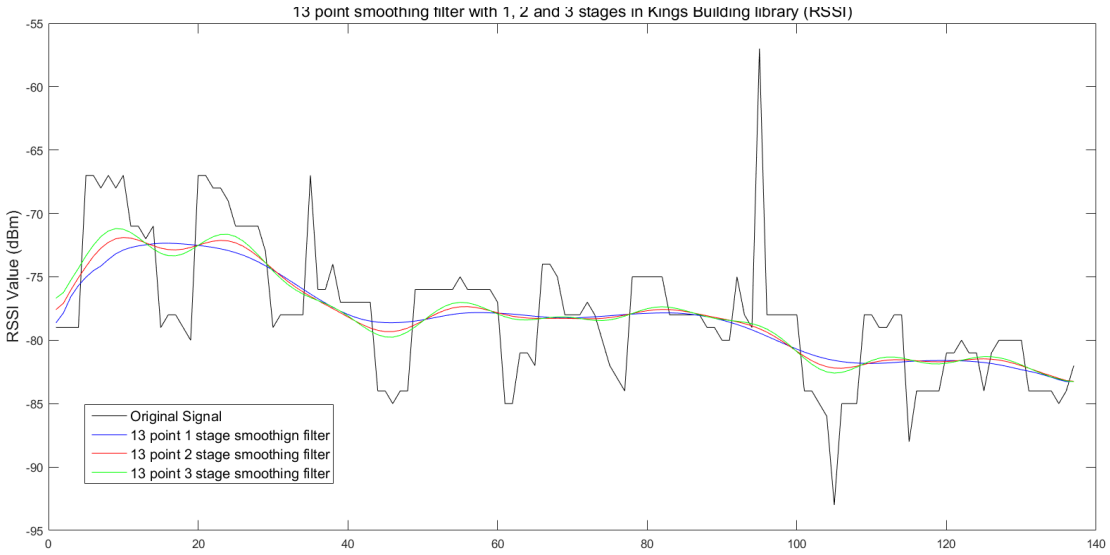

Figure 3. 36 13-point smoothing filter with 1, 2 and 3 stages in library (RSSI)

According to the experimental results shown from Figure 3.33 to Figure 3.36, the 13-point smoothing filter could de-noise the interference caused by small scale fading, which appeared as a fluctuation in the RSSI sequence. Also, the attenuation of the RSSI sequence is higher in a Non-LOS environment than s LOS environment. This is because in a Non-LOS environment, obstacles and moving people result in more reflection which increases the transmission path and deceases the signal strength.

In particular, higher stage smoothing filters show better performance of sensitivity for detecting users' motion when distance is changing. In addition, the fluctuation of the RSSI sequences only display a slight variation when the sequence was kept stationary (as can be observed in the period from 60 seconds to 80 seconds in Figure 3.36). In fact, high stage smoothing filters work like an 'amplifier': when the RSSI sequence is kept stationary, the processed curve does not exhibit big changes, meanwhile when the distance was changing, high stage smoothing filters could sensitively detect the users' motion and then feedback the location

information to the computing system immediately. By considering that the working conditions of proposed indoor positioning systems in most cases are environmental conditions which are Non-LOS, a 13-point, 3-stage smoothing filter could produce the best performance in most indoor areas. Furthermore, the response delay caused by smoothing filters is around 7 seconds, which is also acceptable for most civilian-used indoor positioning systems.

3.5 Conclusion

In this chapter, firstly, the theory of the Free Space Propagation Model was introduced, followed by the formula for derivation of path loss mode that developed from the Free Space Propagation Model. Also, the principle of the indoor transmission equation was presented, which is based on the path loss mode. Secondly, the analysis of transmission interference in an indoor environment was discussed, with the conclusion that small scale fading plays a major role in the causation of fluctuation in the RSSI sequence. Afterwards, the methodology of smooth filters was presented, which also included a discussion of its limitations. Following this, the implementation of smooth filters was demonstrated, accompanied by sets of experimental results of the application of smoothing filters under different parameters and in different environmental conditions.

During experimentation, two of the key parameters of smoothing filters, window width and stages, were tested in different environments and user motion patterns separately. The performance of smoothing filters with different window widths was tested in LOS (cabin office) and Non-LOS (Kings Building library) environments while the distance between transmitter and receiver was either stationary or

dynamic. Experimental results indicated that when the distance between the receiver and transmitter is fixed, the performance of smoothing filters for de-noising the RSSI sequence and the corresponding response time had a direct relation with the window width: long width smoothing filters produced a smoother curve, and longer response time. The performance of smoothing filters with different stages was then tested with the same experimental process. The test results showed that increasing the number of stages of a smoothing filter increased the sensitivity of detecting any change in distance, whilst the amount of fluctuation was not increased by applying a higher stage smoothing filter.

During these sets of experiments presented above, a set of 13-point smoothing filters with 3 different stages were tested in order to determine the final parameters utilized in this research. As a result, the 13-point, 3-stage smoothing filter was selected in order to de-noise the RSSI sequence and increase the positioning accuracy and stability of the positioning system which is introduced in chapter 5 and 6.

Chapter 4 : The employment of Tailor-made Wavelet filters

4.1 Introduction

Wavelets are mathematical functions that segment data into different frequency domains, and then process each data pieces with a resolution matched to its scale [73]. The key theory of wavelets is to process data according to scale [73]. Around 300 years ago, Joseph Fourier discovered the utilisation of the superposition of sines and cosines to represent the other functions [74]. However, in wavelets, the scale that is applied to observe data is different. Wavelet algorithms process data at different rent scales or resolutions [73]. For traditional Fourier transforms, if we apply a narrow window to scale the data, we will get a high resolution on time domain; if we use a wide window to scale the data, we will get a high resolution on frequency domain. In short, by applying Fourier transforms, high resolution on frequency and time domain cannot be acquired at same time. However, wavelets are different. The result in wavelet analysis allows one to see both the ‘big picture’ and the ‘detail’ [74].

Applied fields that are making use of wavelets include astronomy, acoustics, nuclear engineering, sub-band coding, signal and image processing, neurophysiology, music, magnetic resonance imaging, speech discrimination,

optics, fractals, turbulence, earthquake-prediction, radar, human vision, and pure mathematics applications such as solving partial deferential equations [74].

In this research, the RSSI sequence can be defined as a non-stationary process, in this instance, a wavelet can be applied to denoise the RSSI sequence with high performance. In this chapter, the background behind wavelets, which is the Fourier transform, is introduced. The theory of wavelets and the motivation of its utilisation is given, followed by a set of experimental results and a chapter conclusion.

4.2 Fourier transform, Discrete Fourier transform and Wavelet transform

4.2.1 Fourier Transform

Fourier's representation of functions as a superposition of sines and cosines has become ubiquitous for both the analytic and numerical solution of differential equations and for the analysis and treatment of communication signals [75]. There is a strong relationship between Fourier transform and Wavelet transform.

Specifically, Fourier transform is applied to present a signal’s frequency feature but analyses the signal in a time domain. Firstly, the signal function is translated from the time domain to the frequency domain. Then, the frequency content of this signal can be analysed as the frequency components (normally presented in sine and cosine waves) at each frequency can be presented by referring to the coefficients of the transformed function. Finally, an inverse Fourier transform is applied to transform the data from the frequency domain back to the time domain.

In this research, by considering the power consumption, frequent communication in full-duplex will reduce the cruising ability dramatically. As a result, the RSSI in

the receiving end is discrete. In this situation, the discrete Fourier transform (DFT) can be utilized to process the discrete RSSI signal. The DFT estimates the Fourier transform of a function from a finite number of its sampled points [75]. These sampled points should have the outstanding characteristics of the original signal. Because the DFT and continuous Fourier transform have the same properties of symmetry, the key feature of the original signal will not drop off. Moreover, the formula for the inverse DFT is also relatively simple to achieve, as it is nearly same as the formula of DFT.

4.2.2 Windowed Fourier Transforms

In actuality, the received signal strength under real environmental conditions is non-periodic progress, which means the signal strength cannot be represented accurately from the summation generated by periodic functions. One of the solutions is to extend the RSSI sequence to make an artificially periodic sequence. However, the disadvantage of this is that, at the endpoints, additional continuity of this artificially extend sequence is required. Another solution is to apply a windowed Fourier transform (WTF) [73] for representing the non-periodic RSSI sequence. The WFT could be applied to simultaneously provide information about signal in both time and frequency domains.

Specifically, the RSSI sequence is segmented into pieces, and the frequency content for each fragment is separately analysed. If the signal has sharp transitions, we window the input data so that the sections converge to zero at the endpoints [75]. This process is accomplished by using a weight function that deploys more emphasis around the interval's middle points than in the end area. The function of the window is to locate the signal in the time domain.

4.2.3 Wavelet Analysis

Wavelet analysis is also a function for analysing signal in the time domain for its frequency content. Wavelet analysis differs from Fourier transform in that wavelet analysis does not analyse signals with sine or cosine waves but analyses signals by applying wavelet functions.

The orthogonal wavelet basic function, can be presented below:

$$\Phi_{(s,l)}(x) = 2^{-\frac{s}{2}}\Phi(2^{-s}x - l) \tag{4.1}$$

Where:

s is the scale index for indicating the wavelet's width

l is the location index which is applied to give its position.

Notice that Φ is rescaled by powers of two and translated by integer s and l. The key point of a wavelet function is that a wavelet displays self-similarity, which is because of scale and dilation. At the moment when the mother functions are acquired, all of the detail about the basis can be obtained.

In order to measure our data with different resolutions, a scaling equation is applied to analyse the wavelet:

$$W(x) = \sum_{k=-1}^{N-2}(-1)^k c_{k+1}\Phi(2x + k) \tag{4.2}$$

Where:

$W(x)$ is the scaling function,

c_k are the coefficients of the wavelet.

These coefficients must be satisfied linearly and should be constrained quadratically with the following form:

$$\sum_{k=0}^{N-1} c_k = 2, \sum_{k=0}^{N-1} c_k c_{k+2l} = 2\delta_{l,0} \quad (4.3)$$

Where:

δ is the delta function and l is the location index.

For wavelets, the coefficients c_k can be defined as a filter. These coefficients can be applied in a transformation matrix. The coefficients have two functions: one as a smoothing filter, another to provide the specific information of data. These two orderings of the coefficients are called a *quadrature mirror filter pair* in signal processing parlance [76].

The transformation matrix is applied in a pyramidal algorithm, which is a hierarchical algorithm. These wavelet coefficients are ordered: the odd rows of the matrix works like smoothing filters, while the even rows are applied for bringing out the detail of the data information. Firstly, the transformation matrix is appropriate for the original vector which is full-length. For the next step, the vector is smoothed by the odd rows of the matrix and decimated to 0.5 by the even rows of the matrix. This step is repeated constantly unless a trivial number of 'smooth-smooth- smooth...' data remain [73]. In such a case, each employment of the matrix results in data with higher resolution, while the rest of the data is also smoothed. The outcome of the discrete wavelet transform (DWT) is composed by the rest of the remaining smoothed result with all of the accumulated data information specifically.

4.2.4 Comparison between Fourier Transform and Wavelet Transform

In this research, the RSSI signal sequence is non-stationary, which means the statistical property of the sequence cannot be predicted and changes with time. This is easy to understand because the users' motions are normally random and unpredictable. Meanwhile the interference caused by the antenna orientation and obstacles are also uncertain. A solution for these issues is to apply windowed Fourier transform.

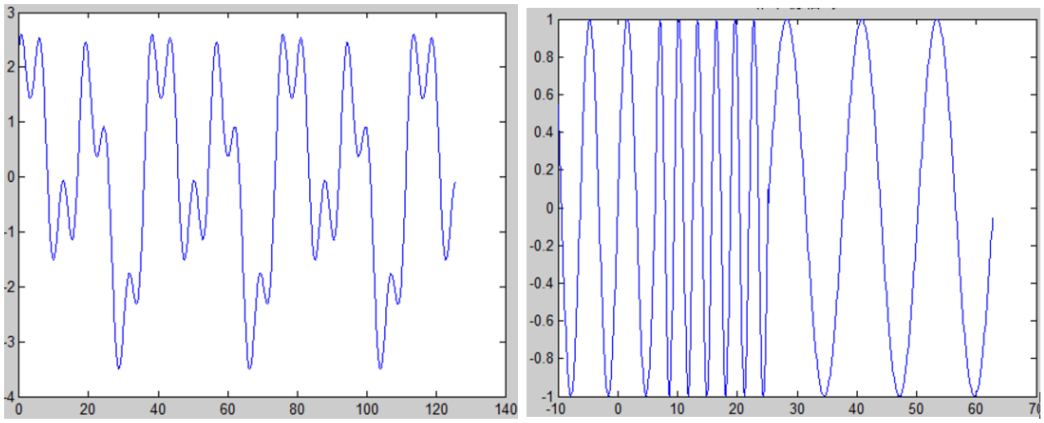

Figure 4. 1 Stationary and none stationary sequence [75]

Figure 4.2 gives a description of windowed Fourier transform. Normally, windowed Fourier transform is applied to process a non-stationary signal sequence. The theory is to reduce the window size until the signal inside the window is stationary. In such cases we can use Fourier transform to observe the fragment of the original signal. This process is referred to as 'short time Fourier transform' (STFT).

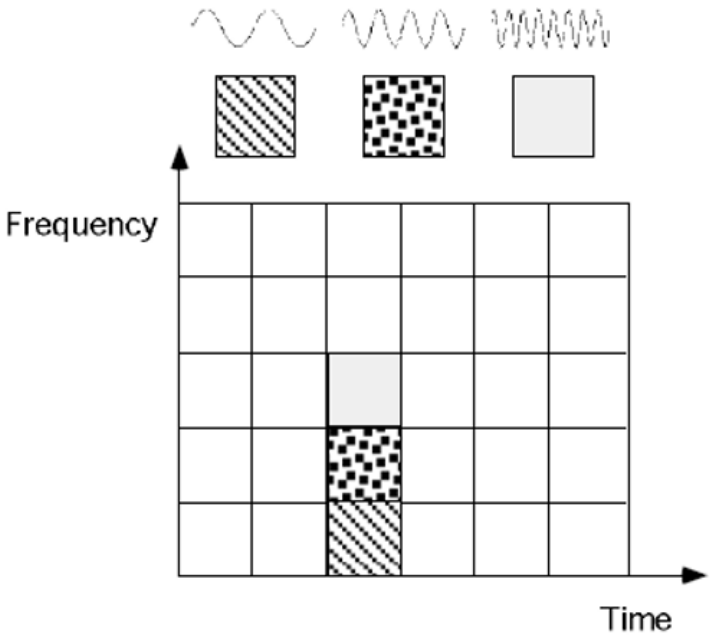

Figure 4. 2 Time resolution and frequency resolution of Fourier transform [73]

STFT only differs slightly from Fourier transform. In STFT, signals are cut into pieces which are small enough, those pieces can be defined as a stationary process. Based on this theory, a window function is needed. The width of the window should be the same with the width of each signal segment otherwise the stationary condition of the STFT is invalid.

As discussed previously, the resolution of STFT is fixed. This is because the width of the window function cannot be changed. If the width of the window is infinite, a perfect frequency resolution can be acquired after processing Fourier transform. However, the temporal information is not available to be obtained as the time span of the window is infinite.

However, what we desire is to achieve the stationary nature of the signal sequence. In this regard, the width of the window function should be as short as possible until the signal segment within the window width is stationary. As a result,

a narrow window could produce a high time resolution and stability of the signal, but result in a low resolution in frequency domain.

An analysis of STFT with different window widths is given in the diagrams, which is shown in the Figure 4.3:

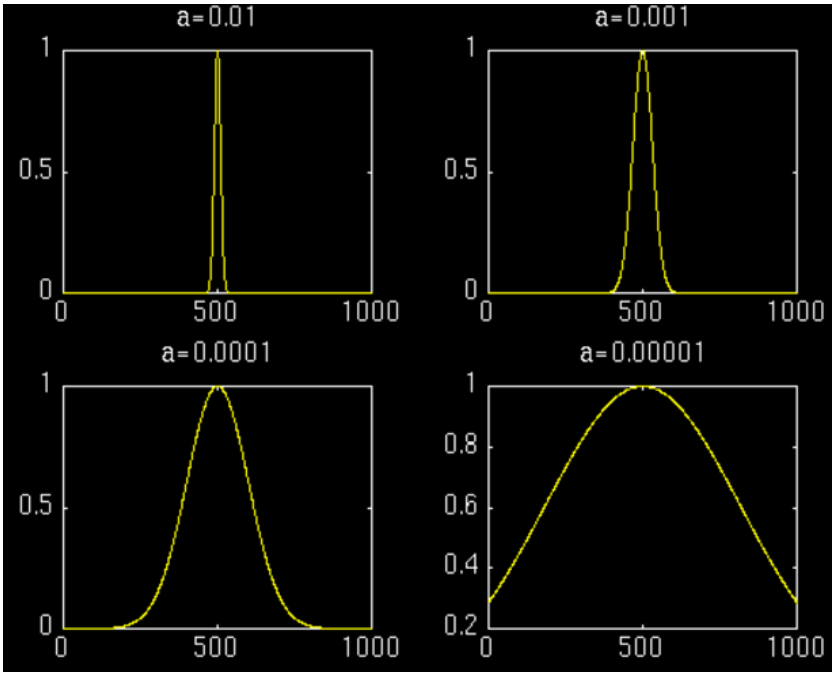

Figure 4. 3 Examples of STFT with different window widths [75]

Figure 4.3 gives a set of examples of STFT with different window widths. For the narrowest window width, the time-frequency resolution diagram is shown below in Figure 4.4, the frequency of the signal is 500Hz:

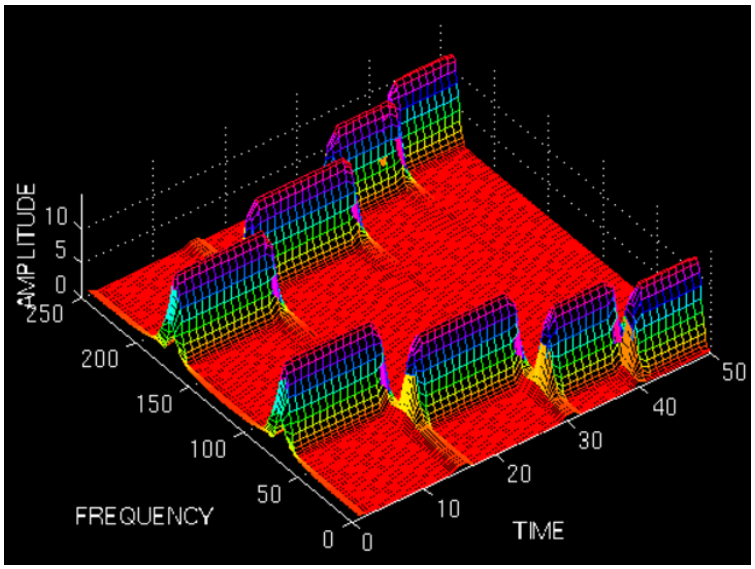

Figure 4. 4 Time and frequency resolution: High time resolution [75]

It is clear to see that, the time resolution of the signal is accurate. However, the curve in the frequency-axis overlaps, the amount of overlap in the curve on the frequency-axis can be observed, which means the frequency resolution is inaccurate.

In comparison, a time-frequency resolution diagram for a wider window width is given below:

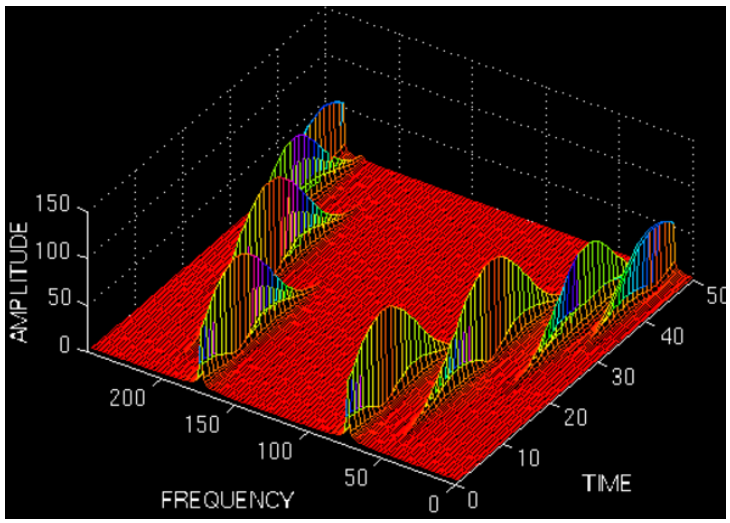

Figure 4. 5 Time and frequency resolution: High frequency resolution [75]

As can be seen in figure 4.5, with the increase of the window width, the resolution in the time domain decreases while the frequency resolution is more accurate. For the widest window for STFT, the result is shown in Figure 4.6:

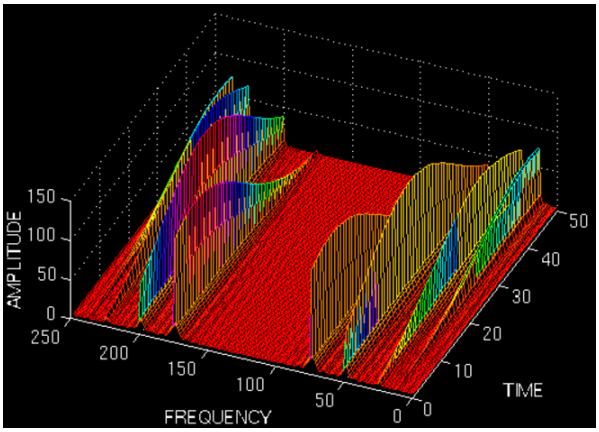

Figure 4. 6 Time and frequency resolution: Highest time resolution [75]

In this case, the time resolution is inaccurate but the frequency resolution is accurate. In summation: a narrow window results in a high time resolution and low frequency resolution; a wide window produces a low resolution in the time domain and a high resolution in the frequency domain. In short, the selection of the window width for the window function's needs is important when processing data with STFT.

For the wavelet transform, one advantage is that the width of the windows can be changed dynamically. In order to insulate the discontinuities of the signal, a short basis function can be a good choice. At the same time, a long basis function can be applied to observe the frequency analysis in detail. In such a case, a basis with different scaling functions, in other words, windows with different window widths may be applied to process the signal in different frequency domains at the same time. An example of this process is shown in Figure 4.7:

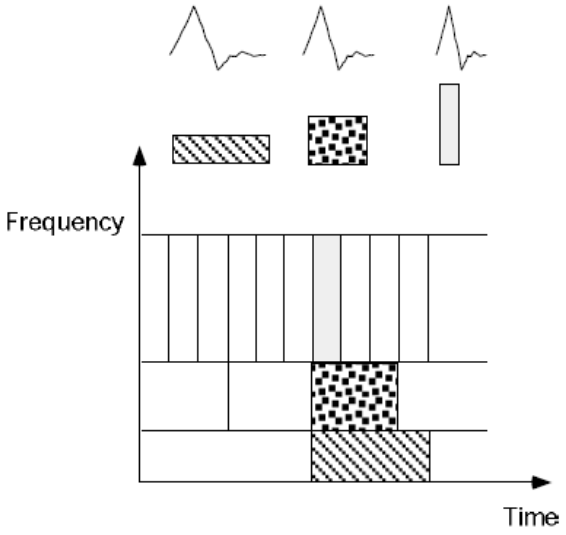

Figure 4. 7 Time resolution and frequency resolution of Wavelet transform [73]

As shown in the figure above, a wide window is applied to process the low frequency components because a low frequency signal requires more time to present. For high frequency component analysis, a shorter basis is employed as the information of high frequency signals can appear in a short time.

In summary, Fourier transform applies a set of basic functions which are sine and cosine waves. In comparison, the scale of the wavelet basis function can be extended or shrunk for application to different frequency components. This characteristic gives wavelets a strong adaptability in dealing with non-stationary processes. As mentioned above, the RSSI signal sequence can be a non-stationary process. In this situation, wavelet transform can be a better choice when compared with Fourier transform.

4.2.5 Gibbs Phenomenon

Gibbs phenomenon, discovered by Henry Wilbraham and rediscovered by J. Willard Gibbs [77].Gibbs phenomenon clarified a phenomenon that：

When a signal fluctuates violently due to Fourier transformation, a large number of triangular waves are required to be fitted irrespective of the size of the transformation.

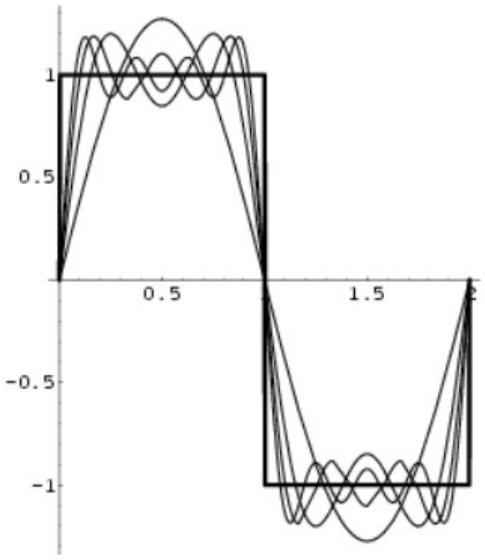

Figure 4. 8 example of Gibbs phenomenon [78]

The wavelet transformation avoids the Gibbs phenomenon because the mother wavelet is 0 for most positions and is not a periodic signal. Using wavelets can effectively avoid Gibbs phenomenon when dealing with violent and rapid non-stationary progress.

4.3 Implementation

The concrete realisation of the wavelet process can be expressed by the following formula [73]:

$$F(w) = \int_{-\infty}^{\infty} f(t) * e^{-iwt} dt \rightarrow WT(\alpha, \tau) = \frac{1}{\sqrt{a}} \int_{-\infty}^{\infty} f(t) * \Psi\left(\frac{t-\tau}{\alpha}\right) dt \quad (4.4)$$

Where:

α is the scale, τ is the translation.

Scale controls the scaling of the wavelet function and τ controls the translation of the wavelet. Scale is inversely proportional to frequency, τ corresponds to time. By using wavelets, we can know both the frequency component of the signal and the position of the time domain corresponding to the frequency component. Further, when we pan in every scale and then multiply the original signal, we get the frequency components contained in all the positions. Therefore, by using Fourier transformation, the frequency can be obtained, and by using wavelets, we can obtain a time-frequency spectrum.

In this research, the wavelet filter is utilized with following steps. Firstly, the original RSSI sequence, which is the f(t) in equation 4.4, were decomposed at different frequencies by using different α value. By applying different levels of hard and soft thresholds on different scales, the component of the noises caused by small scale fading can be removed and finally the rebuilt RSSI sequence was dramatically stabilized and the features of the users' behaviours were retained.

4.3.1 Mother Wavelet

In the process of concrete realisation of the wavelet filter, the choice of mother wavelet is crucial. Some examples of wavelets are shown in Figure 4.9, which are: Daubechies, Haar, Morlet, Symlets, Coiflets and Meyer. [73]

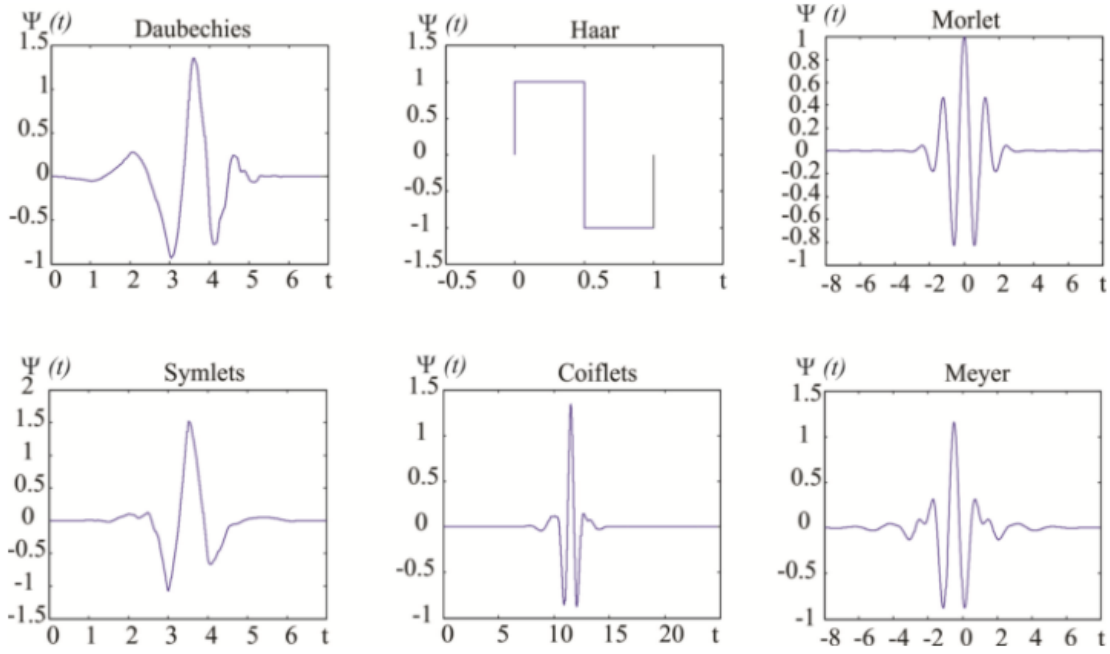

Figure 4. 9 Examples of different types of mother wavelet [73]

In the specific use of the wavelet process, we directly use the wavelet function has been pre-set in Matlab to operate directly on the data. For the mother wavelet, we chose Daubechies in this research because the Morlet wavelet waveforms generally resemble the fluctuations of the RSSI sequence and can also reduce Gibbs phenomenon due to fitting.

4.4 Experimental Results

In this chapter, the wavelet filter is chosen to de-noise the RSSI sequence. First, we employed the Daubechies wavelet in terms of mother wavelet selection. Then, in order to compare with the results of chapter 2, we directly used the wavelet filter

to compare with the data in chapter 2. In this section, we have chosen a different wavelet filter for the window width to perform noise reduction on the RSSI sequence. The experimental results are compared with those in chapter 3.

Experiment 1

As seen in chapter 3, smoothing filter static and dynamic tests were conducted in a 'cabin office'. The environment of the cabin office can be defined as a LOS environment. First of all, different window widths of smoothing filters were tested to make a comparison. The follow figures show the results of the RSSI sequence processed by wavelet filters at 3, 4, 5 and 6 metre distances. The windows widths are 11, 21 and 31 points.

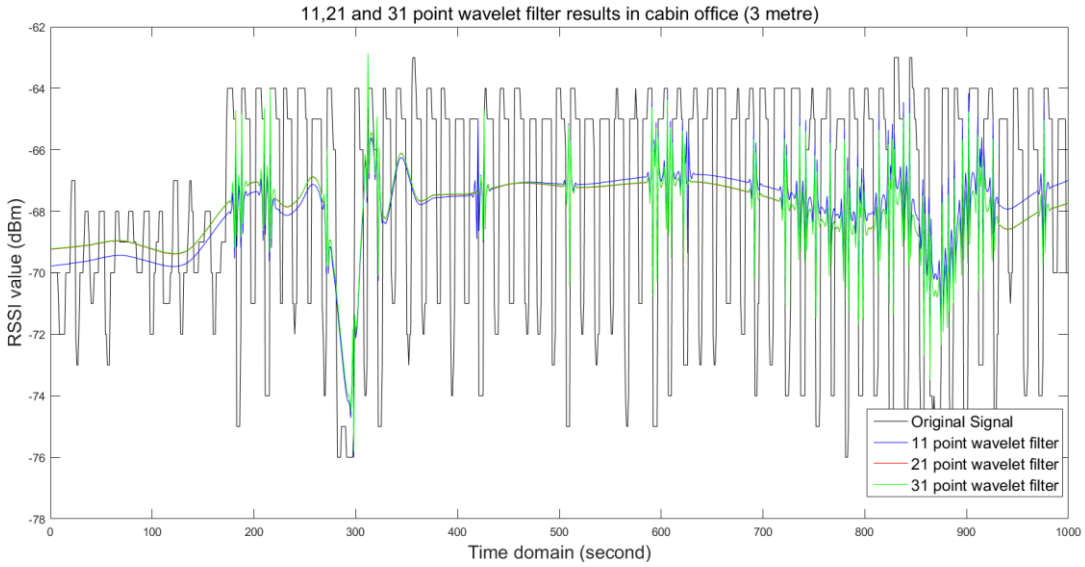

Figure 4. 10 11, 21, and 31 point wavelet filter results of RSSI sequence at three distance under in cabin office

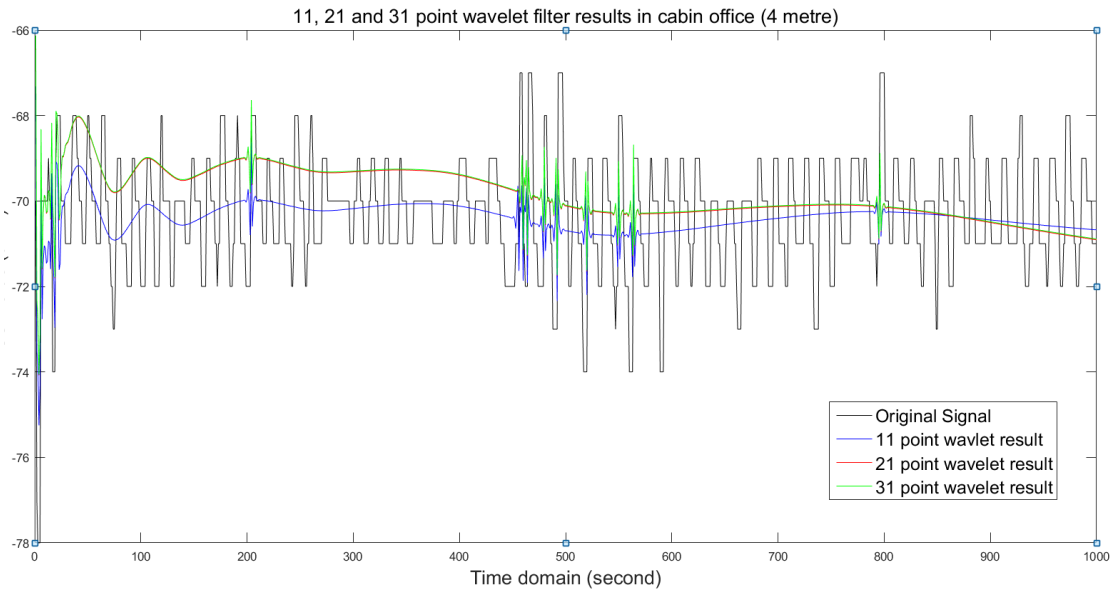

Figure 4. 11 11, 21, and 31 point wavelet filter results of RSSI sequence at four metre distance in cabin office

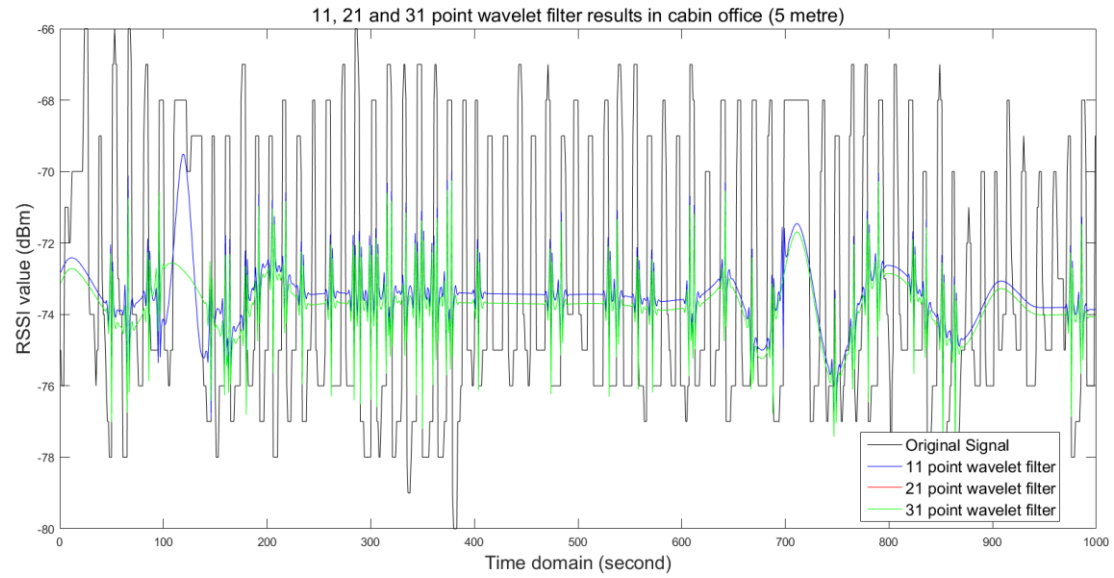

Figure 4. 12 11, 21, and 31 point wavelet filter results of RSSI sequence at five metre distance in cabin office

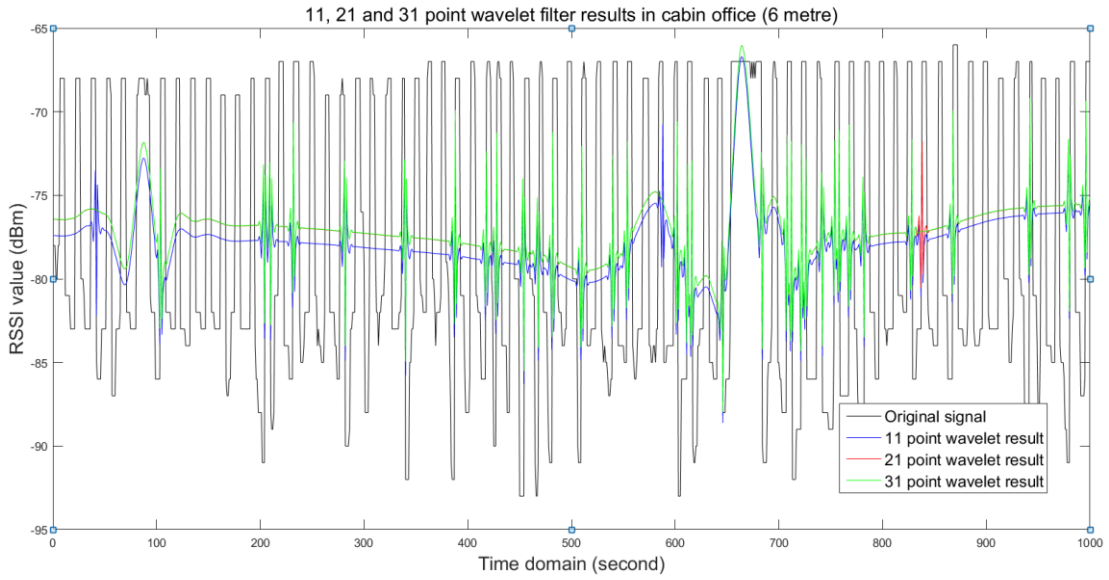

Figure 4. 13 11, 21, and 31 point wavelet filter results of RSSI sequence at six metre distance in cabin office

Table 4. 1 Average value of 11, 21 and 31 point wavelet filter results in cabin office

	Original signal	11 point	21 point	31 point
3 metre	-67.90	-67.93	-68.01	-68.00
4 metre	-70.34	-70.38	-69.84	-96.82
5 metre	-73.16	-73.47	-73.73	-73.73
6 metre	-78.33	-77.82	-77.09	-77.08

Table 4. 2 Standard deviation of 11, 21 and 31 point wavelet filter results in cabin office

	Original signal	11 point	21 point	31 point
3 metre	3.92	1.46	1.37	1.37
4 metre	1.38	0.45	0.66	0.66
5 metre	3.77	1.06	0.98	0.98
6 metre	8.51	2.46	2.42	2.41

As can be seen from Figure 4.10 to Figure 4.13, only a small amount of change in the average value can be observed. The reason for this is that the wavelet filter removes some of the noise from some soft thresholds. In this case, although the average power of the mother wavelet is zero, a very small fraction of the power is still removed, causing the application of soft and hard thresholds. Furthermore, as can be seen that, most of the volatility has been removed, but a small amount of volatility remains. The undulating shape can be clearly seen as a superposition of Daubechies wavelet at different scales. This shows that conditions such as 'Gibbs Phenomenon' may still occur when using the wavelet filter. Also, the standard deviation of the results of using wavelet filters with different window widths is not particularly significant. Therefore, using a wavelet filter with a narrower window does not obviously reduce the filtering effect. In this case, the use of a narrower window width wavelet filter does not significantly reduce the filtering effect, and can significantly reduce the response time of the system.

Experiment 2

The following test observed the wavelet filter's ability to detect user's motion in a dynamic distance. As with the test in chapter 3, the distance between the BLE beacon and the mobile device is 3-4-5-4-5-6 metre. In order to increase the contrast, 5, 15, and 50-point wavelet filters were used.

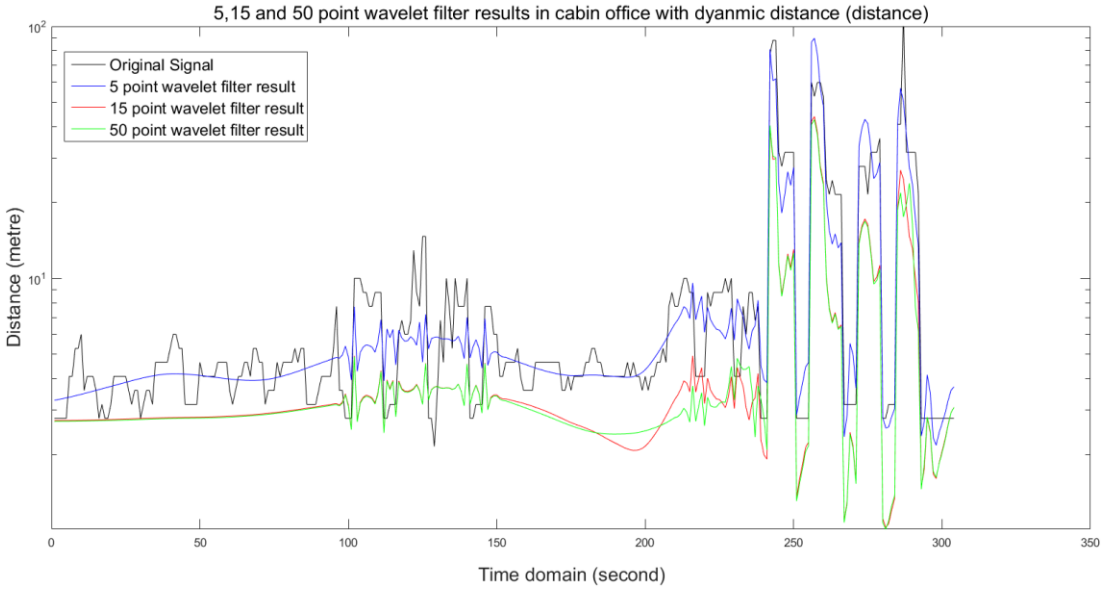

Figure 4. 14 5, 15, and 50 point wavelet filter results of dynamic distance under LOS environment (distance)

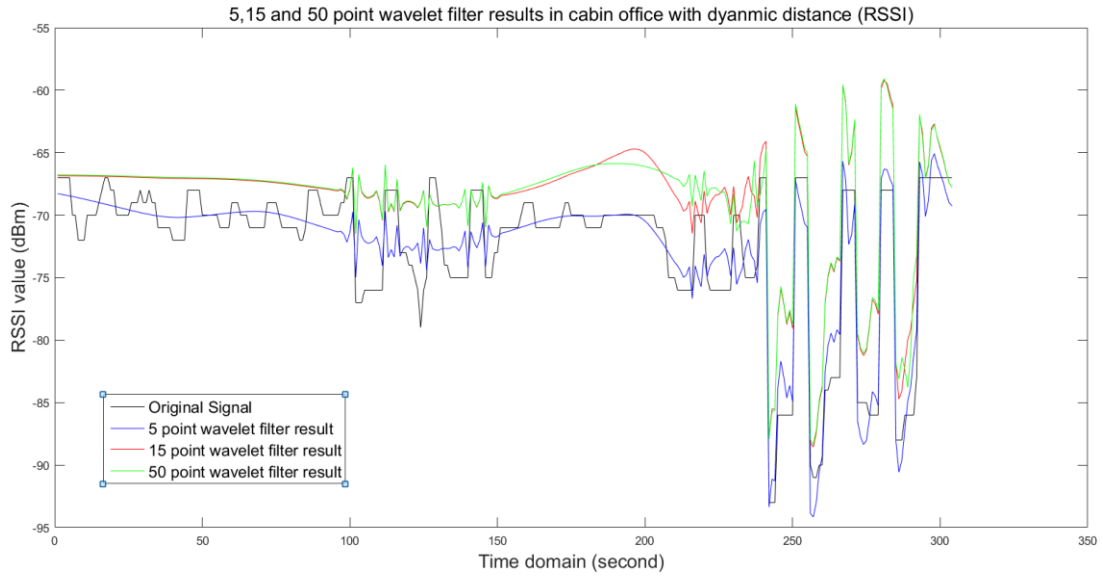

Figure 4. 15 5, 15, and 50 point wavelet filter results of dynamic distance under LOS environment (RSSI)

As can be seen from the figures above, using a narrow-band wavelet filter gives better sensitivity to changes in distance. As shown in Figure 4.14 and Figure 4.15, the 5-point wavelet filter represented by the blue line has a higher sensitivity to change of distance and can significantly distinguish RSSI values corresponding

to different distances. However, the RSSI waveforms processed by the wavelet filter at 15 second and 50 second do not show a good distance change. At the same time, the waveforms of the 15-point and 50-point wavelet filters do not change significantly. Specifically, in other experiments, the results of the 100-point wavelet filter waveform is very similar to the 15 and 50-point wavelet filters. In general, there is no significant difference in de-noising the wavelet filter when the window is longer than 10-points. Moreover, by comparing with the waveforms at 3 and 6 meters, it can be seen that the narrow-band wavelet filter can detect the distance more accurately in the 3-metre area. However, in the 5-metre area, we can see that the original waveform fluctuates violently. The wavelet with a narrow window enlarges the error and the remaining mother waveform leads to a further increase in error. Meanwhile, the wavelet filter using a wider window reduces the fluctuation of the RSSI sequence.

In general, the use of narrow windows gives better sensitivity to changes in distance, while wider window width wavelet filters provide better noise reduction.

Experiment 3

In chapter 3, the smoothing filter was used to process the measured RSSI data in the kings building library environment. This environment can be defined as a complex Non-LOS environment. In contrast, this set of data was also processed by the wavelet filter to detect the wavelet filter's ability to reduce noise in the RSSI sequence in complex environments. Static distances of 3, 4, and 5 metres were handled by wavelets with different window lengths respectively. In the second part of the experiment, wavelet filters with different window lengths were used to reduce noise in the RSSI sequence over a dynamic range.

The figures below show the RSSI sequence and the results of being processed by wavelet filters with 11, 21, and 31-point window widths at a distance of 3, 4, and 5 meters in the library environment.

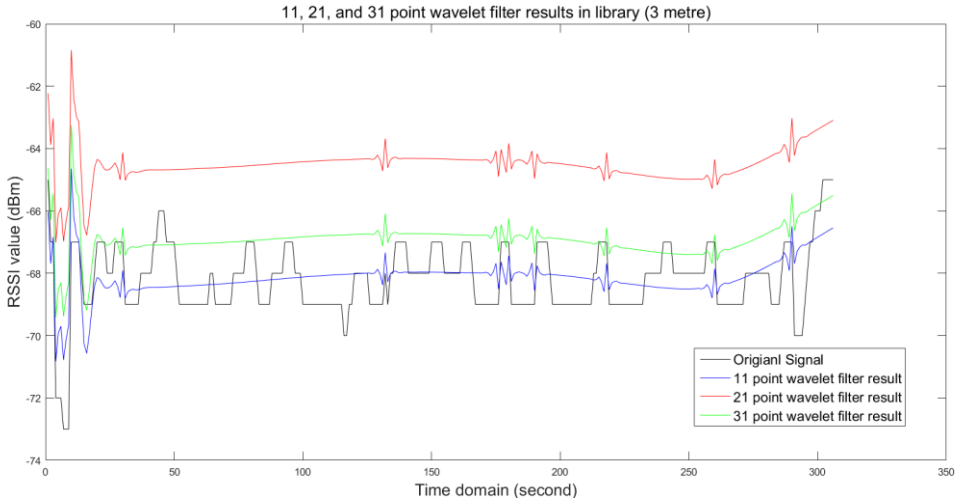

Figure 4. 16 11, 21, and 31 point wavelet filter results of 3 metre RSSI sequence in library

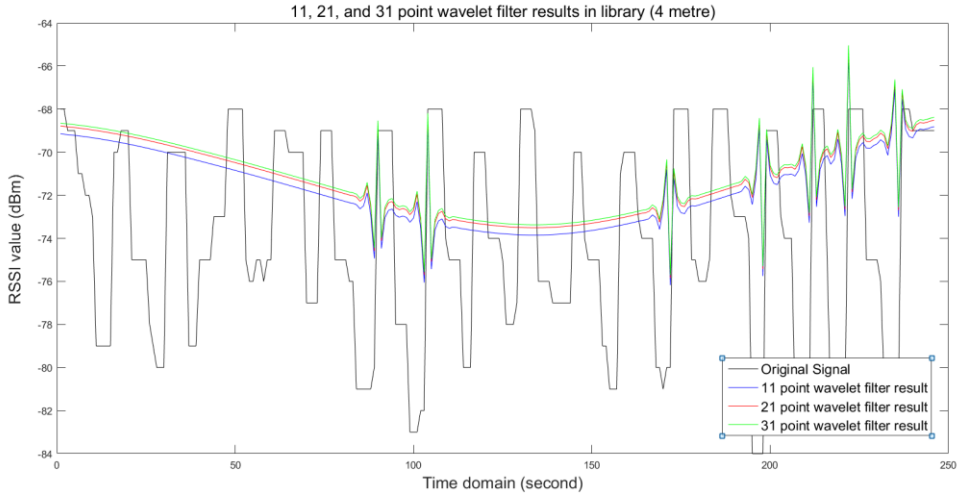

Figure 4. 17 11, 21, and 31 point wavelet filter results of 4 metre RSSI sequence in library

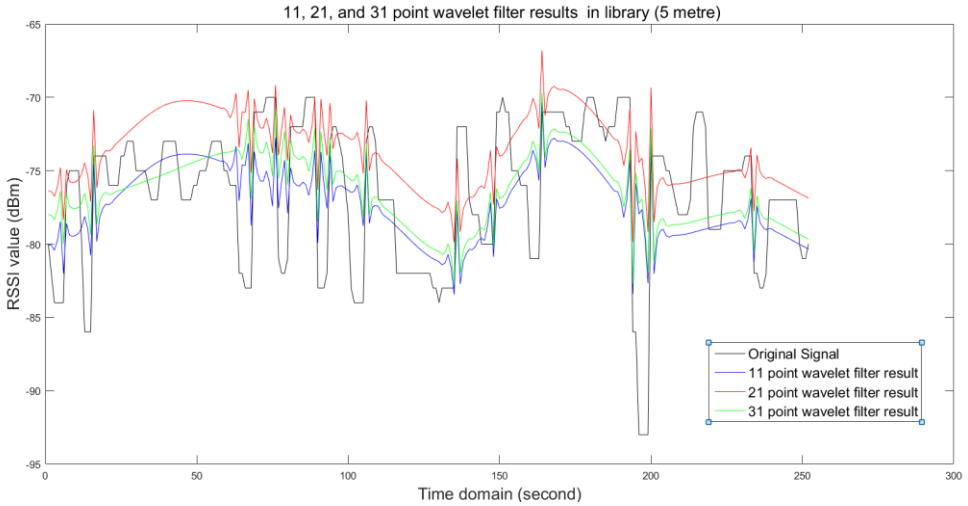

Figure 4. 18 11, 21, and 31 point wavelet filter results of 5 metre RSSI sequence in library

Table 4. 3 Average error of 11, 21 and 31 point wavelet filter results in library

	Original Signal	11 point	21 point	31point
3 metre	-68.21	-68.13	-64.50	-66.91
4 metre	-74.02	-71.66	-71.32	-71.18
5 metre	-76.56	-77.17	-73.60	-76.43

Table 4. 4 Standard deviation of 11, 21 and 31 point wavelet filter results in library

	Original Signal	11 point	21 point	31point
3 metre	1.15	0.60	0.57	0.57
4 metre	4.82	1.81	1.81	1.81
5 metre	4.82	2.56	2.58	2.48

As shown in Figure 4.16, at the time of 3m, the results of the 11, 21, and 31-point wavelet filters do have some differ but not greatly. An average value of 2dBm

difference can be observed between each filters, at the same time, the standard deviations were 0.6, 0.57, and 0.57 (the standard deviation in the original data was 1.6), showing a better de-noising effect. At 5 metres, it can be seen that the RSSI sequence measured over 250 m at time 180 and time 195 due to violent fluctuations in the environment. By using wavelet filters, fluctuation and interference are greatly reduced. In general, in a complex environment, the use of wavelet filters can significantly reduce the fierce interference caused by small scale fading, thereby improving positioning accuracy and system stability.

Experiment 4

The figures that follow show the result of a process in which the distance varies from 3 to 5 metres in the library environment. In contrast, wavelet filters at 5, 15, and 50 points are used for comparison.

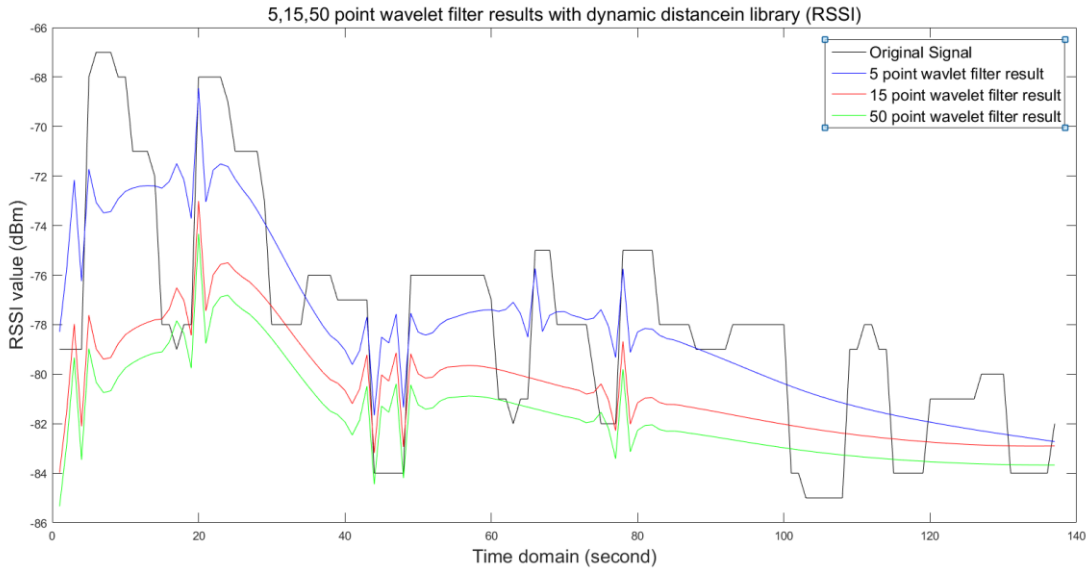

Figure 4. 19 5, 15, and 50 point wavelet filter results of dynamic distance in library (RSSI)

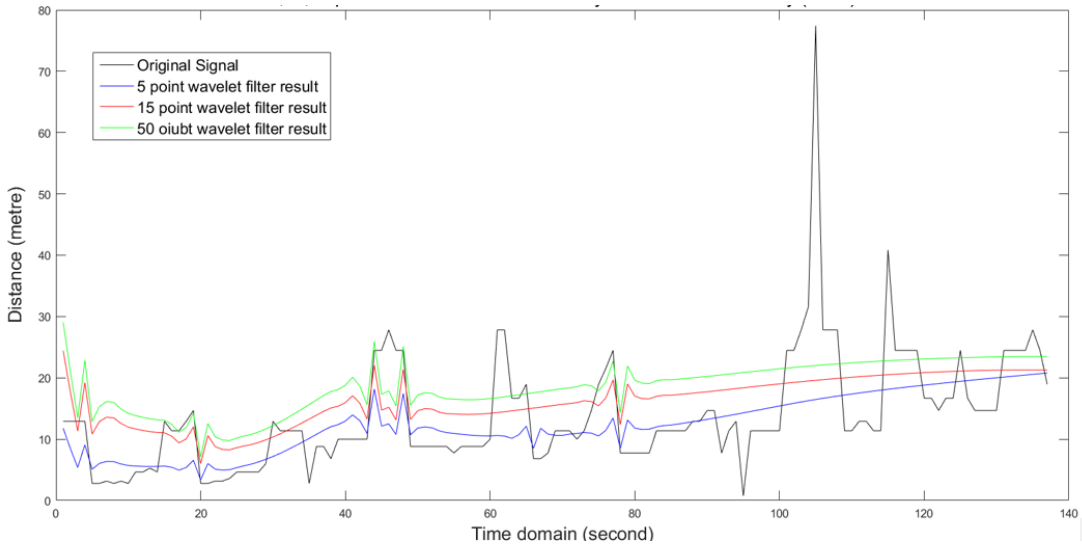

Figure 4. 20 5, 15, and 50 point wavelet filter results of dynamic distance in library (Distance)

As can be seen from the figures, the blue line, which is the 5-point wavelet filter result, shows extremely good performance in the area of detecting the user's motion and distance change. The wavelet filter result cannot clearly distinguish the distance change. When comparing the performance of the 15-point and 50-point results, one can see that their average value and standard deviation do not differ greatly. Furthermore, the overall trend of the waveforms is also highly similar, which proves that the result of wider windows is not significantly different in both Non-LOS and LOS environments. Considering this research, the aim of the proposed systems is to establish an indoor positioning system that can provide a positioning error of not more than 5 metres in a complex Non-LOS environment (because the maximum detected distance is 10 metre if the RSS is -59dBm at 1 metre distance). Under these conditions, the response time of the system should not be too long, and the system should have appropriate sensitivity to distance and location changes, so the window width should not be higher than 11 in general.

Experiment 5

Finally, the data of the dynamic range collected in the kings building library were processed and compared using a smoothing filter of 2 orders of 15 points and an 8-point wavelet filter respectively. The results are shown in Figure 4.21 and Figure 4.22 below:

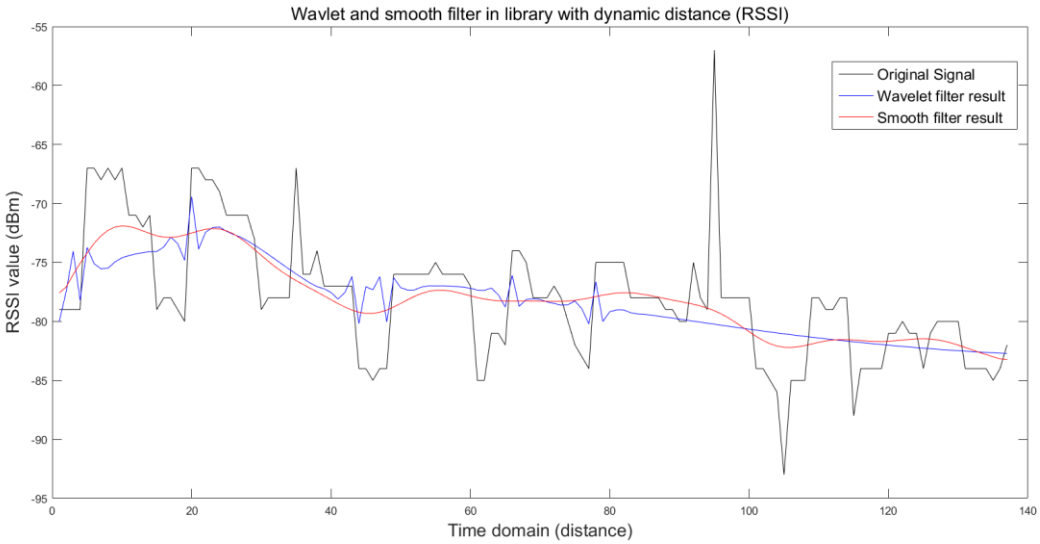

Figure 4. 21 Different filters results in library with dynamic distance (RSSI)

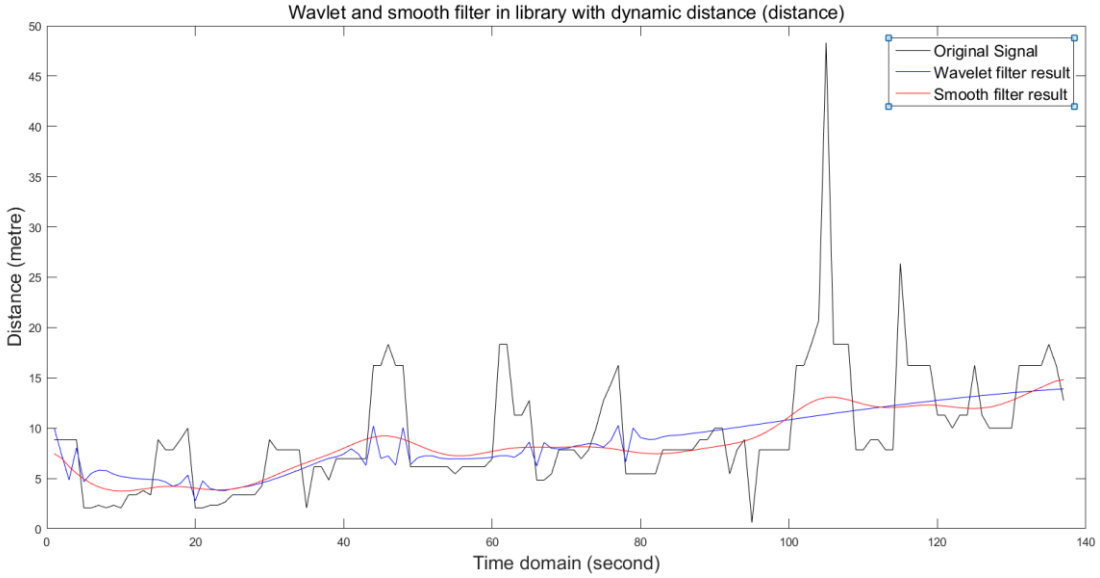

Figure 4. 22 Different filters results in library with dynamic distance (distance)

As can be seen from the figures, both wavelet and smoothing filters can reduce the error caused by the noise of small scale fading, thereby increasing system stability and positioning accuracy. In comparison, the wavelet filter is more sensitive to the fluctuations of the RSSI at a relatively close distance, whereas the smoothing filter performs more evenly both at short distances and at long distances. Moreover, neither the smoothing filter nor the wavelet filter can completely remove errors due to the additional attenuation caused by a complex environment. In a complex environment, a distance of 5 metres produces an instantaneous error of 100 metres or more without filter processing. But by using the filter, this error can be reduced to about 10 metres. The above error can be further reduced by adjusting the filter coefficients, but this will result in the positioning system being unable to detect the change of distance sensitively.

4.5 Conclusion

In this chapter, the basic principles of wavelets were introduced. Before introducing the wavelet filter, the principles of the Fourier filter as well as its advantages and disadvantages were first introduced. The Fourier filter is a filter based on frequency domain decomposition of signal processing. The principle involves the use of sin and cos waves of the signal frequency decomposition, followed by removal of the noise frequency range, to achieve the signal de-noising. The principles of the wavelet filter and the Fourier filter are similar; they both decompose the signals using different bases and perform noise reduction processing. The biggest problem with Fourier filters is their inability to achieve double high resolution in the frequency and time domains simultaneously. Wavelet filters are different in this regard. The wavelet's base is an aperiodic function.

Relatively speaking, Fourier's fundamental and its wave are both periodic functions. By using different scales, the wavelet can use different size window functions for different frequency intervals, so that the wavelet can obtain high resolution in the time domain and the frequency domain simultaneously for different frequency ranges. Furthermore, the Gibbs phenomenon is drastically reduced because the base of the wavelet is a non-periodic function. Wavelet filters have different shapes of mother wavelet. In this research, Daubechies wavelet is used as mother wavelet for the wavelet filter. In the experimental section, wavelet filters with different window widths were used to perform noise reduction on the RSSI sequence. The sets of filters de-noising the dynamic and static data collected in the small cabin and library environments respectively, are the same set of data as that collected in the third chapter. The aim of using the same data is to compare the performance gap between the two filters, which includes stability and accuracy. Finally, after many comparisons, an 8-point wavelet filter is selected for noise reduction of the RSSI sequence. This filter, and the 15-point, 2-stage smoothing filter were also used to process a set of complex, dynamic distance data in the environments. The results show that both wavelet and smoothing filters can significantly reduce the error due to small scale fading; the error can be reduced from 100 meters to 9 meters in the case of poor signal quality. However, neither the wavelet nor smoothing filters can completely remove the error caused by signal attenuation due to environmental interference. Therefore, this situation needs to be fully considered when designing the localization algorithm.

Chapter 5 : Offset Centroid Core Based Positioning Algorithm Combining with a Weighted Framework

5.1 Introduction

In this chapter, the basic trilateration positioning algorithm is introduced firstly, including its advantages and disadvantages. Afterwards, the proposed offset centroid core based positioning algorithm is demonstrated combining with a tailor-made weighted framework. In order to decrease the complexity of the proposed system, fitting formula of the weighted framework is utilized. Finally, a sets of experimental results under different indoor environments are exhibited in order to test the performance of the proposed system.

In the area of geometry, trilateration can be defined as the process of computing absolute or relative positions of points by measurement of distances by applying the geometry of circles, spheres or triangles [79]. Recently, trilateration has actual utilization in surveying and navigation, including global positioning systems, cellular based network positioning and indoor positioning. Compared with triangulation, trilateration does not require the measurement of angles.

Theory of Trilateration Positioning algorithm

In a 2-D environment, it is a common known method that if three BLE beacons are not deployed in one line, the user position will be located in the common point

of the three circles which are generated by the RSSI signal. An example of trilateration is shown below:

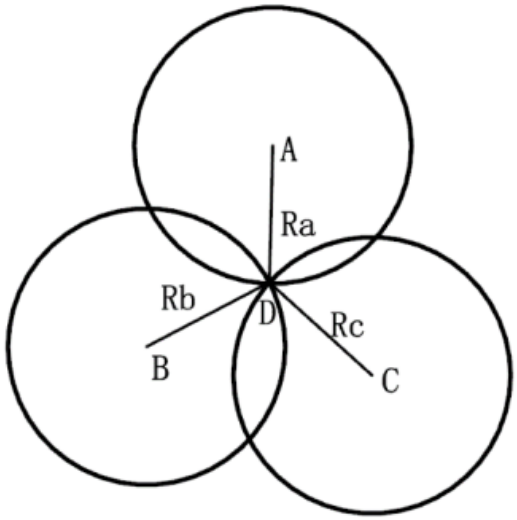

Figure 5. 1 Trilateration algorithm under ideal LOS environment

As shown in Figure 5.1, A, B, and C are the APs with the location A(x_1,y_1), B(x_2,y_2), and C(x_3,y_3). If the unknown coordinate D is D(x,y), the position of node D can be calculated by using the position of the nodes A, B, and C and the calculated distance R_a, R_b, and R_c. The algorithm to calculate the distance between the unknown anchor node D and the known anchor nodes Ra, R_b and R_c is shown in the RSSI algorithm.

The equations used to compute R_a, R_b, and R_c are shown below.

Where:

$$R^2_{(a,b,c)} = \left(x - x_{(1,2,3)}\right)^2 + \left(y - y_{(1,2,3)}\right)^2 \quad (5.1)$$

In a real environment, because of reflection and other factors, the distance calculated by the RSSI algorithm is inaccurate. The calculated result will be larger than the actual distance. As a result, the three circles A, B, and C will not cross at

one point, which should be the node D in Figure 5.1. As shown in Figure 5.2, three common points E, F, and G between each of two circles will instead show the unknown anchor node D.

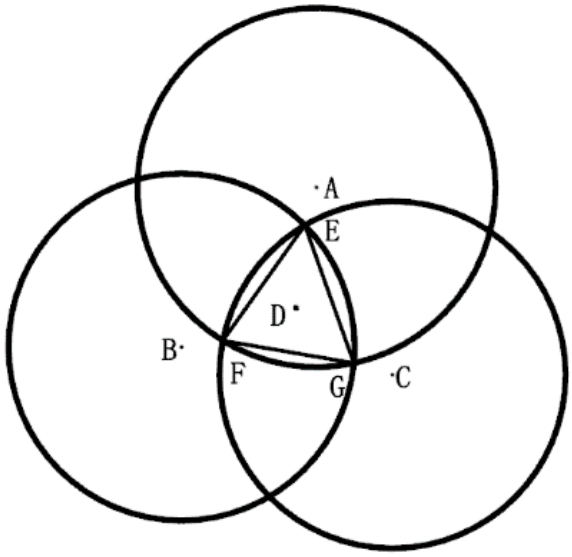

Figure 5. 2 Trilateration algorithm under real environment

In such a case, the centroid core of the triangle composed by the three common points E, F, and G is applied as a solution to instead determine the position of the unknown anchor node D. In fact, with the decrease of interference on the RSSI signal, node E, F, and G will eventually coincide on the node D. Assuming that the location of the common points are E(x_4,y_4), F(x_5,y_5), and G(x_6,y_6), the position of D(x,y) is derived by the following equations:

$$\begin{cases} x = \frac{x_4+x_5+x_6}{3} \\ y = \frac{y_4+y_5+y_6}{3} \end{cases} \tag{5.2}$$

This algorithm has certain limitations. The user's position will only be calculated when the three circles have crossed points with each other. Two examples of an unexpected situation are shown in Figures 5.3.

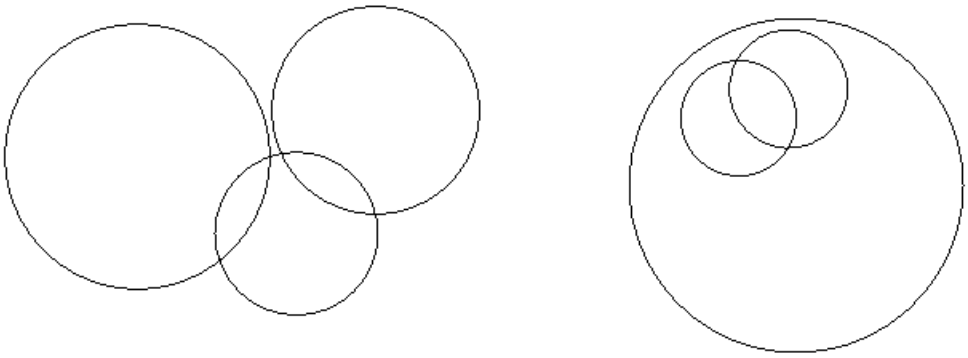

Figure 5. 3 Three circles do not have cross points between each other

In Figures 5.3, one or two circles do not have crossed points with each other. In this case, at least one root of the equation is an imaginary number which will stop the calculation process. In order to solve this problem, the use of algorithms such as the least-square based algorithms [80] has been proposed. However, many additional cases which are not limited in Figures 5.3 must be considered, and creating corresponding sub-algorithms for each unexpected case is difficult. An excessive number of sub-algorithms could not only decrease the compatibility of the algorithms, but may also increase the computation and hardware workload dramatically.

5.2 Offset Centroid Core Based Positioning Algorithm

This research proposes the use of off-set triangulation in order to provide a solution to the problem mentioned above. This algorithm is different from the traditional triangulation algorithm, and the cross point based triangulation principle has been abandoned. Instead of calculating the centroid core coordinate of the triangle generated by the three cross points, the centroid core of the triangle

generated by the three APs which the user position belongs to is used as a datum point. The user's specific position is calculated by achieving the offset to the datum point and the offset margin according to the distance ratio between the user's position and each AP. As long as three Bluetooth signals have been received by the mobile device and the three APs were not deployed in one line, this algorithm can be employed no matter whether the result is accurate or not. In this case, if the triangle consisting of APs which the user position belongs to can be determined accurately, the localisation error will normally be no larger than half of the distance between two beacons.

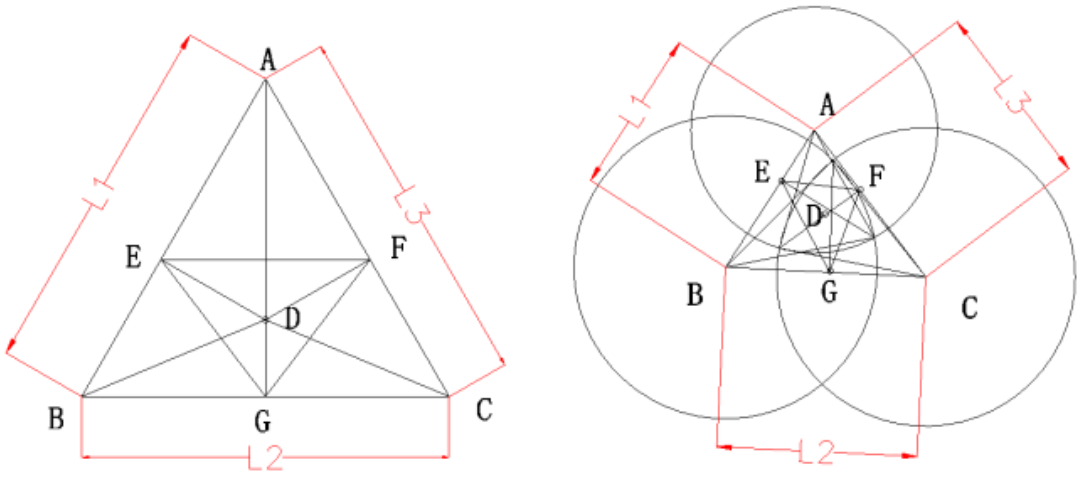

Figure 5. 4 Off-set triangulation algorithm under ideal (left) and real (right) environment

According to Figure 5.4, three APs named A, B, and C were deployed on the map in a triangular formation with measured coordinates. The user's mobile device was located within the triangle. The reference distance between the mobile device and each AP (L1, L2, and L3) were calculated according to equation 4. Next, three reference points – E, F, and G - were calculated by applying the distance ratios

L1/L2, L2/L3, and L3/L1. The centroid core of the triangle EFG will then become the coordinates of the mobile device.

5.3 Weight Framework

In the previous section, an off-set triangulation algorithm has been proposed to compute the user's position. Specifically, the key idea of this algorithm is to calculate the user's coordinates by applying a triangle consisting of three BLE beacons. Three off-set vectors are generated to fix the X and Y coordinates of the centroid core of the triangle generated by the three beacons.

In real environmental conditions, users may normally receive amount of RSSI values from more than three BLE beacons. In such an event, providing an effective system to choose the best beacon with the most accurate location information could increase the localization accuracy dramatically; meanwhile, an appropriate triangle with suitable size and reasonable length sides could also increase the average localisation accuracy and stability of the localisation system.

In this section, a weighted framework is applied to make a selection of the best signal provider and best BLE beacon group (3 Beacon comprising a group). This weighted framework consists of three key parameters: *Wa*, *Wr*, and *Wq*. A specific explanation of these parameters is given below.

5.3.1 Absolute Weight (Wa)

Absolute Weight (Wa) is applied to compute the reliability of the RSSI value from each beacon. In Chapter 3, equation 3.11 figured out the relationship between RSSI and distance. Similarly, the negative effects caused by fading and multipath

have been discussed. In this section, the method of the weight evaluation of each beacon in different cases will be given, which includes LOS and Non-LOS indoor conditions.

As discussed in chapter 3, the distance between users' position and the BLE beacon is computed according to the path loss model. Ideally, the received signal strength should keep stable if users' actions are motionless. However, the interference caused by fading and multipath produces a fluctuated RSSI signal sequence. By considering that normally more than three RSSI signal sequences from different beacons are received at the same time, selecting the best signal provider could increase the localisation accuracy dramatically.

In this section, Wa is applied to provide this function mentioned above, where a is absolute. For Wa, we decompose the problem of computing it into two conditions:

1 the RSSI signal strength is strong or weak;

2 the transmission channel is LOS or non-LOS.

With the assumption that there are two BLE beacons deployed in room 1, which are Beacon A and Beacon B, and another pair of BLE beacons deployed in room 2, the layout is shown in Figure 5.5 below:

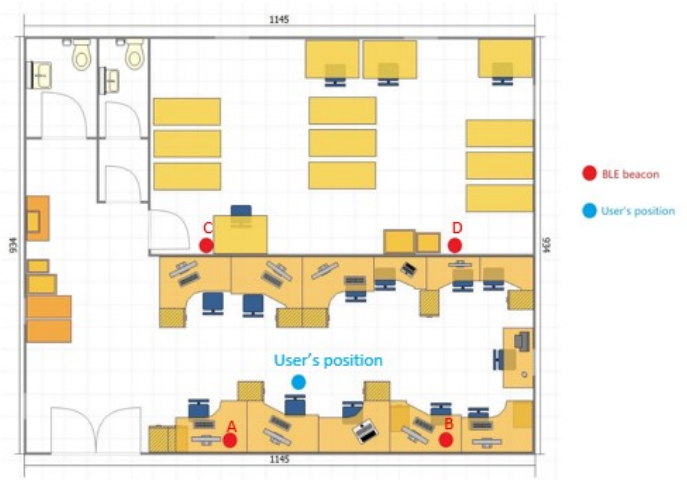

Figure 5. 5 Example of indoor testing under LOS environment

In Figure 5.5, the user is located at the blue point. As can be seen, two BLE beacons are deployed in the same room as the user while two beacons are deployed in the next room. Assuming that the transmission channel in each room is a LOS environment, specifically, that the distance between the user and BLE beacon A is 2.5 metres, and for beacon B is 3.5 metres, for beacon C is 4 metres, and beacon D is 5 metres. In this condition, beacon A is the nearest beacon with the strongest RSSI value. Therefore, beacon A will be given as the highest weight value, which is dependent on the specific RSSI value. As a result, beacon A will be given the highest weight, beacon B is the second highest, C is the third highest, and beacon D will be given the lowest weight value.

Meanwhile, if BLE beacons are settled in the same room as the user, the reliability of this beacon is also higher than the ones deployed in a different room. Thus, a special ID is given to each beacon to justify whether the beacon is located in the same room as the user. Specifically, the same ID will be given to these beacons which are deployed in the same room. When the signal strength of beacon A is received, which is the strongest one presently, other beacons with the same ID of

beacon A will be identified by the receiver. The beacon with the same ID as the strongest signal provider will be evaluated with a high weighting coefficient, while beacons with a different ID will be evaluated with a lower weighting coefficient.

According to the experimental results, when distance between user and BLE beacon was less than 3 metre, the RSSI value could figure out the distance information accurately. Meanwhile when distance is larger than 6 metre, the relationship between RSSI and distance was not as clear as 1-3 metre. In addition, when distance was larger than 8 metre, the RSSI value cannot be received. As a result, the Wa was classified to three stages: 1-3 metre. 4-5 metre and 6-7 metre.

Also, when the transmit path was Non-LOS environment, the RSSI value cannot be received when distance was larger than 5 metre. In the meantime, distance information provided by RSSI under Non-LOS environment was not as reliable as LOS environment. By considering the stability of the proposed system, the impact factor of Non-LOS signal provider should be lower than the one under LOS environment because the Non-LOS one is not ‘reliable’. In this proposed system, the weight value of those Non-LOS signal provider is half of LOS signal provider.

5.3.2 Relative Weight (Wr)

Under the discussed conditions, three beacons namely A,B and C are selected as a group of signal providers and a triangle generated. As discussed above, the valid localisation region is the interior of the triangle ABC. For a triangle with a certain perimeter, the area of this triangle has a direct relationship with the quality of this triangle in positioning. In geometry, it is easy to prove that, if the length of a triangle is certain, then an equilateral triangle has the largest area. The detail of

this proof is easy to achieve and will not be discussed in this thesis. If we assume, L_A, L_B and L_C are the length of side for triangle ABC, and L is equal to the total length L, we have the following equation:

$$L_A + L_B + L_C = L \tag{5.3}$$

If we normalize L to L, the equation can be:

$$K * (L_A + L_B + L_C) = 1 \tag{5.4}$$

Where:

K is the normalizing factor, which is equal to 1/ L.

According to the Helen theorem, the area of a triangle can be derived by the following equation:

$$S^2 = 0.5 * L * (0.5 * L - L_A) * (0.5 * L - L_B) * (0.5 * L - L_C) \tag{5.5}$$

Where:

S is the area of triangle.

Assume that:

$$\{L'_{A,B,C}\} = K * \{L_{A,B,C}\} \tag{5.6}$$

Let:

$$L'_A + L'_B + L'_C = 1 \tag{5.7}$$

If the triangle A'B'C' is an equilateral triangle, the area of the triangle is:

$$S^2 = 0.5 * (0.5 - 0.33)^3 = 0.048 \tag{5.8}$$

According to the calculated result, the maximum area of a normalised triangle is 0.048. Similarly, the area of an equilateral right triangle is 0.042. According to the beacon deployment problem, the minimum appropriate triangle area is 0.036,

which means a triangle with an area lower than 0.036 after normalisation will be considered to be selected in general.

5.3.3 Quality of Triangle (Wq)

When many signals (more than three) are received from different APs, multiple triangles will be produced. Applying good-quality triangles as optimal solutions will increase the localisation accuracy dramatically. Wq in this weighted framework is used in these circumstances to compute the quality of the triangle by considering the overall length of the side of a triangle.

According to the experimental results, in an indoor area, the valid transmission distance for BLE and mobile devices is normally 8 metres. We assume that three beacons' signals are received by the mobile device, namely A, B, and C, and the shape of the triangle ABC is equilateral. Under this assumption, the maximum length of the triangle ABC should not be larger than 7m.

By considering the interference under real environmental conditions, a triangle length of 6.5 metres could be a valid choice, which means a triangle with an overall length which is larger than 19.5 metres will not be selected in general. In addition, an irregular triangle may cause a larger transmission distance. In such a situation, the overall length should be decreased. The final value for the overall length in general should be 18 meter.

5.4 Implementation

Three key parameters which are Wa, Wr and Wq were introduced in the previous session. As the target device for this algorithm is a mobile device, the computation and complexity of this algorithm needs to be considered. In addition, power consumption is also a key factor. A complex system will increase the power consumption dramatically and decrease the cruising ability of mobile devices. In this instance, a fitting formula could be utilised to decrease the logical judgement and reduce the computation.

Wa

The relationship between signal strength and distance is shown in with the following table:

Table 5. 1 Wa under LOS and Non-LOS environment

	Weight value under LOS environment	Weight value under Non-LOS environment
1 metre	8	4
2 metre	6	3
3 metre	5	2.5
4 metre	4	2
5 metre	3	N/A
6 metre	1	N/A
7 metre	0.5	N/A

As seen in Table 5.1, the weight value for the non-LOS signal is half of the signal under LOS conditions. 1 and 2 metre distances are given additional weight values which are 8 and 6.5 under LOS conditions, while the weight for 6 and 7 metre distances is 1 and 0.5. In this model, the beacon with strong signal strength will be given a higher priority to be selected for calculating the user's position.

The relationship of weight value and distance is shown in Figure 5.6:

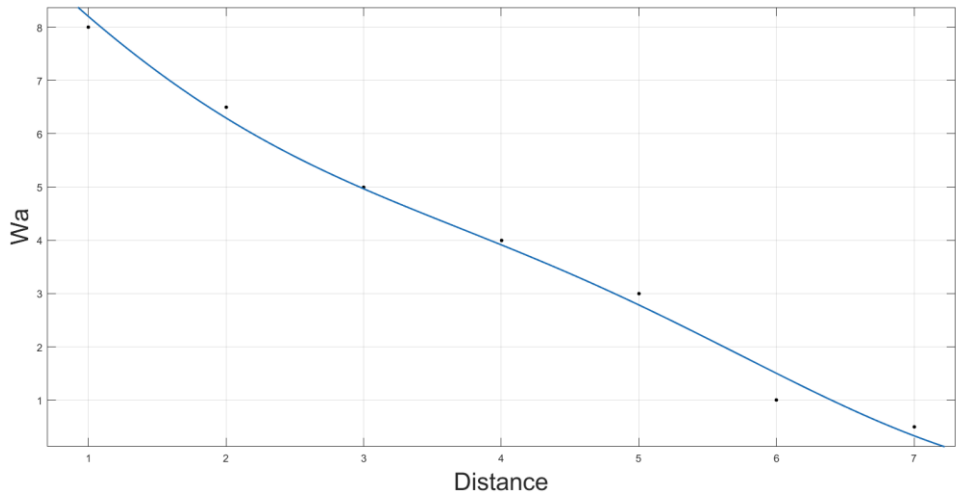

Figure 5. 6 Fitting formula of Wa under LOS environment

Where:

In this situation, the linear model is applied to fitting the formula. The equation is shown below:

$$W_a = a * [\sin(distance - \pi)] + a * [(distance - 10)^2] + c \quad (5.9)$$

Where:

The coefficients of a, b and c are (with 95% confidence bounds):

a = 0.4265 (-0.1302, 0.9832)

b = 0.1105 (0.0942, 0.1267)

c = -0.3847 (-1.1, 0.3301)

The Sum squared error (SSE) is 0.4179 and adjusted R-square: 0.9862.

Wr

When three BLE beacons are selected, a triangle will be produced by the selected BLE beacons if they are not deployed in one line. Afterwards the centroid of this triangle will be calculated as a reference point and this point will be applied to calculate the user position.

Wr is controlled by the following conditions: the shape of the triangle. It is easy to prove that equilateral triangles provide the best computing environment. By applying Helen theory, the area of the triangle can be calculated according to the perimeter and length of the three sides, which is the equation 5.5. If we assume that, in equation 5.5: L_A=L_B=L_C=0.3333 metre (L_A+L_B+L_c=L_C metre). The S of the triangle is then equal to 0.048 m^2.

As introduced in previous section, a normalisation factor is applied to normalise the length of side L_A,L_B and L_C to allow the normalised perimeter to be equal to 1.

In this case, the performance WR can be calculated: 0.048 is the maximum area and the weight of this triangle is set to 1. The area of an isosceles right triangle is 0.042 and the weight of it is set to 0.8. When the area of a triangle is less than 0.036, this triangle will not be suggested to be applied to provide the users' location. The diagram below shows the relationship between the normalised area and the weight value:

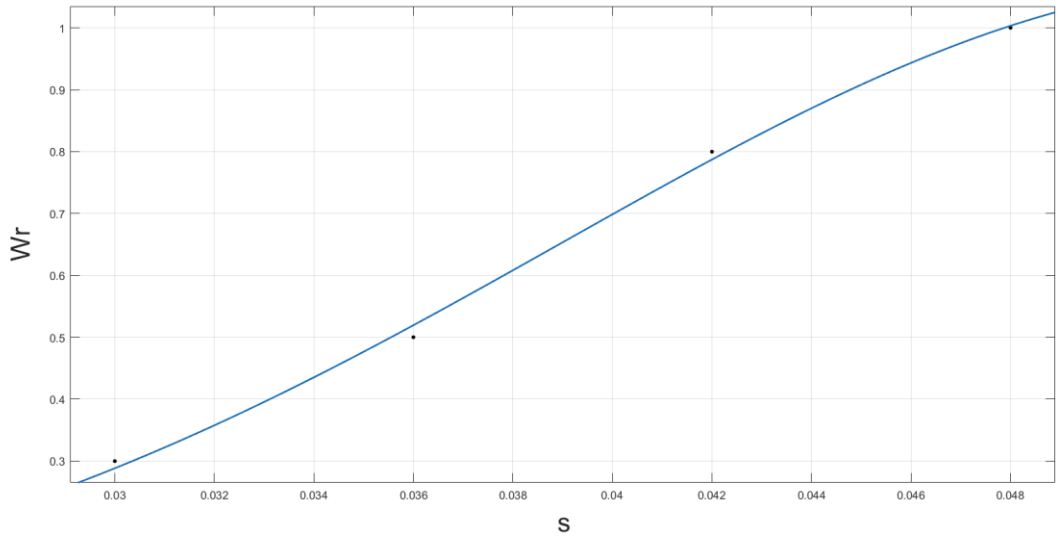

Figure 5. 7 Fitting formula of Wr

Where:

s is the area of the triangle.

For W_r, an exponential model is applied for fitting formula:

$$W_r = a_1 * e^{\left\{-\left[\frac{(S-b_1)}{c_1}\right]^2\right\}} \tag{5.10}$$

Where: a_1, b_1, and c_1, Coefficients are (with 95% confidence bounds):

a_1 = 1.077 (-0.1233, 2.277)

b_1 = 0.05342 (0.009123, 0.09771)

c_1 = 0.0204 (-0.01566, 0.05646)

For the fitting formula error:

SSE: 0.0006905

R-square: 0.9976

Wq

Wq in this weighted framework is used in these circumstances to integrate these signal providers together and increase the influence of APs with high-quality signals. Specifically, inside a selected triangle, the distance between each two beacons plays a major role on justifying the value of Wq. According to the experimental result, the distance between beacons and mobile devices should normally be no more than 7 metres (as fading and multi-path will increase the error dramatically), the distance between each pair of two beacons should be no larger than 8 metres (on average). Thus, the L of the triangle should be no larger than 24 metres. As a key parameter, Wq is also a multiplicative factor (from 0 to 1). The relationship between weight value and the perimeter is shown in Figure 5.8:

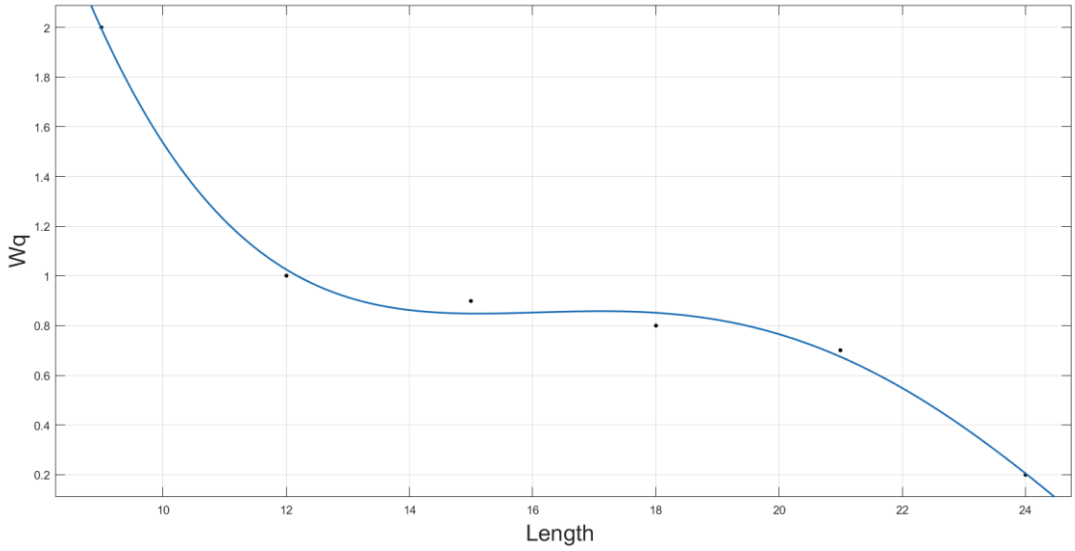

Figure 5. 8 Fitting formula of Wq

Where:

W_q is the weight value and $length$ is the perimeter of the triangle.

For W_q, Fourier model is applied for fitting formula:

$$W_q = a_0' + a_1' * \cos(length * \omega) + b_1' * \sin(length * \omega) + a_2' * \cos(length * 2\omega) + b_2' * \cos(length * 2\omega) \quad (5.11)$$

Coefficients:

a_0' = 2.142e+08

a_1' = -2.855e+08

b_1' = -8.197e+06

a_2' = 7.13e+07

b_2' = 4.097e+06

ω = 0.001378

The error of fitting formula is:

SSE: 0.006707

R-square: 0.9962

5.4.1 Implementation of Weighted framework

As introduced, the Wa is a based weight model and Wr and Wq are multiplicative factors. The final equation for computing the weight value of a selected triangle is:

$$W_{overall} = \sum x_{a,b,c} * W_r * W_q$$

$$= \left(\sum a * sin\left(Distance_{a,b,c} - \pi\right)\right) + b * \left[\left(Distance_{a,b,c} - 10\right)^2 + c\right] * a_1 * e^{\left\{-\left[\frac{(S-b_1)}{c_1}\right]^2\right\}} * [a_0' + a_1' * cos(length * \omega) + b_1' * sin(length * \omega) + a_2' * cos(length * 2\omega) + b_2' * cos(length * 2\omega)] \quad (5.12)$$

Where:

$Distance_{a,b,c}$ are the distances between mobile device and respective BLE beacons,

s is the area of the triangle (generated by 3 beacons),

$length$ is the perimeter of the triangle (generated by 3 beacons).

Coefficient:

a = 0.4265 b =0.1105 c =-0.3847

a_1 =1.077 b_1 =0.05342 c_1 =0.0204

a_0' =2.142e+08 a_1' =-2.855e+08 b_1' =-8.197e+06

a_2' =7.13e+07 b_2' =4.097e+06

ω = 0.001378

5.4.2 System Implementation

Initially, all of the BLE beacons are deployed inside a room with a reasonable distance where the average distance between each pair of two beacons should be no larger than 10 metres in the most extreme case. Beacons deployed in the same room will be given the same identification (ID) number to identify the condition of the signal transmission channel in future. The coordinates X and Y are also recorded for user location computation.

At the moment when the BLE signal RSSI is received by mobile device, the BLE beacon with strongest signal strength is selected and this beacon will be set as the reference beacon which means the propagation path of this beacon is in a LOS environment. Thus, the propagation path of the beacons with the same ID as the selected beacon will be recognized as LOS. Following this, all of the received beacons will be randomly grouped, each group comprising three beacons. All of the position results will be computed while the weight value of each triangle is also computed. Those results with a low weight value will not be applied to calculate users' position. The flow chart of this process is shown below:

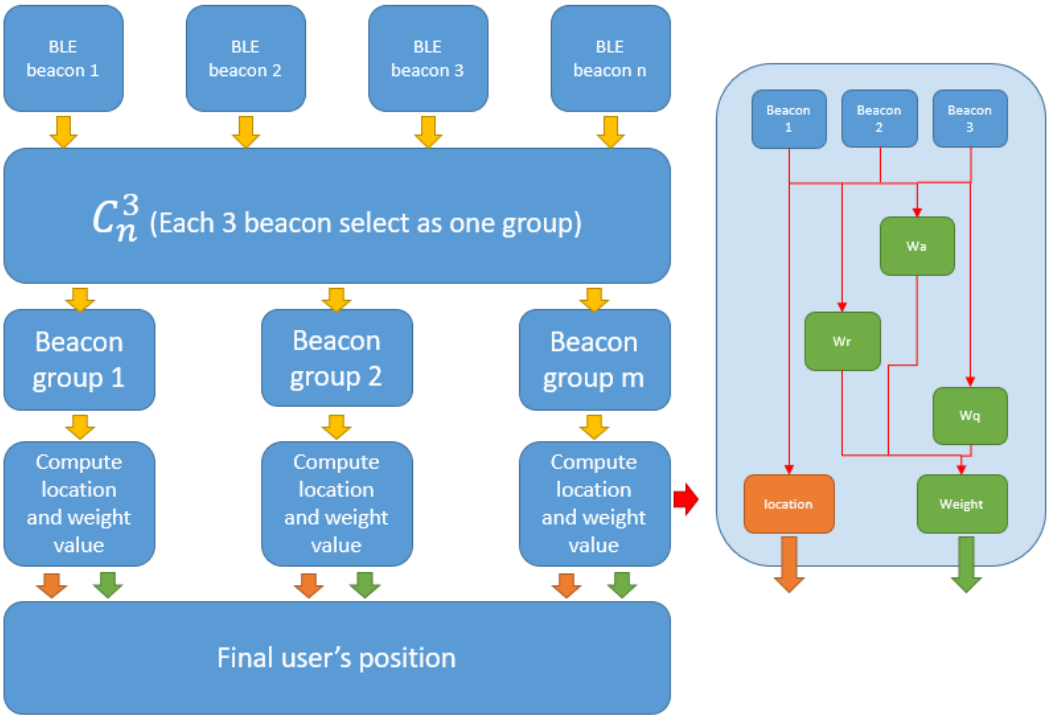

Figure 5. 9 Working progress of the weighted framework

Notice that the beacons with a non-LOS propagation path could also take part in the calculation process with a 50% off weight value. As introduced previously, signal providers with the strongest signal strength may not be the best choice for calculating users' position. This is because these triangles are obtuse triangles, or some of the propagation path of these signal providers is not LOS. By applying this weight framework, the final results of users' positions are measured by multiple beacons. In this situation, the potential of maximal accuracy is decreased however the standard deviation of accuracy is also decreased. As introduced in chapter 2, the desired accuracy is between 1 to 5 metres, which means a centimetre grade maximal accuracy is not necessary in this research.

5.5 Experimental Results

5.5.1 Filter Test Results

In chapter 3 and chapter 4, smoothing filters and wavelet filters were used to reduce inaccurate distance results due to small scale fading. Before using the weight framework for beacon selection, the performance of these filters needed to be tested separately with the offset centroid core algorithm.

The figures below show the results of LOS (data is collected in the cabin office) environments, as well as the result of not using any filter, using the wavelet filter, and using the smoothing filter. The red star point in the middle of figures is the real coordinate of the user. Each blue circle is the result of the algorithm. As can be seen from the figures, the accuracy of positioning is greatly increased, irrespective of using either the wavelet or smoothing filters. As a result of comparison, in Figure 5.10, the RSSI data is not processed by any filter, and the positioning result is uniformly dispersed in the triangle. In other figures, most of the results, whether employing smoothing or wavelet filters, were located around the red star dots. It is worth noting that after a large number of tests, it was found that both wavelet and smoothing filters have similar noise reduction performance in most cases. Therefore, in the following experiments, default RSSI results have been processed by wavelet or smoothing filters. At the same time, the use of two different filters led to a very slight gap that was not considered significant and will not be further discussed or compared.

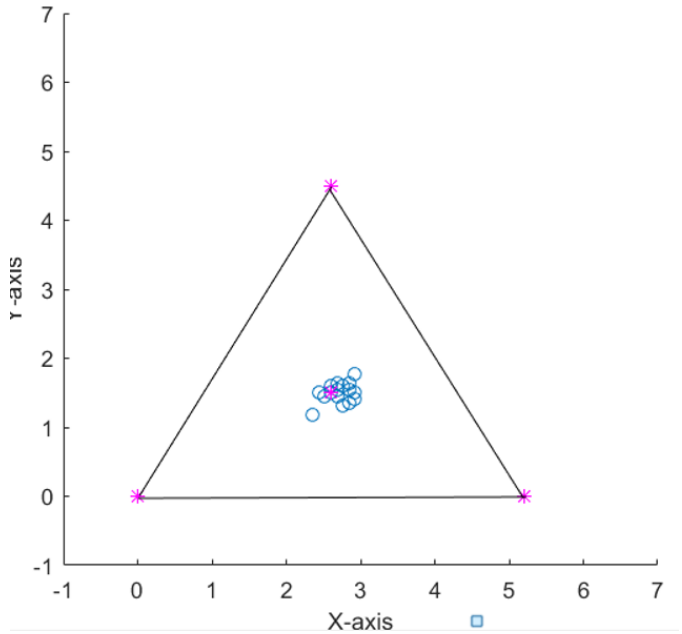

Figure 5. 10 Example of centroid core positioning algorithm (using original RSSI sequence)

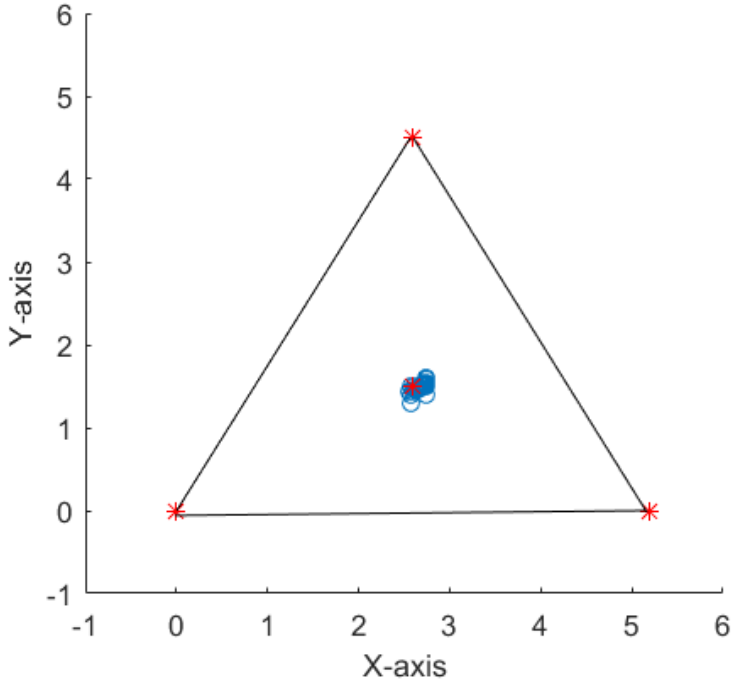

Figure 5. 11 example of centroid core positioning algorithm (processed by smooth filter)

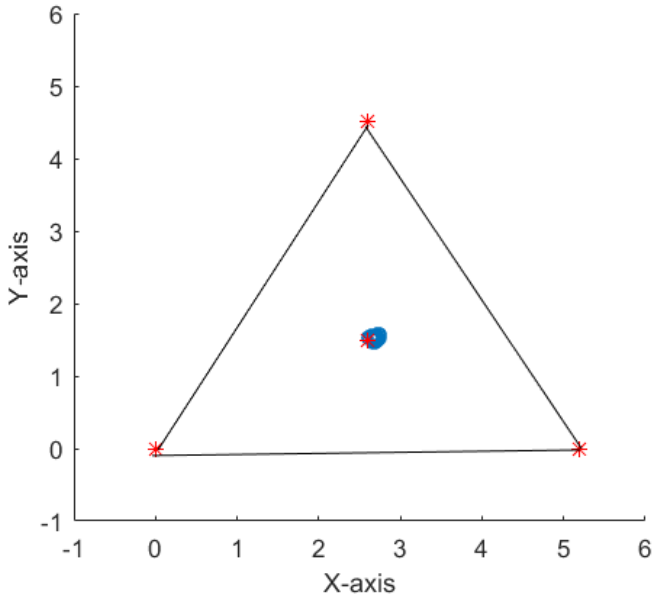

Figure 5. 12 Example of centroid core positioning algorithm (processed by wavelet filter)

5.5.2 Experimental Results of Proposed System under Different Environmental Conditions

In order to test the performance of the proposed system integrally, three different experimental environments were selected. These were: the cabin office belongs to Scottish Microelectronics Centre [81] of University of Edinburgh (a LOS environment), the Kings Building library [82] of University of Edinburgh (a non-LOS environment) and a Sainsbury supermarket located in Carmon toll [83] (a complex non-LOS environment). The detail of these three experiments is shown below:

Experiment 1 in small cabin.

The first experiment was tested in the cabin office. A total of four BLE beacons were deployed in the four corners of the room. The whole environment can be considered a LOS environment. The details of the deployment of BLE beacons are shown in Figure 5.13 below. The main purpose of this experiment is to measure the performance of the system under the BLE deployment density condition of the LOS environment. A total of six test points were measured. The results of the error and standard deviation are shown in Figure 5.14 and Table 5.1 below:

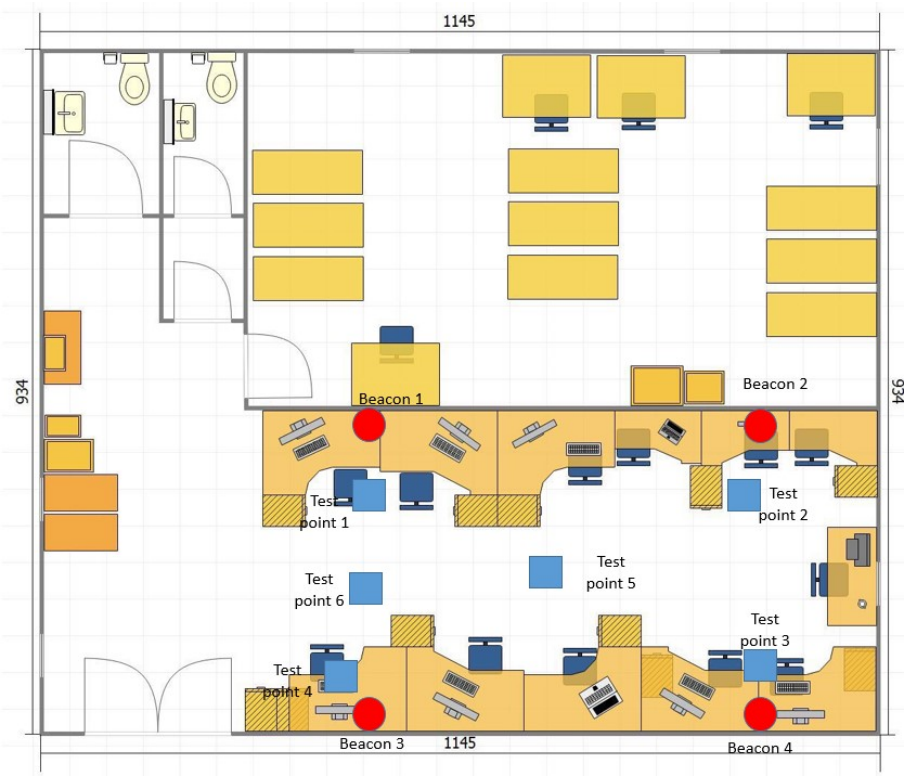

Figure 5. 13 Set up of the experimental environment in cabin office

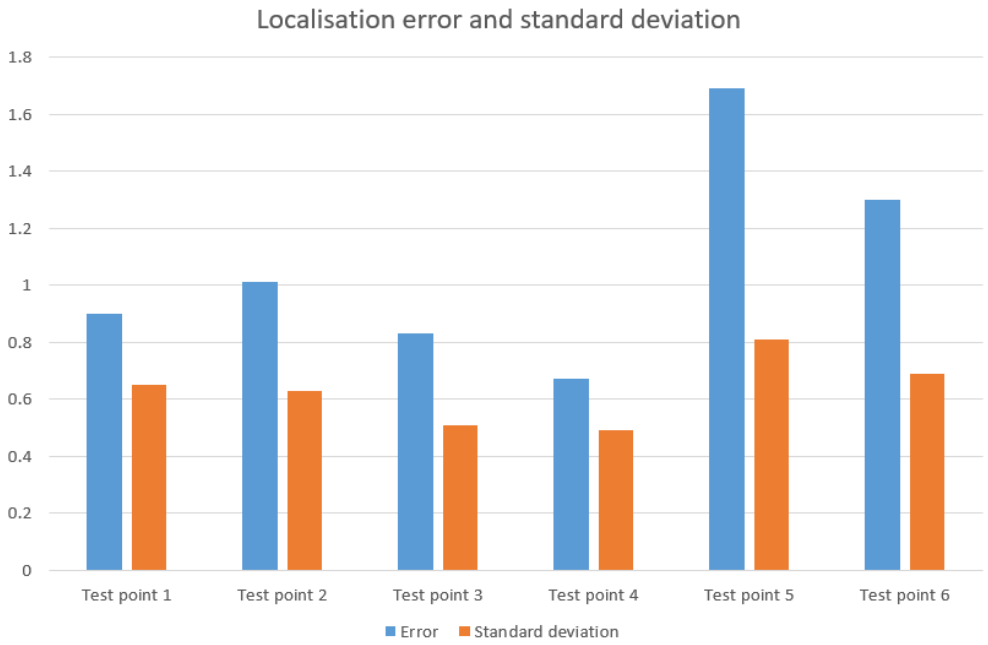

Figure 5. 14 Localisation error and standard deviation of the experimental result in cabin

Table 5. 2 Localisation error and standard deviation of the experimental result in cabin

	Error	Standard deviation
Test point 1	0.9	0.65
Test point 2	1.01	0.63
Test point 3	0.83	0.51
Test point 4	0.67	0.49
Test point 5	1.69	0.81
Test point 6	1.3	0.69

The positioning accuracy at test points 1, 2, 3, and 4 is very high because the user position is very close to the first of the four beacons and the average RSSI received is above -65 dBm. The system greatly increased the weight of the nearest beacon due to the weighting system being set so that the positioning coordinates were forcibly positioned to the beacon position. In this case, because the RSSI signal is greater than -65 dBm, its position must be within a radius of 2 metres of one of the four BLE beacons, so the maximum positioning error is between 1 and 2 metres.

For test point 5, its position is in the middle of the map, and the positioning result actually reciprocates back and forth near the middle of the map. For test point 5, the positioning error is still no more than 2 metres, but it can be seen that the standard deviation of test point 5 is slightly larger than test points 1, 2, 3, and 4. The position of test point 6 is located at the boundary of the positioning area, and it can be seen that the overall positioning error is still not more than 2 metres. The

position of the positioning result swings left and right in the actual position because, in this case, the BLE beacon with the highest weight is either beacon 1 or beacon 2 due to the fact that the measured location is mainly determined by these two beacons. Because the values of the RSSI sequence for beacon 1 and 2 still fluctuate slightly after they have been processed by the filter, their positioning results bounce back and forth to the left or right of the actual result.

In summary, the test results at the cabin office show that the system provides a stable error of 1-2 meters in the LOS environment. The stability of the system is still determined by the stability of RSSI.

Experiment 2 in small cabin.

The second experiment and the first experiment were conducted in the same environment, but for experiment 2, a pair of BLE beacons were placed in the next room. In this case, there are two Beacon signal transmission paths which are Non-LOS. The purpose of this experiment is to test whether the Non-LOS beacons can successfully provide relatively accurate distance information to the positioning system to calculate the users' position. There are 4 test points in this experiment, the distribution of which is shown in Figure 5.15. The error of each test point and the standard deviation are shown in Figure5.16 and Table 5.2.

Figure 5. 15 Set up of the experimental environment in cabin office (2)

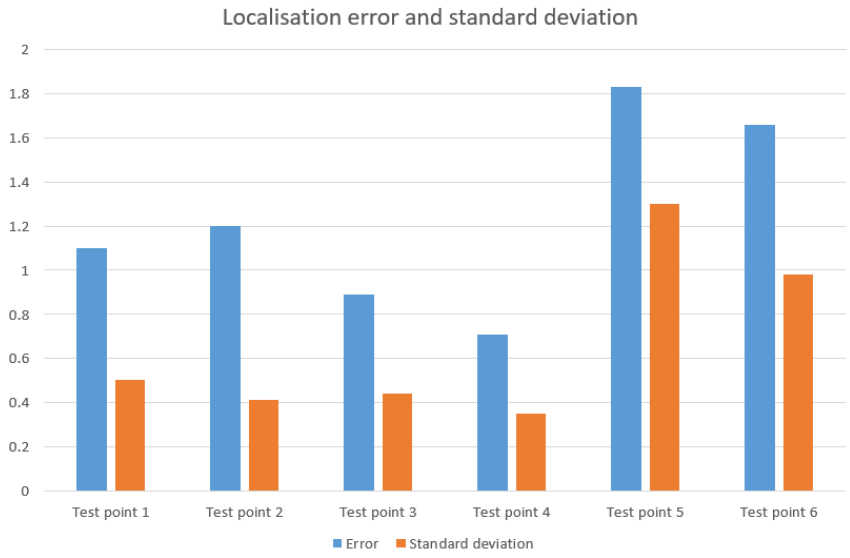

Figure 5. 16 Localisation error and standard deviation of the experimental result in cabin (2)

Table 5. 3 Localisation error and standard deviation of the experimental result in cabin (2)

	Error	Standard deviation
Test point 1	1.1	0.5
Test point 2	1.2	0.41
Test point 3	0.89	0.44
Test point 4	0.71	0.35
Test point 5	1.83	1.3
Test point 6	1.66	0.98

According to the experimental results, test point 1 and test point 2 are essentially the same as those of the previous experiment. Because of the existence of a plywood wall, the transmission paths of beacon 1 and beacon 2 is Non-LOS. However, since the strongest signal provider is beacon 3 or beacon 4, the RSSI values for beacon 1 and beacon 2 are added to a + 5dBm off-set to correct for the additional attenuation of the signal due to the plywood obstruction. Therefore, there is no significant difference between the positioning results of test points 1 and 2 and the previous test. The error of test point 4 is relatively large. During the experiment, it was found that when the user stood at test point 4, their position was judged to be the room where beacon 1 was located at some moments because the algorithm is operating under a special case scenario. For example, the user being located near the wall, and the next room happening to have a BLE beacon. In this case, although the beacon transmission path is Non-LOS, because the user is close enough to this beacon, the RSSI value of this beacon may still be higher than -65 dBm. Moreover, if no other beacon can provide a stronger RSSI

value, the beacon placed in the next room will be selected as the reference beacon, and the user area in which the user is located will also be forced to be the next room. In actual testing, this situation does not occur often unless the user's location is very close to the beacon located in the next room. In this event, although the indoor area where the user will be judged to be is incorrect, the distance error will still not be greater than 2 metres.

For the next step, the positioning system proposed in this chapter was tested in the Kings Building Library. A total of two sets of tests were conducted separately, with the first set in two adjacent learning rooms, and the second set of tests in several rows of shelving. The library environment can be considered a complex non-LOS environment. Bookshelves and books are the main source of interference in this environment, while a small number of moving people can also increase the error of positioning results.

Experiment 3 in library

The first group of six BLE beacons were deployed in two rooms and in the corridor in front of the rooms. Among them, the room on the left hand side deployed three beacons, and the other room deployed two beacons. There was also a beacon deployed in the corridor. The specific beacon deployment condition is shown in Figure 5.17. A total of 14 test points were tested in this experiment and the results are shown in Figure 5.18 and Table 5.4.

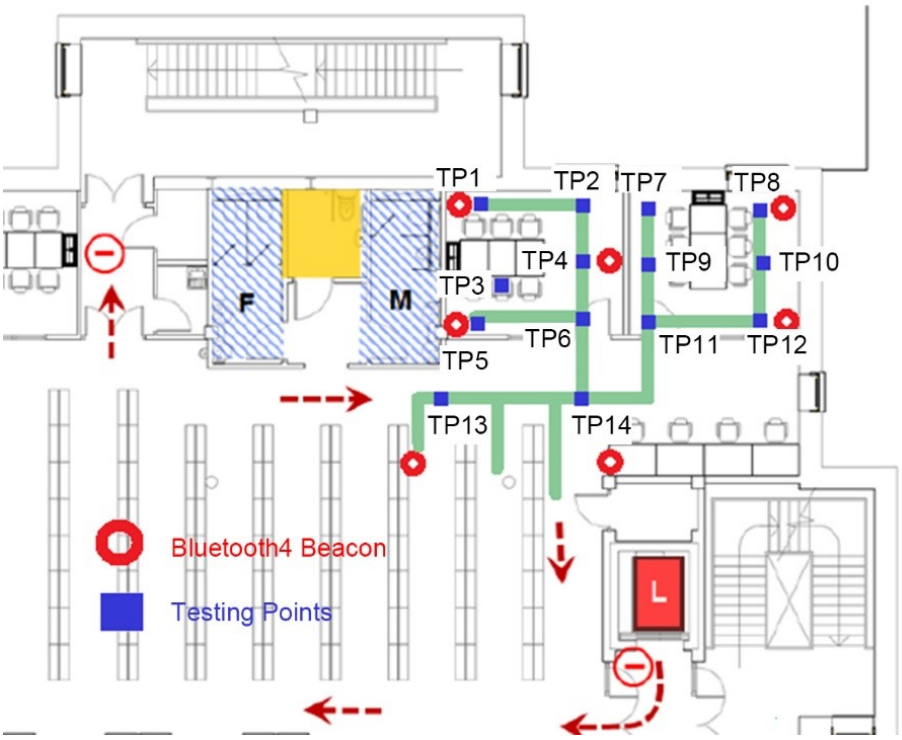

Figure 5. 17 Set up of the experimental environment in library

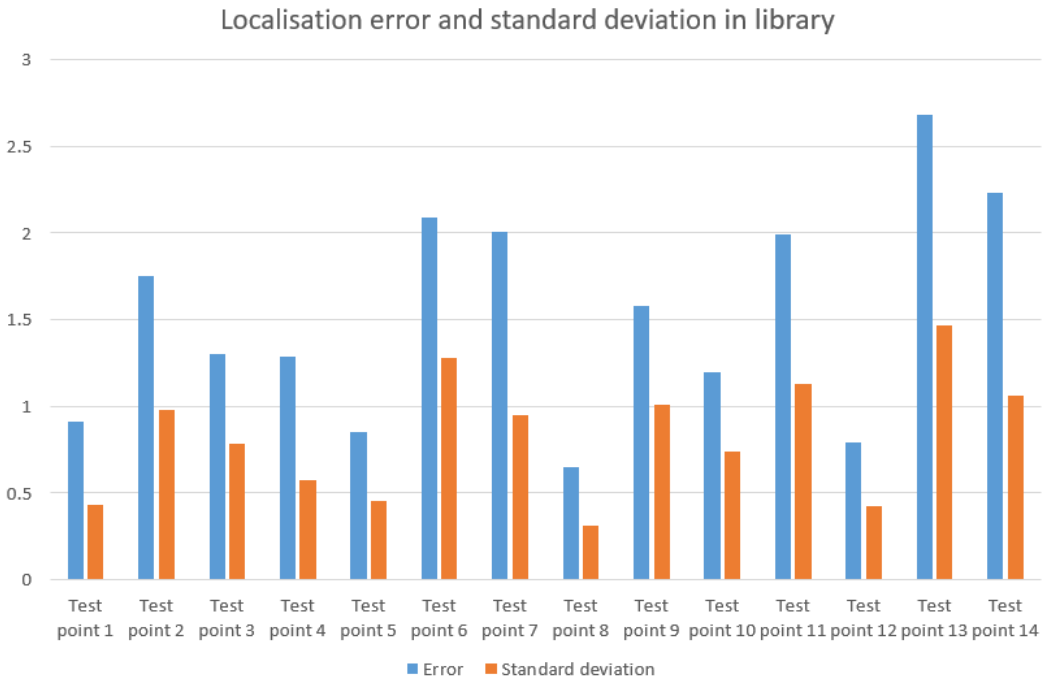

Figure 5. 18 Localisation error and standard deviation of the experimental result in library

Table 5. 4 Localisation error and standard deviation of the experimental result in library

	Error	Standard deviation
Test point 1	0.91	0.43
Test point 2	1.75	0.98
Test point 3	1.3	0.78
Test point 4	1.29	0.57
Test point 5	0.85	0.45
Test point 6	2.09	1.28
Test point 7	2.01	0.95
Test point 8	0.65	0.31
Test point 9	1.58	1.01
Test point 10	1.2	0.74
Test point 11	1.99	1.13
Test point 12	0.79	0.42
Test point 13	2.68	1.47
Test point 14	2.23	1.06

It can be seen that test points 1, 5, 8, and 12 have higher positioning accuracy. This is because their location is more consistent with the BLE beacon, when it is less than 2 metres away from a beacon, its position is forced to be the beacon's location. The error of test point 4, though not high, but in some cases its location will be determined as in the wrong room, this situation, and the previous test in

the cabin environment share this similarity. However, in the corridor, positioning accuracy is slightly lower, and the standard deviation higher than the other points because the transmission path of the two BLE beacons that make up the area in which they are located is Non-LOS. Even so, the overall positioning error is still not more than 3 meters.

Experiment 4 in library

The next experiment was also conducted in the library, the test environment for the book area. Five BLE beacons were deployed on shelves, the details as shown below. There were 9 test points in this experiment, where test points 1-6 were within the effective positioning area, and test points 7-9 were outside of the effective positioning area. The exact positioning error and standard deviation are shown below.

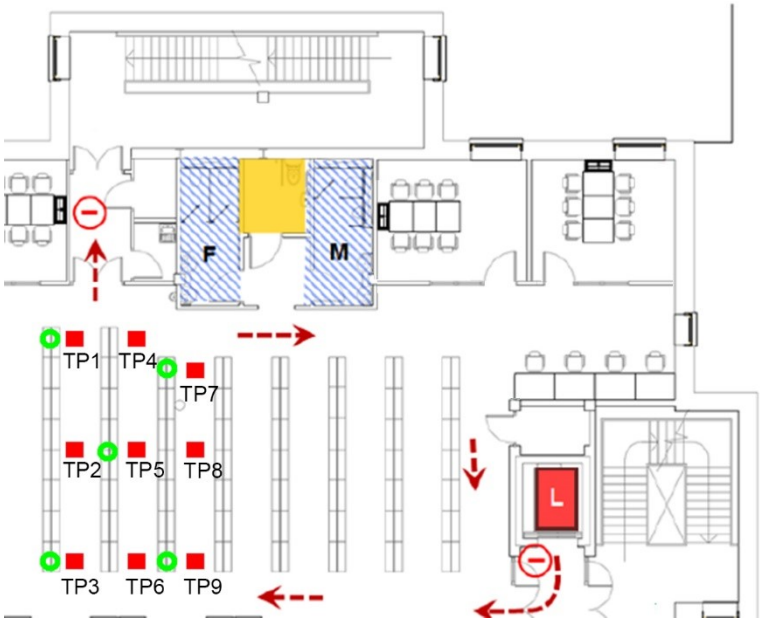

Figure 5. 19 Set up of the experimental environment in library (2)

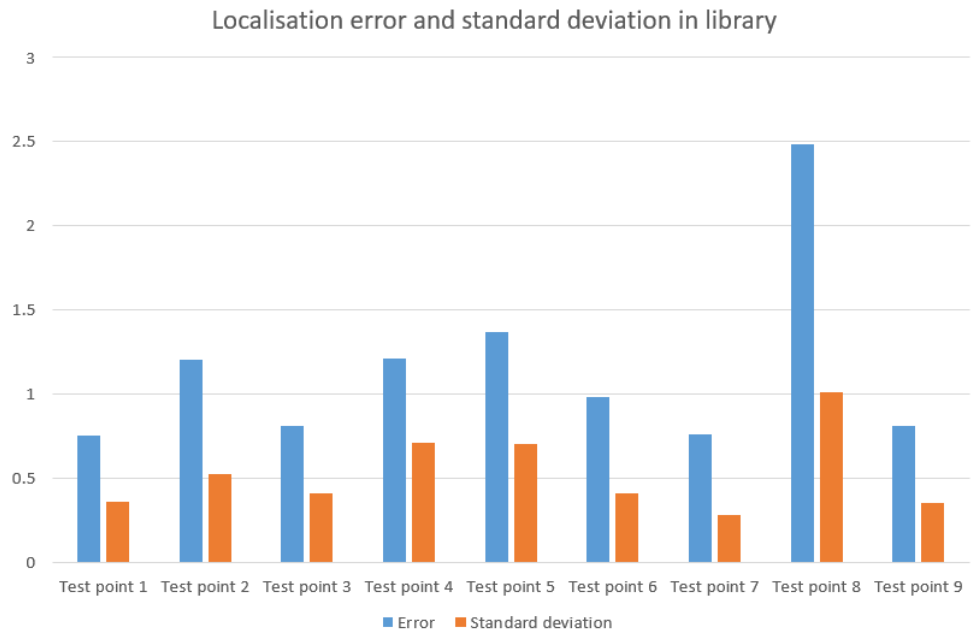

Figure 5. 20 Localisation error and standard deviation of the experimental result in library (2)

Table 5. 5 Localisation error and standard deviation of the experimental result in library (2)

	Error	Standard deviation
Test point 1	0.75	0.36
Test point 2	1.2	0.52
Test point 3	0.81	0.41
Test point 4	1.21	0.71
Test point 5	1.37	0.7
Test point 6	0.98	0.41
Test point 7	0.76	0.28
Test point 8	2.48	1.01
Test point 9	0.81	0.35

The results show that the positioning error of Test points 1-6 were about 2 metres, of which the test points 1, 3, 7, and 9 returned minimum error. Positioning error of test point 2 and test point 5 were slightly higher, and the standard deviation was also higher than test points 1, 3, 7, and 9. At the same time, the error of test point 5 was slightly higher than that of test point 2. According to the analysis of the specific signal strength, it was found that the error of test point 5 was mainly due to the signal strength of beacon 4 being slightly higher, resulting in a tendency of test point 5 to move toward beacon 4.

From the results, it can be seen that test points 7 and 9 were forcibly locked at the BLE beacons 4 and 5 positions. This is because points 7 and 9 were very close to BLE beacon 7 and 9. In addition, test point 8 was positioned on the shelf where beacon 4 and beacon 5 resided, and outperformed beacon 4 and beacon 5 consistently.

Experiments in the library have shown that in a complex Non-LOS environment, the overall positioning error is slightly higher than in a LOS environment. However, as long as the user is located inside an effective positioning area, the error will not exceed 3 meters. When the user's position in the effective positioning area strays into the border area, the positioning error can still be controlled within 3 meters. However, if the user strays out of this effective area, then the positioning accuracy cannot be guaranteed.

Experiment 5 in supermarket

The last set of tests were conducted in a supermarket. The test area was in the shelving area. The entire shelf is made of metal, and the two sides were full of

goods. Furthermore, there were a large number of people buying goods and moving back and forth between the shelves. In order to ensure deployment density, all beacons were placed on the top of the double-sided shelves, and were covered by small amounts of produce. This resulted in all transmission paths being Non-LOS. The aim of this experiment was to test the feasibility and positioning accuracy of the proposed system in a very complex Non-LOS environment.

In the first experiment, five BLE beacons were deployed on three rows of shelves, a total of 12 test points were tested in this experiment, the details of which are shown in Figure 5.21:

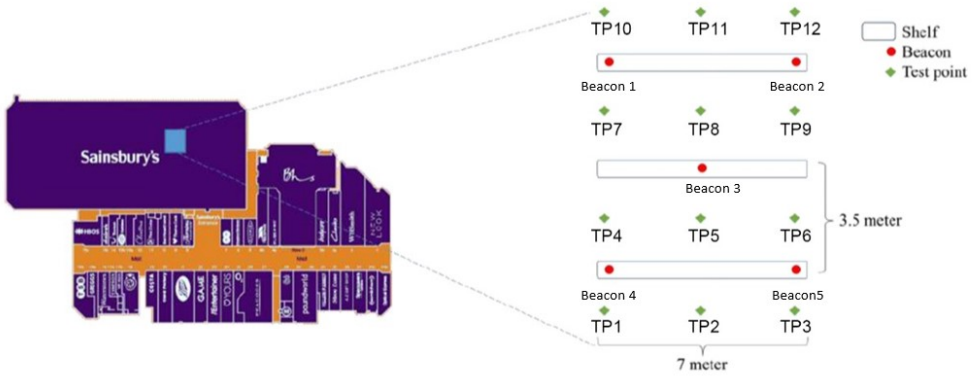

Figure 5. 21 Set up of the experimental environment in supermarket

Of the 12 test points, test points 4-9 were deployed in the effective area, while the rest of the test points were located outside the effective positioning area. The error of each point is shown in Figure 5.22 and Table 5.5.

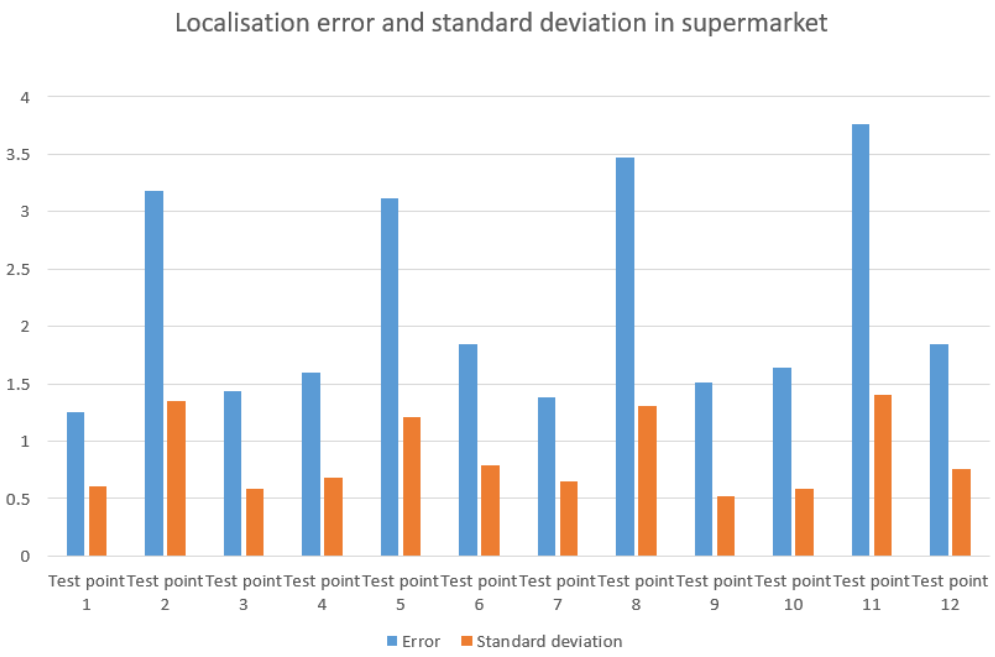

Figure 5. 22 Localisation error and standard deviation of the experimental result in supermarket

Table 5. 6 Localisation error and standard deviation of the experimental result in supermarket

	Error	Standard deviation
Test point 1	1.25	0.61
Test point 2	3.18	1.35
Test point 3	1.44	0.59
Test point 4	1.6	0.68
Test point 5	3.26	1.21
Test point 6	1.84	0.79
Test point 7	1.38	0.65
Test point 8	3.47	1.31
Test point 9	1.51	0.52

Test point 10	1.64	0.59
Test point 11	3.76	4.43
Test point 12	1.84	2.09

From the overall data, the positioning error in the supermarket was greater than in the library. Reading each beacon's RSSI reading at each test point, it was found that even though filters were used to remove noise and interference, the error in the entire RSSI sequence was still quite large. Because when choosing the parameters of the filters, the most important point is to keep valid distance information, so the window width of filters cannot be too long, and the smoothing effect cannot be too high. With regards to this, the local positioning error of the entire positioning system was in excess of 1 metre greater than that of the previous tests. The overall system localisation error was about 3 meters.

The measured location of test point 4 was located next to BLE beacon 4. The reason for this and the previous conditions present in the cabin office and library was different. The user stood at test point 4 and was located about 1.5 meters away from beacon 4. However, the average RSSI from beacon 4 at test point 4 is less than -65 dBm because of the interference from the shelf and the produce. So, the user's position was not forced by the location system to set the coordinates of beacon 4. However, after analysing the RSSI value of each beacon specifically, it was found that the instantaneous RSSI value of BLE beacon 1 was less than -100dBm and the instantaneous RSSI value of BLE beacon 5 was less than -90dBm. After filtering, beacon 1’s average RSSI value was -93dBm, and beacon 5’s average RSSI value was -88dBm. After distance conversion (the attenuation

due to all shelves had been compensated by 5 dBm), the measured distance of beacon 1 to test point 4 and beacon 5 to test point 4 were much greater than 10 metres, which resulted in a very large distance ratio. As a result, the centroid of triangles which consisted of beacons 1, 3, and 4 and beacons 3, 4, and 5 would be offset by a powerful vector around beacon 4. The end result was amazing: test point 4's error was no greater than 3 metres. In fact, incorrect measurement data was used to get a more accurate result.

Test point 5 sometimes appeared incorrectly positioned on the other side of the shelf, which was test point 8’s position. After checking the RSSI sequence, it was found that the signal strength from beacon 5 and beacon 6 would be dramatically decreased when a customer pushed the trolley station at test point 4 and test point 6. At this moment, the signal strength of beacon 1 and beacon 2 would be greater than beacon 4 and beacon 6 even though the latter two were closer to test point 5. Even so, the positioning error was still about 3 metres, and did not exceed 4 metres.

Test points 1, 2, 3, 10, 11, and 12 were different. These test points were all located outside the effective area. Because according to the positioning results, their position would be located inside the effective area. For example, test point 10 in the test would be located between test point 7 and test point 8, and test point 11 would be positioned around test point 8.

Experiment 6 in supermarket

The final test details in the supermarket are shown below. A total of 6 BLE beacons were deployed on two shelves. BLE deployment density was higher than

in the previous experiment. The aim of this experiment was to detect whether the same deployment environment can increase positioning density significantly. Of these, only Test Points 4, 5, and 6 were deployed in the effective positioning area, and the other test points were all located outside the effective area. The error and standard deviation for all test points are shown in figure 5.24 and table 5.7.

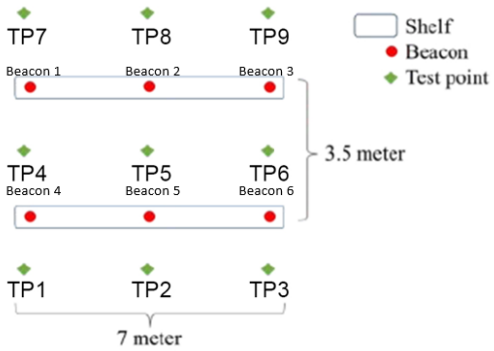

Figure 5. 23 Set up of the experimental environment in supermarket

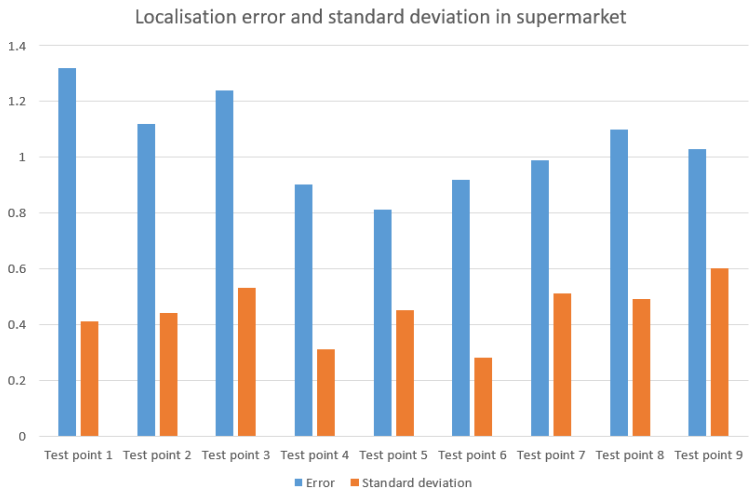

Figure 5. 24 Localisation error and standard deviation of the experimental result in supermarket (2)

Table 5. 7 Localisation error and standard deviation of the experimental result in supermarket (2)

	Error	Standard deviation
Test point 1	1.32	0.41
Test point 2	1.12	0.44
Test point 3	1.24	0.53
Test point 4	0.9	0.31
Test point 5	0.81	0.45
Test point 6	0.92	0.28
Test point 7	0.99	0.51
Test point 8	1.1	0.49
Test point 9	1.03	0.6

According to the above test results, the localisation error of test point 4 had some different from the test point 4 of the previous test, and the average error was decreased by 60cm. The main reason for this was that the deployment density is too high. For example, test point 4 was significantly affected by both beacon 1 and beacon 4. As a result, the positions of test point 4 sometimes were either located at the location of beacon 1 or beacon 4, meanwhile some of the measured locations were located between beacon 1 and 4. The situation of test point 5 and 6 is similar with test point 4. At the same time, the error of Test Points 1-3 and 7-9 is similar to the test points 1,3 and 9,12 of the previous test, although the standard deviation was slightly decreased. The reason for this was mainly because more beacons provide more distance information, and each piece of distance information fluctuates with environmental interference. The interference

of multiple pieces of distance information will add up at different moments, and the offset value will be determined by different beacons. This leads to a decrease in the standard deviation of the overall system, because that some dramatic fluctuations of the error will be averaged and smoothed by the results from other beacons. The overall error from test point 1 to test point 9 is around 1 metre however, the beacon deployment density under this test cannot be utilised in most of practical applications.

In general, using the proposed off-set centroid core positioning algorithm in combination with the weighted framework, system positioning errors are between 1-2 metres in a LOS environment. In a very complex Non-LOS environment, the positioning error will not be greater than 4 metres. In some cases, the user's location within a certain room may be misjudged as being inside the next room, but in this case, the average error will still be under 4 metres.

5.6 Conclusion

In this article, the basic trilateration positioning algorithm was introduced first. The shortcomings of the algorithm were also described in detail: measurement distance error can lead to many inaccuracies, circles sharing no common intersection point cannot be used to calculate results. In order to solve these problems, an off-set centroid core positioning algorithm combined with a weighted framework was proposed in this paper. The positioning algorithm uses the triangular centroid core as a reference point and the distance ratio provides the off-set value, resulting in a vector offset centroid core as a positioning result. Weighted framework consists of a total of three main weights. By using the Wa Wq and WR parameters, the system can choose the right BLE beacons more efficiently and accurately as the primary distance information provider, and can correctly select more efficient triangles to increase positioning accuracy.

The novelty of this proposed system is described as follow:

1: The weak points of most trilateration based position system are not existed. As mention in this chapter, when three circles generated by RSSI value do not have common point between each other, those trilateration based systems could not generate a ‘reasonable’ results as the users’ position cannot be an imaginary number. By applying this proposed system, the calculated result will not be limited by the ‘common point’ based technique, which means the stability and adaptability of system is increased.

2: A tailor made weighted framework is proposed for this system in order to increase the localisation accuracy and system stability in addition. By applying this

weighted framework, multiple beacons (more than 3) can be utilised to provide users' location information at same time. Meanwhile, this weighted system could also select the best signal provider and combination of beacons dynamically.

The system was tested separately in three different environments. The three environments were: the cabin office room (LOS), Kings Building Library (Non-LOS), and supermarket (complex Non-LOS). The experimental results showed that the positioning accuracy of the system could be maintained at 1-2 metres in a LOS environment, while the positioning error was between 3-4 metres in an extremely complicated, Non-LOS environment.

The main disadvantage of this algorithm is that it requires that most indoor environments be covered by BLE beacons. In other words, the deployment density and condition of BLE beacons requires additional restrictions.

Meanwhile, as mentioned above, the minimum number of the BLE beacon required in this system is three. Increasing the number of beacon, in other words, increase the signal deployment density could increase the positioning accuracy slightly. Based on such situation, it seems that using more than 4 beacon based algorithm should be a better choice than 3 beacon based. However, by considering the cost performance, those extra beacons could not increase the localisation accuracy markedly because of the RSSI noised analysed in chapter 3. As a result, developing more than three beacon based algorithms could not provide a significant performance improvements but only increase the complexity of the proposed system. These mentioned problem limit the utilisation range of

this proposed system. The hybrid Monte Carlo localization algorithm discussed in the next section addresses the above problem.

Chapter 6 : Application of Optimised Monte Carlo Localisation Using Bluetooth Low Energy, Accelerometer and Compass

6.1 Introduction

The Monte Carlo filter, which can also be referred to as particle filter, has become an established means for solving state-space models [84]. Particle filters have applications in areas such as signal processing, tracking, neuroscience and biochemical networks. The Monte Carlo technique was initially developed in the 1950s [85] [86], However, since the introduction of the bootstrap filter [87] there has been a resurgence of research in this field.

Prior to the relatively recent popularity of particle filtering methods, The Kalman filter [88] was the standard method for solving state-space models [84]. It was, at one time, the most effective choice for solving linear Gaussian state-space models. When the requisite linearity or Gaussian conditions were not met, variants of the basic Kalman filter: the extended Kalman filter or the unscented Kalman filter, could be employed. The Kalman filter does exhibit certain limitations however, specifically, it cannot perform well when dealing with highly non-linear and non-Gaussian problems [89].

Particle filtering techniques provide a more elegant solution to the problem than the Kalman filter and its variants [89]. Particle filtering techniques estimate the

latent process's marginal distribution as observations become available. Sampling is used at set time points to approximate distribution of particles, each with a corresponding weight and set of discrete values [90]. There are several articles and books which give detailed reviews of particle filters and their applications, for example [91], [92], [93] and [94]. In addition, an overview of more general sequential Monte Carlo methods is given by [95].

In this chapter, the MCL algorithm is employed to build a system targeting indoor positioning. The theory of MCL, which is expanded from the Bayes filter [96] is introduced. Afterwards, methods of applying an accelerometer and compass as a means of estimation update for MCL is discussed. The method of implementing BLE to provide observation updates is also given. In addition, implementation of this system is demonstrated, followed by a set of experimental results. Finally, a comparison between MCL, the proposed off set centroid algorithm in chapter 5, and other positioning algorithms is made.

6.2 Methodology of MCL

6.2.1 Hidden Markov Model

A 1-D example of the position model is presented to explain the methodology of MCL. The example is shown below:

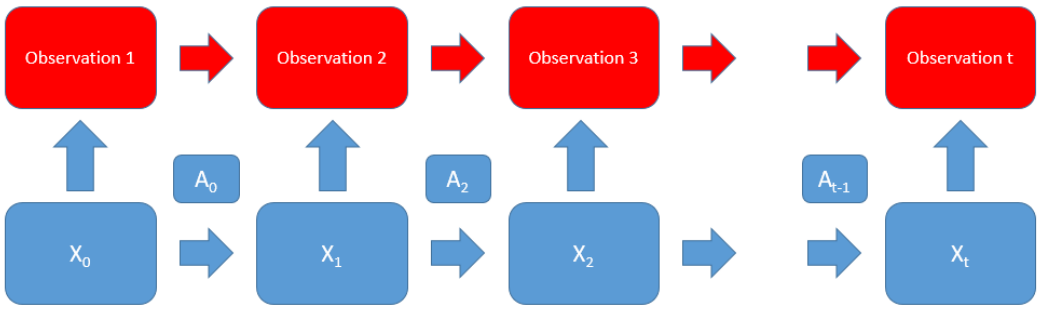

Figure 6. 1 Example of Hidden Markov Model

The initial user position is assumed as x_0 and an observation result o_0 is observed. For the next step, an estimation, namely a_0 occurs. At this point, the updated user position is x_1, together with an observation result o_1. This process works continually until the user is located at position X_t, with an observation O_t. The penultimate step of the estimation update is a_{t-1}.

This model can be resolved by the HMM. The explanation of the HMM is given below. Actually, the HMM is a special state of the Bayes mode.

A HMM is a statistical Markov model in which the system being modelled is assumed to be a Markov process with unobserved (hidden) states [97]. An HMM can be presented as the simplest dynamic Bayesian network. The mathematics behind the HMM were developed by L. E. Baum in [98]. In basic Markov models,

the states can be observed directly. In such cases, the state transition probabilities are the only impact elements. However, In the HMM, states cannot be observed directly, but the outputs which are related to the state, can be observed. During observation, a probability distribution for each state is generated. In this event, the sequence of outputs produced by the HMM provides information about the states. An example of a HMM is shown below.

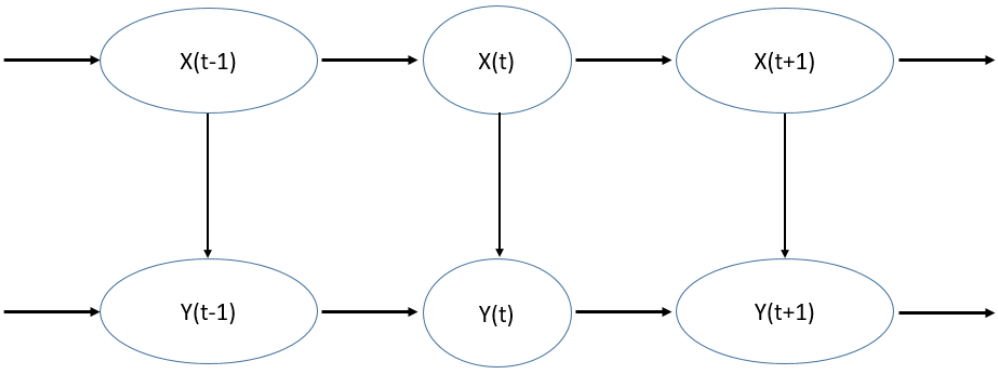

Figure 6. 2 Explanation of Hidden Markov Model

In this HMM, the arrow points out the relationship between X_t. As can be seen from the diagram, X(t) is only controlled by X(t-1) which X(t) is justified by X(t-2). Meanwhile, each Y(t) is only related to their corresponding X(t). In this model, X(t) is referred to as the hidden variable, which is the hidden state discussed above. This variable is invisible.

It can be assumed that the dimensionality of determinate elements for each X(t) is N, which means the possibility of X(t) is N. Hence, the possibility from X(t) to X(t+1) is N^2, because the possibility of X(t+1) is also N. Similarly, if we assume that the possibility of the observation result, which is the Y(t) in this model, is M, the complexity of the output model from X(t) to Y(t) will be O(N M). If Y(t) is a

vector of M dimensionally, the final complexity of the output model will be O(N M^2).

If the observation is Y:

$$Y = y(0), y(1), \dots, y(L-1) \tag{6.1}$$

The hidden state is X:

$$X = x(0), x(1), \dots, x(L-1) \tag{6.2}$$

The probability of HMM can be presented as:

$$P(Y) = \sum_X P(Y|X)P(X) \tag{6.3}$$

Where: L is the length of the model.

6.2.2 Particle Filter

MCL is a recursive Bayes filter that estimates the posterior distribution of users' poses conditioned on sensor data. In fact, MCL can be summarised as an application of particle filters, and the manifestation of it can be described by the HMM.

Bayes filters address the problem of estimating the state *x* of a dynamical system (partially observable Markov chain [99]) from sensor measurements. The basic Bayes equation is shown below:

$$P(A|B) = \frac{\sum_i P(B|A)P(A)}{P(B)} \tag{6.4}$$

The key idea of Bayes filtering is to estimate a probability density over the state space conditioned on the data. This posterior is typically called the belief and is denoted:

$$Bel(x_t) = p(x_t|d_{0\ldots t}) \tag{6.5}$$

Where:

x denotes the state, x_t is the state at time *t* and $d_{0\ldots t}$ denotes the data starting at time 0 up to time *t* .

In this research, two types of data are distinguished: perceptual data which derive from BLE beacon sensors, and odometry data, which are provided by accelerometer and compass to provide information about users' motions. Expressing the former by *o* (for the observation update) and the latter by a (for motion update), we have the following equation:

$$Bel(x_t) = p(x_t|o_t, a_{t-1}, o_{t-1}, a_{t-2}, \ldots o_0) \tag{6.6}$$

In this model, it can be assumed that the action update and observation update are received alternately. It must be noted that in the process from *X*(t-1) to *X*(t), *a*(t-1) is applied to present the latest motion update.

In a Bayes filter, the belief is estimated recursively. The initial belief describes the initial information about the user's state. However, normally users could not have the knowledge of their initial position. In this case, a uniform initial distribution is utilised to present the user's location, where the initial user's position is unknown.

In order to drive the update equation recursively, the equation 6.6 (as shown above) can be transformed by the equation 6.4 which is the Bayes rule:

$$Bel(x_t) = \frac{p(o_t|x_t, a_{t-1}, o_{t-1}, a_{t-2}, \dots o_0)p(x_t|a_{t-1}, o_{t-1}, a_{t-2}, \dots o_0)}{p(o_t|a_{t-1}, \dots o_0)} \quad (6.7)$$

In the equation 6.7, the denominator has a constant relationship with X(t). Therefore, the equation 6.7 can be simplified to:

$$Bel(x_t) = \eta\, p(o_t|x_t, a_{t-1}, o_{t-1}, a_{t-2}, \dots o_0)p(x_t|a_{t-1}, o_{t-1}, a_{t-2}, \dots o_0) \quad (6.8)$$

Where:

η is equal to:

$$\eta = p(o_t|a_{t-1}, \dots o_0)^{-1} \quad (6.9)$$

Bayes depends on the assumption that the current state X(t) only depends on the previous state X(t-1), which can be referred to as a Markov assumption [100]. In such a case, the equation 6.8 can be simplified to:

$$Bel(x_t) = \eta\, p(o_t|x_t)p(x_t|a_{t-1}) \quad (6.10)$$

The final equation is shown below:

$$Bel(x_t) = \eta\, p(o_t, x_t|a_{t-1}) \quad (6.11)$$

6.2.3 Estimation Update

As mentioned above, MCL is a recursive Bayes filter that estimates the posterior distribution of users' conditions on sensor data. Bayes filters address the problem of estimating the state x of a dynamical system (partially observable Markov chain) from sensor measurements. Bayes filters assume that the environment is Markov, which means, past and future data are independent if one knows the current state.

In this research, two types of data are distinguished: perceptual data which is BLE beacon sensor data, and odometry data, which is the accelerometer and compass data to provide information about users' motions.

The implementation of estimation update and observation update sections rely on a specific estimation problem. In indoor localisation, both models can be achieved straightforwardly with several lines of code. The specific methodology of the implementation has been introduced in depth at the beginning of this chapter. Thus, in this section, a cursory explanation is given only.

The estimation update section, which is the motion element, can be generalised as users' kinematics in a probabilistic environment. As mentioned, for user position, the position x and x' are two dimensional variables. Each pose comprises the users' two dimensional coordinates, which can be divided into direction and displacement. The method of measurement in this research has been achieved by accelerometer, and the direction information is produced by a compass integrated within the mobile devices. The function of a is an odometry reading of a control command. In the area of indoor positioning, changes of pose or position can be called kinematics [99]. However, the basic kinematics equation

only describes the excepted position x' as an idea result, and the noise and physical error of the mobile device are not extant.

In a real system, the estimation update provided by the accelerometer and compass is erroneous, in this case, the position of x' is uncertain. In order to present this inherent uncertainty, a sampling model of $p(x'|x,a)$ is applied as a solution. The sampling model is a routine that package x and a as a group of inputs and generates random poses x' according to $(x'|x,a)$, which is easier to apply a close-form description of the motion. Figure 6.3 gives an example of the sampling model based model $p(x'|x,a)$, which is applied to present odometry measurement. As can be seen in this figure, the sequence of particle sets approximates the position of users that only utilise accelerometer and compass.

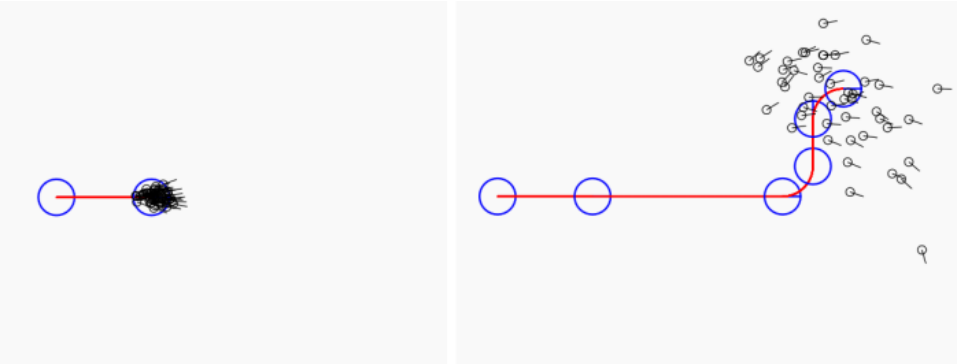

Figure 6. 3 Uncertainty caused by errors of accelerometer and compass

The employment of Accelerometer and Step counter

In this section, the theory of using the accelerometer and compass are explained specifically. This includes the principles of the accelerometer and compass, and method of implementing them into MCL.

- **Introduction of Step counter**

People are paying increasing attention to daily exercise. Step counters are widely applied as an efficient way to record a user's physical training history in their daily life. Recently, two different types of step counters are commonly utilised in different devices. These are: mechanical step counters and electronic step counters.

- **Mechanical step counters**

Mechanical step counters account the user's steps by sensing the shaking of certain sections of human body such as arms and legs. A threshold is utilised in the mechanical step counter: when the accelerated velocity caused by human motion is larger than the threshold, this behaviour will be detected by a built-in mechanism and this motion will be counted by the step counter.

However, mechanical step counters have certain limitations. Firstly, sometimes step counters cannot capture human motion accurately when the scope of swing is small and could potentially not trigger the step counter. This is due to the fact that it is difficult to dynamically set up the threshold value of mechanical step counters. Secondly, gross movement could also activate the step counter and result in an error count, such as hand raising or head scratching.

- **Electronic step counters**

Electronic step counters normally consist of an accelerometer and a microprogrammed control unit (MCU). The accelerated velocity can be detected by the accelerometer, and the actual steps will be computed by the MCU.

Three-axis acceleration sensors are widely implemented into modern electronic step counters. This sensor can detect the user's motion in 3 dimensions. As a result, electronic step counters which utilise this technique have the advantage of higher accuracy and higher capacity of resisting disturbance.

Recently, with the rise in popularity of mobile smartphone devices with integrated accelerometer units, most smart devices can supply the application of step counters without significant additional hardware expenditure by directly installing the relevant software. Meanwhile, this technique is also implemented into smart watches and smart bracelets with step counting algorithms to let users record their exercise history. An example of three-axis acceleration sensors based on IOS devices is shown below.

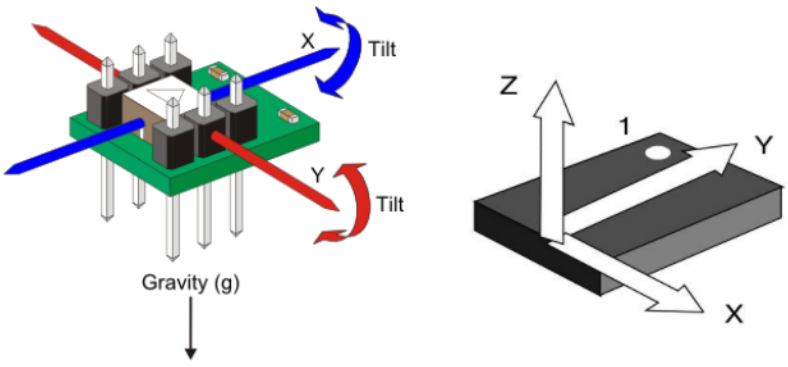

Figure 6. 4 Example of accelerometer in mobile devices [101]

Specifically, the accelerometer is a circuit based on a Micro Electro Mechanical System (MEMs) that measures the value of acceleration which is caused by gravity of movement or titling action. Figure 6.5 gives an example of a capacitance based accelerometer. When accelerated velocity is generated, the position of seismic mass changes and these changes result in a change in capacitance. This capacitance change is equivalent to the current change, and finally this variation will be recognised as a change in force.

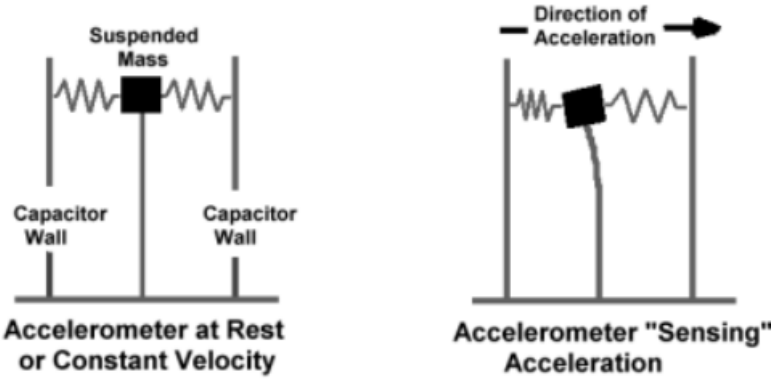

Figure 6. 5 Example of capacitance based accelerometer [101]

6.2.4 Implementation of Step Counting

Step counting algorithms can be divided into four categories: peak to peak, Frequency domain transformation such as Fast Fourier Transform (FFT) algorithms, and filter based algorithms, and pattern recognition.

In this research, it is assumed that users hold their mobile device stably in their hand, or put it inside their pocket, which means that mobile devices normally keep stationary until movements occur. In such cases, a peak to peak algorithm could be applied to compute user motion accurately. Meanwhile, with considering for

the computing workload, the computation of this algorithm is also appropriate for mobile based indoor localisation systems.

When users engage with the indoor positioning application, their mobile devices are either put inside their pockets or held in their hands. In this situation, the direction and rotation of these mobile devices is uncertain. The period of users' motions can be obtained by calculating their accelerated velocity in 3-D vectors, which is an approximate sine curve. Furthermore, the direction of current accelerated velocity can be acquired by referring to the data collected in the first step. These results are applied to make a comparison with the previous direction of accelerated velocity.

As a result, if this direction is the opposite of the previous direction, this means the recent state is not a part of the peak phase, the counter will increase by one. Otherwise, this stage will be ignored. In this case, users' steps can be computed by counting the number of peak periods.

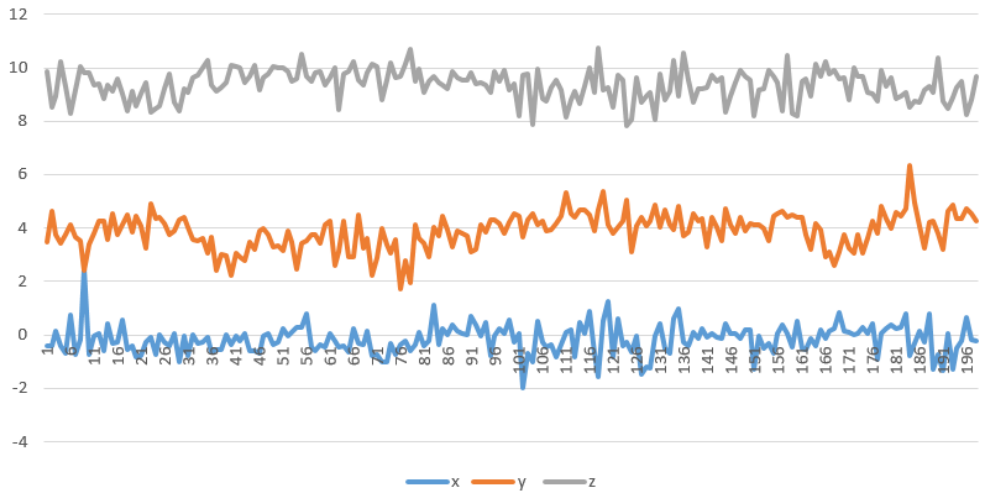

Figure 6. 6 Example of collected data of accelerometer(x,y and z axis)

Denoise

Sometimes mobile devices may suffer a low amplitude but high frequency distribution, such as when mobile users are shaking their hands. The accuracy of step counters will be decreased by these behaviours mentioned above. In such cases, a filter can be implemented into this system to remove and decrease the effect of these interferences.

Currently, the fastest human running frequency is 5Hz (the case of people using auxiliary equipment to travel faster than 5Hz is not considered). To be specific, the time lag between two steps should no less than 0.2 seconds. A low pass filter could be employed to remove noises which are higher than 5Hz. Meanwhile, by comparing the average peak value, the threshold can be set up dynamically, which could also increase accuracy for the step counter.

6.2.5 The Assumption of the Error of Accelerometer and Compass

As mentioned, in this proposed system, accelerometer and compass are applied to provide the estimation update. In specific, accelerometer is utilised to measure the variation of distance and compass is employed to measure the change of orientation.

Assumed that a_t can be presented as:

$$a_t = d_t * \overrightarrow{or_t} \tag{6.12}$$

Where:

d_t is the variation of distance,

$\overrightarrow{or_t}$ is the change of orientation, which is a normalised direction vector.

Because the indoor position is a two dimensional environment, equation 6.12 can be extended as:

$$a_t = d_t \sin\theta_t * \overrightarrow{x_t} + d_t \cos\theta_t * \overrightarrow{y_t} \quad (6.13)$$

Where:

θ is the degree of orientation,

$\overrightarrow{x_t}$ and $\overrightarrow{y_t}$ are orthometric one dimensional reference vectors.

By considering the error of accelerometer and compass, equation 6.13 can be extended to:

$$a_t = d_t' \sin\theta_t{}' * \overrightarrow{x_t} + d_t' \cos\theta_t{}' * \overrightarrow{y_t} \quad (6.14)$$

Where:

$$d_t' = d_t + N(0, \sigma_d{}^2),\ \theta_t{}' = \theta_t * [1 + N(0, \sigma_{ot}{}^2)] \quad (6.15)$$

In equation 6.15, d_t' and $\theta_t{}'$ is the observed value, σ_d and σ_{ot} are the scale parameter of errors, which is presented as Gaussian distribution.

According to a mass of experimental results, the inaccuracy of accelerometer and compass are approximately 10%, the final equation can be presented as:

$$a_t = [d_t + N(0, \sigma_d{}^2)] \sin\theta_t * [1 + N(0, \sigma_{ot}{}^2)] * \overrightarrow{x_t} +$$

$$[d_t + N(0, \sigma_d{}^2)] \cos\theta_t * [1 + N(0, \sigma_{ot}{}^2)] * \overrightarrow{y_t} \quad (6.16)$$

Where:

$$\sigma_d{}^2 = 10\%, \sigma_{ot}{}^2 = 10\% \quad (6.17)$$

6.2.6 Observation Update

Most current smart mobile devices are normally carry BLE functionality. The method of applying BLE to provide approximate distance information has been introduced in previous chapters. The application of BLE in MCL is to provide distance information between users' mobile devices and several BLE landmarks with absolute coordinates.

Assuming that the user's position is x, and the observation o_i present a RSSI from the beacon *i*. In this research, the data observed from the user is the RSSI value from the BLE beacons. The relationship between distance and the RSSI value has been discussed in chapter 3, which is the equation 3.11. Thus, the state between the observed RSSI value and the distance can be expressed by the following equation:

$$d_i = 10^{\frac{P(r_0)+o_i+X\sigma}{10\alpha}} \quad (6.18)$$

As discussed above, a Gaussian distribution parameter which is $X\sigma$, is added in equation 6.18 to mitigate interference. The mean value of this distribution is 0, while the variance is σ^2 according to the discussion in chapter 3.

6.3 Implementation of MCL

6.3.1 The Assumption of Even Distribution and Gaussian Distribution

In each loop, a set of particles will be selected: first, these particles will be removed from the map, and then according to the assigned weight value re-deployed to the map. Specifically, the selected particles will be deployed one by one around the weighted particles. A greater quantity of selected particles will be deployed around weighted particles with higher weight value.

It can be seen that, by using even distribution, particles will be equally deployed within the weighted area. In comparison, Gaussian distribution will be faster because most of selected particles will be deployed in the middle of weighted area. The advantage of even distribution is that the overall computation is lower than Gaussian distribution, however, Gaussian distribution is more in line with probability statistics.

When weight is assigned to particles, both even distribution and Gaussian distribution can be used.

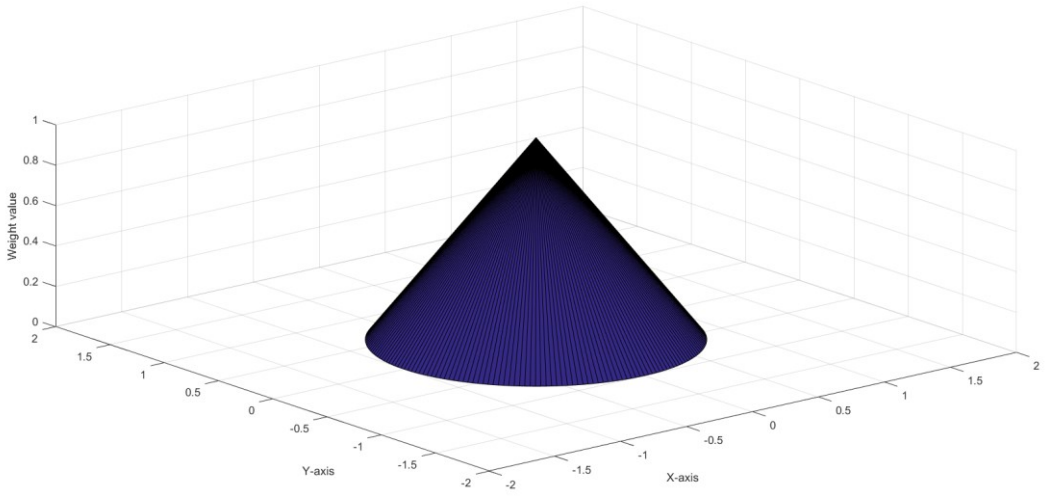

Figure 6. 7 Weight values of weighted areas using even distribution

As shown in Figure 6.7, the assignment of weights follows the principle of even distribution. The weight value of particles distributed around the central circle line will be higher and the weight value of particles in the border area will be lower. Weight distribution follows a linear relationship. In this case year, the selected particle will be evenly distributed between concentric circles, between the numbers of linear relationships.

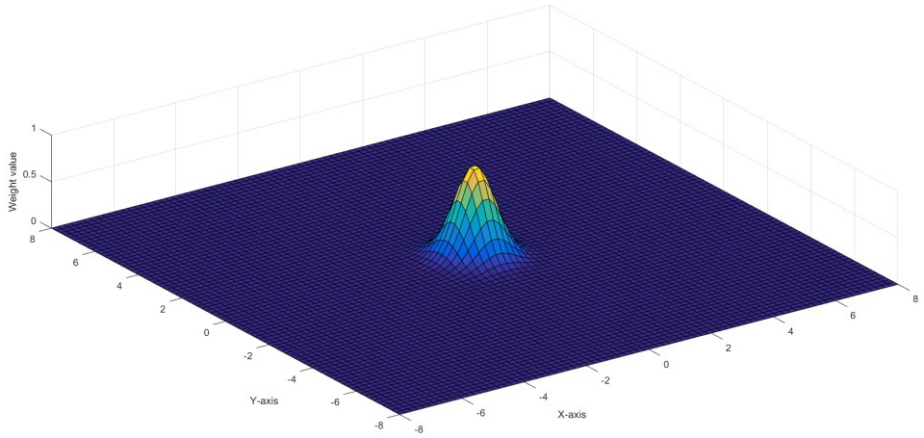

Figure 6. 8 Weight values of weighted areas using Gaussian distribution

As shown in Figure 6.8, the weight assignment follows the Gaussian distribution principle. Similar to even distribution, the weight value of particles around the central circle line will be higher than the particles distributed in the border area. However, unlike even distribution, more selected particles will be assigned to the central area because of Gaussian distribution. As a result, by using Gaussian distribution, the degree of aggregation of particles will be much greater than with the use of even distribution.

The two features are obvious: through the use of even distribution, particles prove difficult to be overly or excessively distributed together. Therefore, the MCL system will have a higher degree of adaptive and error correction capabilities. The use of Gaussian distribution will increase the degree of aggregation of particles, in the case of a stable system, positioning accuracy will be higher than through the use of even distribution.

By adding an additional room ID to all BLE beacons, it can be used to assist in determining whether the signal transmission channel is LOS or non-LOS. Specifically, in most cases (the strongest signal strength is not less than -76dBm),

the system will default to provide the strongest signal BLE beacon and user belonging to the same indoor environment, and BLE beacon, and have the strongest signal strength BLE beacon with the same room ID of the BLE beacon's transmission channel also considered LOS, while the ID of the same BLE beacon will be considered to be deployed in other rooms. In this case, the signal strength of the BLE beacon deployed in other rooms will be supplemented with an additional compensation factor to correct the distance. At the same time, the distance information provided in the non-LOS environment will be given a lower weight.

After all the particles have been deployed in the above steps, estimated result will be used for the next update. By using the accelerometer and compass, the user's motion information will be estimated and then an error assumption will be introduced and then added to each of the particles on the map. As described in the previous section, the error rate of the accelerometer is 10% on average, and the results follow the Gaussian distribution, while the compass error is also 10%, following the Gaussian distribution.

6.3.2 Framework of the Tailor-made MCL

In practice, a set of random numbers consistent with the number of particles will be generated and then substituted into Equation 6.5, and the error factor introduced for a separate particle can be considered random. But all the particle error factors together, will show a Gaussian distribution.

After initialization, firstly, particles are randomly deployed in the targeting area. For the next step, the accelerometer and compass begun to receive the user’s

motion. The estimated motion update which includes the variation of displacement and direction will be added to each particle. Afterwards, the BLE signal detector begin to receive the distance information from deployed BLE beacon. Each RSSI value will generate a weighted area that particle located inside the weighted area will be given a higher weight value. Meanwhile, some particle are randomly removed and refilled around those weighted particles. This infinite loop will keep working and finally most of deployed particles will be crowed together, which is the user's location.

In the last step of each loop, a small amount of particles will be selected: they will first be removed and then re-routed. The purpose of this is to provide the self-reset function to the positioning system. If this step is missing, as the system runs, all the particles will be pooled into a very small range. When an unknown error occurs, the aggregated particles will lose the chance of being broken up and reorganized. In actual use, only 1% of the total particles are needed to provide enough 'seed' for reset.

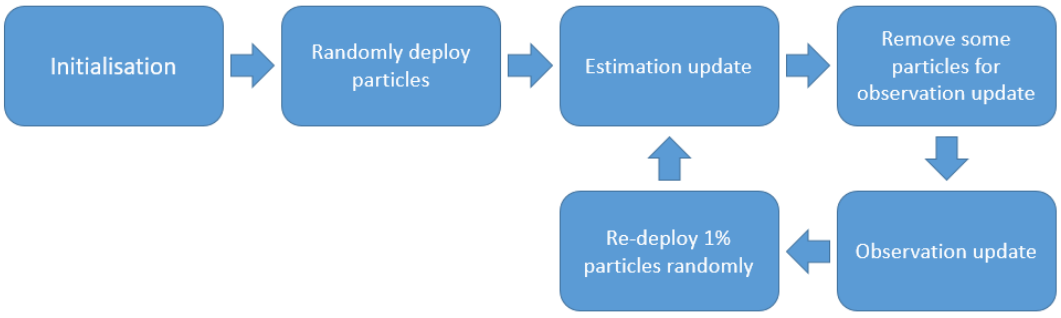

Figure 6. 9 Flow chart of the implementation of MCL

6.4 Experimental Results of MCL and Other Algorithms

6.4.1 Number of Particles

A large number of tests under different circumstances have been conducted. The first three groups of tests were used to test the positioning accuracy of MCL under different parameters and the particle aggregation effect. The first three groups of trials were conducted in the cabin office, where a total of six BLE beacons were deployed in two rooms. Four BLE beacons were deployed in the room above and two BLE beacons were deployed in the rectangular room below. The specific layout of the test point and BLE beacons are shown in Figure 6.10.

In this experiment, a total of four groups of tests were tested using particle numbers of 500, 1000, 2000 and 3000, respectively. Some of the example diagrams are shown below from Figure 6.11 to Figure 6.18:

Figure 6. 10 Layout of the test point and BLE beacons in cabin office

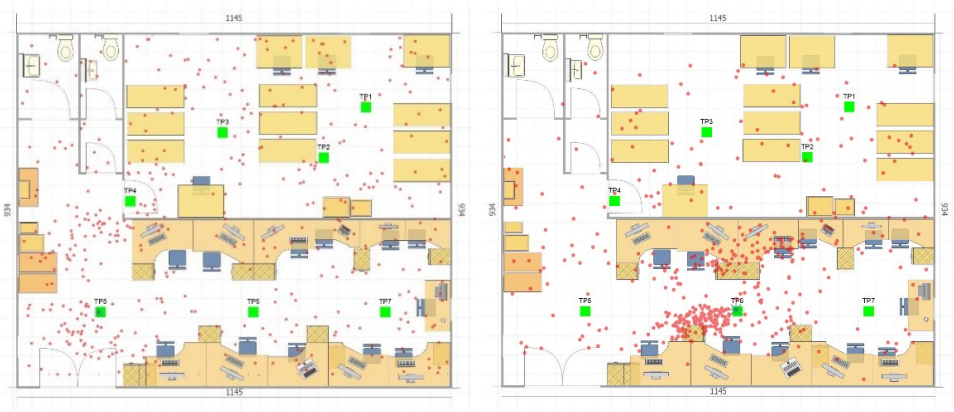

Figure 6. 11 Initial result of 500 point MCL (Left)

Figure 6. 12 500 point MCL result in test point 6 (Right)

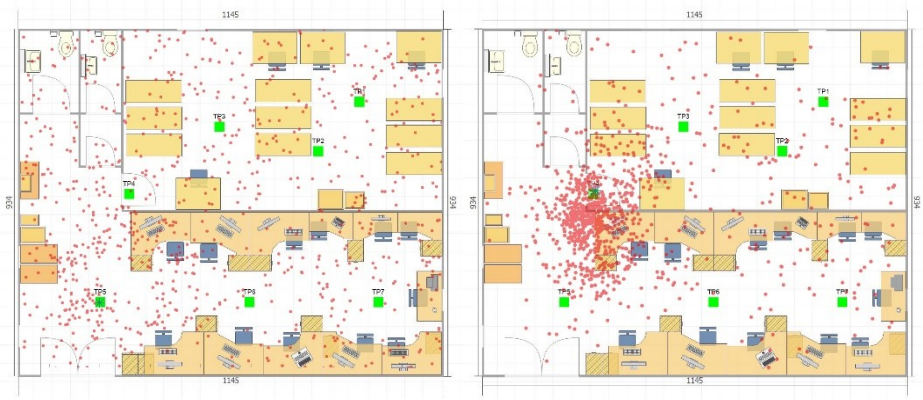

Figure 6. 13 Initial result of 1000 point MCL (Left)

Figure 6. 14 1000 point MCL result in test point 4 (Right)

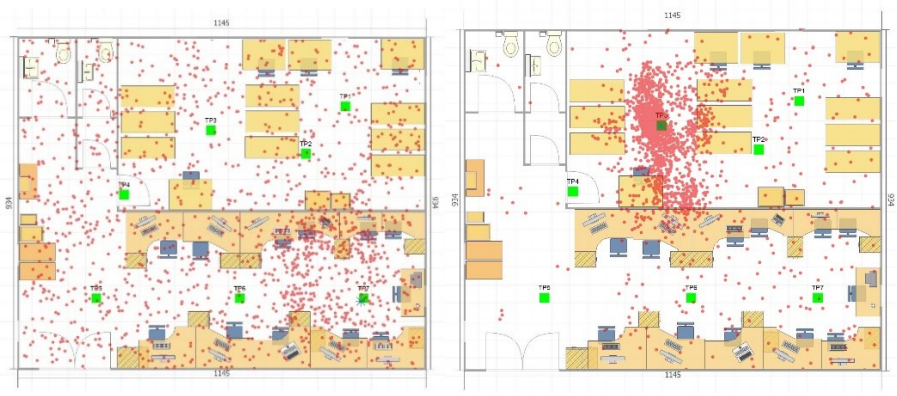

Figure 6. 15 Initial result of 2000 point MCL (Left)

Figure 6. 16 2000 point MCL result in test point 3 (Right)

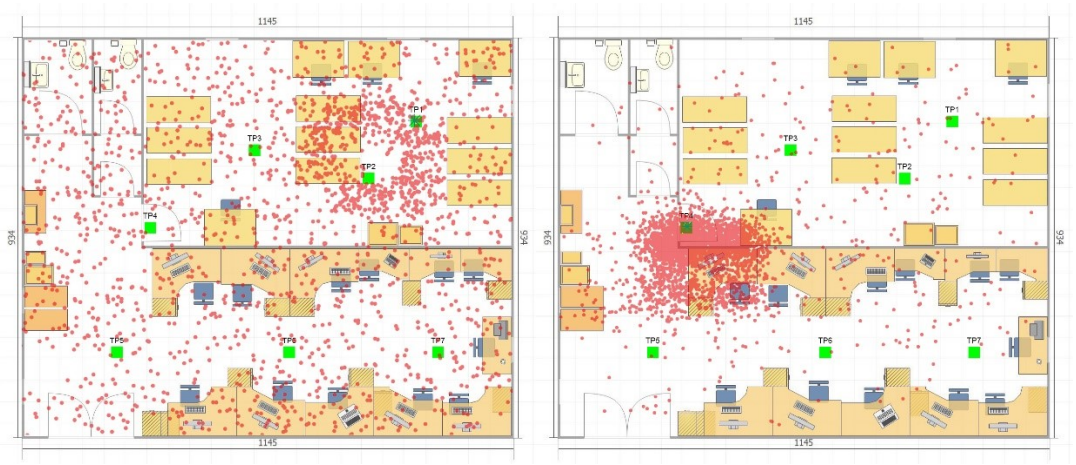

Figure 6. 17 Initial result of 3000 point MCL (Left)

Figure 6. 18 3000 point MCL result in test point 4 (Right)

In these figures, the blue mark is the user position, the green dots are test points from 1 to 7, the red dots are particles and the blue dots are BLE beacons.

As can be seen from the Figure 6.12, the use of 500 MCL positioning results are not very satisfactory, a large number of points are scattered throughout the map. The 1000 point, 2000 point, and 3000 point results, when compared to this difference, are not large. Considering particle dispersion and computation, the number of particles should be between 1000 and 3000. In the actual experiment, too many particles will not only lead to a sharp increase in the amount of computation, but also lead to the convergence of multiple particles appearing. In this case, the localisation error will also increase drastically.

6.4.2 Even Distribution and Gaussian Distribution

The purpose of the second experiment was to test the assumption used by particle deployment. In this experiment, two examples are shown, which are: an even

distribution and a Gaussian distribution of 3000 points MCL. The results are shown below:

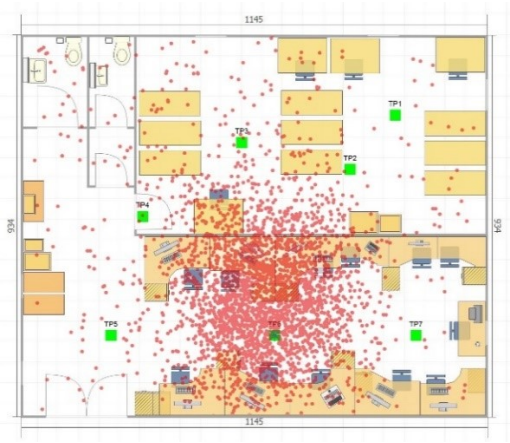

Figure 6. 19 Result of MCL at test point 6 using even distribution

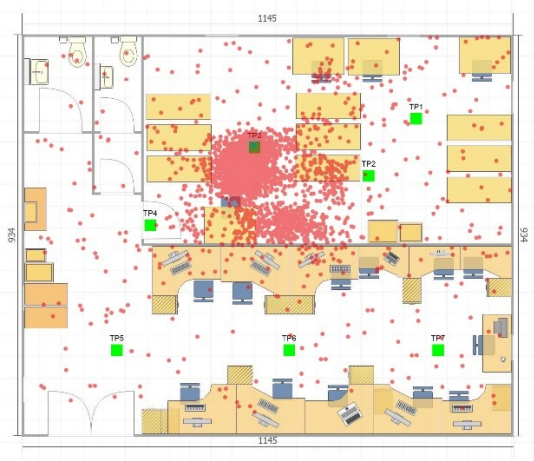

Figure 6. 20 Result of MCL at test point 6 using Gaussian distribution

As can be seen from the results, particle aggregation is less than normal with random distributions. In the actual test, it was found that particles using the normal distribution of the MCL particles aggregation speed was faster than the use of randomly distributed MCL particles. From the final positioning error, the error of using normal distribution is also slightly less than with random distribution. Because under normal circumstances, the use of normal distribution can increase

positioning accuracy while reducing the response time of the system. The advantage of using random distribution is that, because the particle aggregation is small, when there is need for dispersal, the system rebuild time is greatly accelerated.

6.4.3 Redeployment Ratio of Particles

The third experiment was designed to test the effect of different numbers of re-deployed particles' on positioning results. According to the above, in each loop, a portion of the particles were selected, removed from the map, and then re-deployed to weighted particles. The choice of different proportions of re-deployed particle systems will affect accuracy and corresponding time. The first two groups re-deployed 300 and 450 particles respectively among 1500 particles. The last two groups re-deployed 600 and 900 particles, respectively among 3000 particles. A total of 4 examples are shown in the figures below.

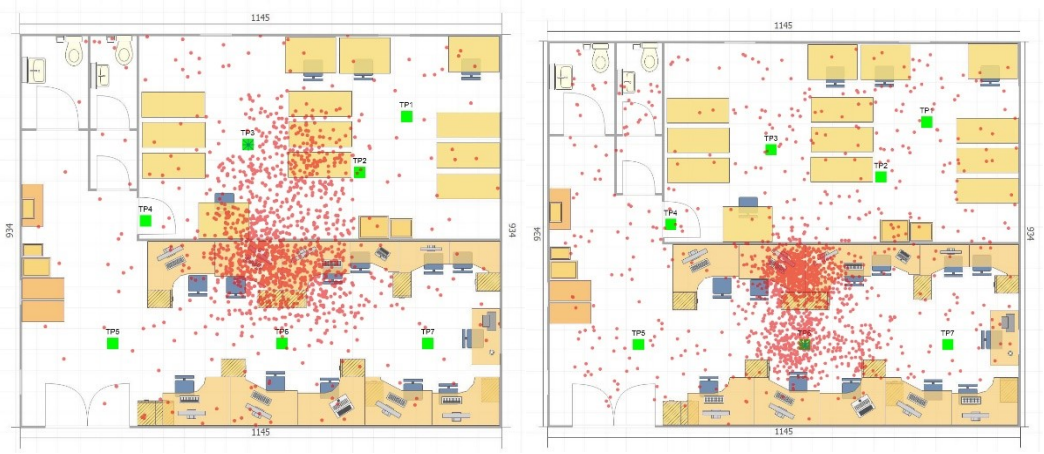

Figure 6. 21 20% redeployment ratio of 1500 particles (left)

Figure 6. 22 30% redeployment ratio of 1500 particles (right)

Figure 6. 23 20% redeployment ratio of 3000 particles (left)

Figure 6. 24 30% redeployment ratio of 3000 particles (right)

The results show that for a total of 1500 particles, it can be intuitively seen from the Figure 6.21 that particle convergence is very low, so the positioning error is also high. The result of using 450 re-deployed particles was significantly better than 300 points. In the case of 3000 particles, there was not much difference between the results of 600 and 900 re-deployed cases. It can be found that when the total number of particles used increases, the proportion of re-deployed particles can be appropriately reduced. In the meantime, after extensive experimentation, it has been shown that using a greater number of re-deployed particles can also significantly reduce the response time of the system. One thing which bears mention is that: using excessive amounts of redeployed particle can lead to a dramatic increase in the amount of computing strain on a system.

After many trials, 3000 particles were chosen with a 30% re-deployment ratio (900 points). The assumption of MCL is Gaussian distribution.

6.4.4 Experimental Result of MCL and Other Algorithms

The following five groups of tests examined MCL under different conditions. The first group of tests was conducted in the cabin office (LOS environment). The second and third experiments were conducted in the Kings building library, a complex Non-LOS environment. The fourth and fifth experiments were conducted in the supermarket, a very complex Non-LOS environment with lots of moving people. The above five groups of experiments are exactly the same as those in chapter 5. In the following experiments, the MCL test results were compared with the centroid core positioning algorithm [102], least square algorithm, basic trilateration algorithm, nearest beacon algorithm [103], and off set centroid core algorithm proposed in chapter 5 respectively.

Experiment 1 in cabin

In the cabin office experiment, a total of eight examples of the diagrams are shown below. They were initialised states and test points 1-7 of the result in the examples. All of these diagrams are shown below:

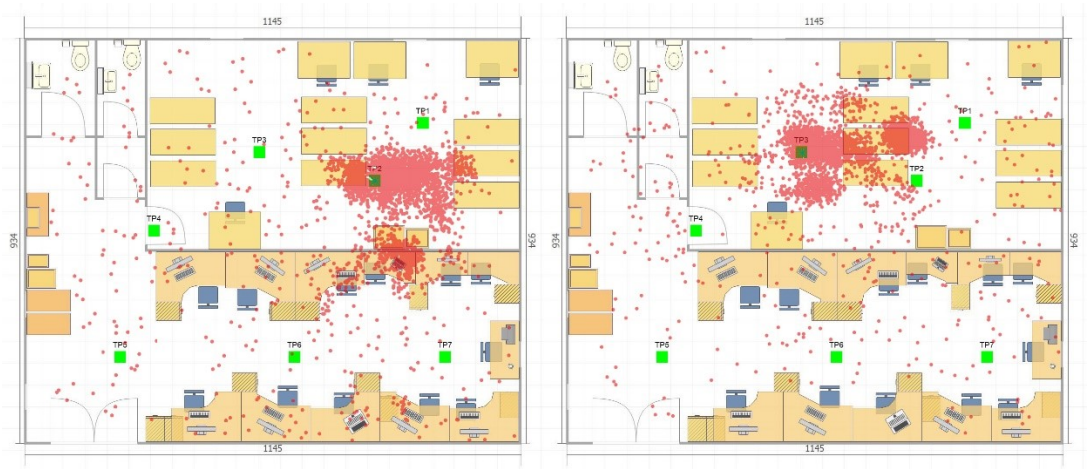

Figure 6. 25 Result of test point 2 (left)

Figure 6. 26 Result of test point 3 (right)

Figure 6. 27 Result of test point 4 (left)

Figure 6. 28 Result of test point 5 (right)

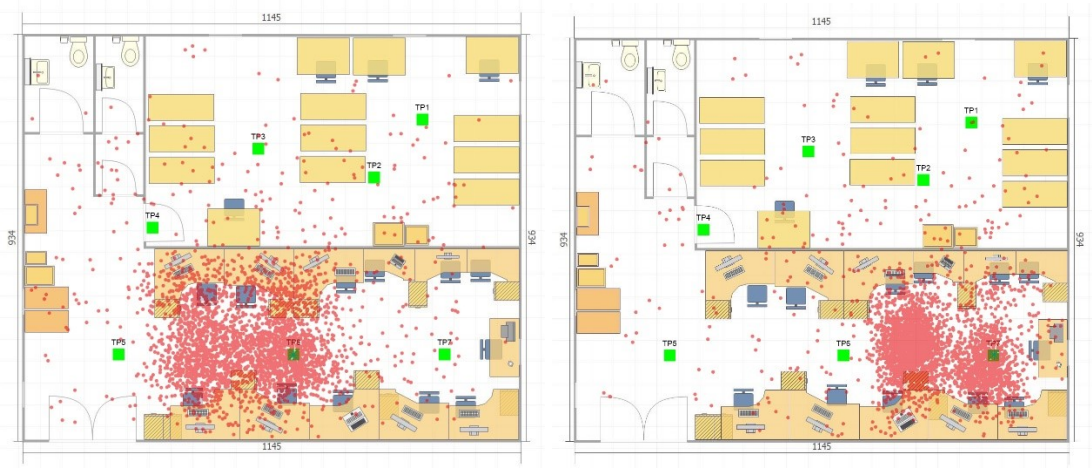

Figure 6. 29 Result of test point 6 (left)

Figure 6. 30 Result of test point 7 (right)

As can be seen from these diagrams, test point 1 to test point 7 have different degrees of error. The main performance map has multiple particle aggregation areas. It is noteworthy that most of the invalid aggregation areas are concentrated near the closest BLE beacon, especially in the examples of test point 2, 4, and 5.

In these cases, one can improve the positioning accuracy by selecting the strongest convergence area, while discarding the aggregation area, which is normally the smaller one. However, in the case of test point 6 and test point 7, a higher positioning error was caused by removing the smaller particle pool. In the cases of test point 6 and seven, the accurate particle pools and user's actual location were more than 2 metres apart. Test point 5's situation was more complicated because, due to its position, it could not receive RSSI values except from beacons 3, 5 and 6. Moreover, beacon 6's RSSI value error was very large. This led to MCL positioning significant errors at test point 5. Therefore, using MCL is still limited by the deployment density of BLE beacons. However, it can be intuitively seen that the effective positioning area of the MCL is much larger than the offset centroid core algorithm using the same deployment density, so the overall positioning accuracy of the MCL is still greater than the algorithm proposed in chapter 5.

The following Figure shows the error results of test points 1-7 with different positioning algorithms. Least square which uses four reference points by default.

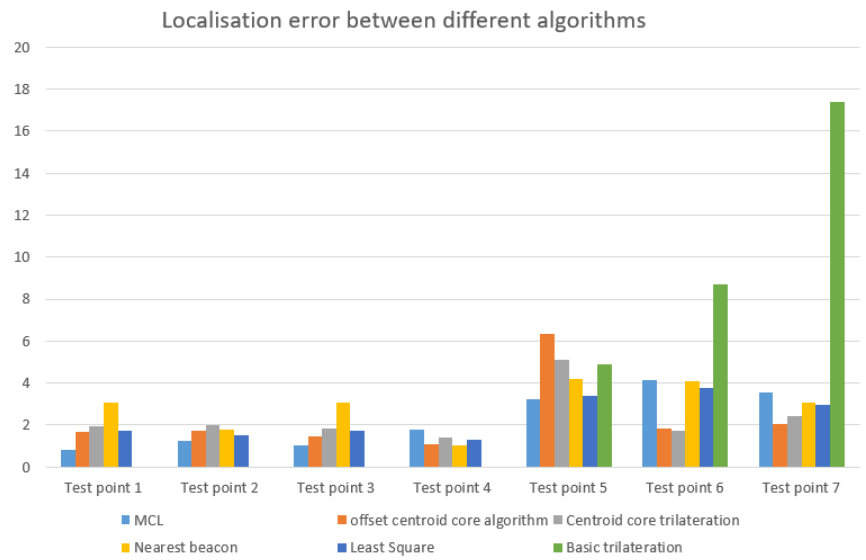

Figure 6. 31 Localisation error of different algorithms

As can be seen from Figure 6.33, the basic trilateration algorithm has a large flaw. In most cases, three circles do not have common points between each, so the algorithm does not give a positioning result. The accuracy of the nearest beacon algorithm is directly related to the distance to the nearest beacon. When the transmission path is LOS and the distance from the nearest Beacon is less than 2 metres, the positioning accuracy can be very high. When located equidistant between multiple beacons, and the distance from all beacon is greater than 2 metres, the algorithm's positioning accuracy will be greatly reduced. The accuracy of using centroid core is similar to that of chapter 5's proposition, but the stability of the system is lower than that of the system proposed in chapter 5. The accuracy of the least square algorithm is higher than that of MCL. Although the Least square algorithm can have a high adaptability, the precision and accuracy of the least square algorithm is high because it is still a positioning algorithm for a single

information source, while its sources and RSSI value instabilities and errors are high. The overall stability is still not as good as MCL.

Experiment 2 in library

The next two sets of tests were conducted in the Kings building library. The first group of experiments was conducted in two learning rooms as well as in the corridor section. A total of seven BLEs were deployed in the hallway and two learning rooms. This test involved a total of 14 test points, in order to save space, only six test results are displayed. These are test points 1, 3, 6,7,12, and 14.

Figure 6. 32 Experimental result of test point 1

Figure 6. 33 Experimental result of test point 3

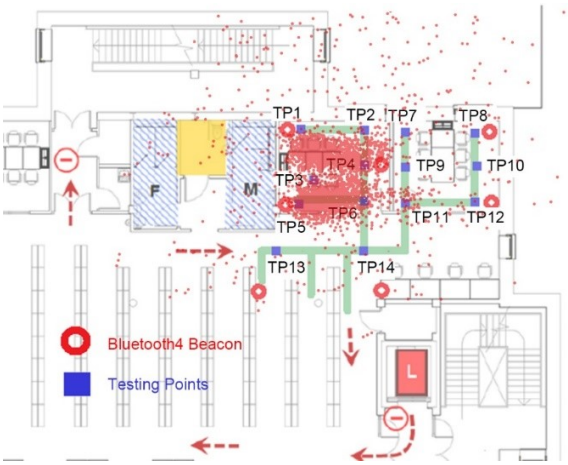

Figure 6. 34 Experimental result of test point 6

Figure 6. 35 Experimental result of test point 7

Figure 6. 36 Experimental result of test point 12

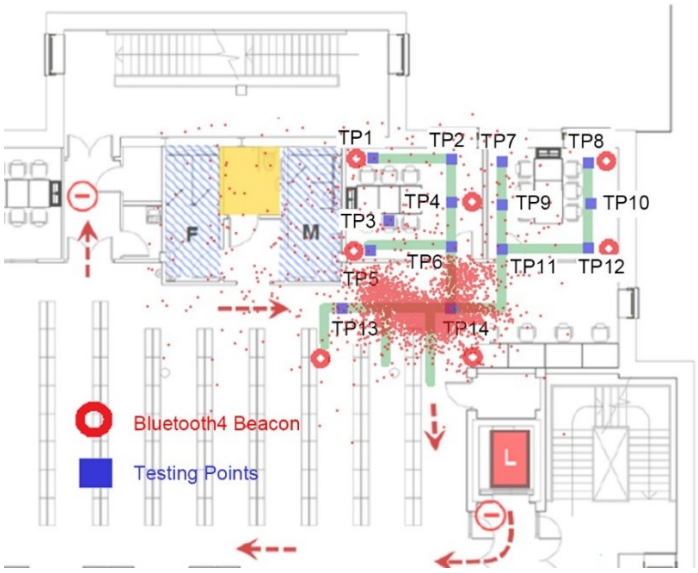

Figure 6. 37 Figure 6. 37 Experimental result of test point 14

It can be seen from the figures that the accuracy of the MCL in the complex Non-LOS environment is slightly lower than that in the LOS environment. Test points 3, 6, and 7 have obvious positioning errors. Where point 6 produces a

conspicuous convergence of two particles. Point 7 is affected by beacon 3. The positioning accuracy of Point 14 is higher than expected. After analysing the RSSI value of beacon 7, we found that the RSSI of beacon 7 is about -65 dBm when the user was at test point 14. At this moment, beacon 7 played a leading role in positioning the user. Without regard to the room judgement error (located at the test point 7 is wrongly positioned to the left of the learning room), the overall positioning error was between 3 and 4 metres.

The figure below shows the positioning error of different algorithms tested in the library. RSSI values are more prone to being degraded in complex environments. In this case, the basic trilateration algorithm could give the positioning results in some test points however most of them are very error-prone. The nearest beacon algorithm is similar to the previous result, when user stands near beacon, the positioning error will be reduced. When the user is more distant from all beacons, positioning error will be very large. The accuracy of Centroid core algorithm is lower than that observed in the cabin office environment. After analysis, we find that the algorithm cannot effectively select the best signal provider under complicated conditions. When some RSSI errors are accepted, the positioning accuracy will be greatly reduced by these inaccurate RSSI values. The accuracy of the algorithm proposed in Chapter 5 is roughly same as that of MCL. Least square algorithm showed better positioning performance in a Non-LOS environment, but its error is still slightly larger than that of MCL, and positioning accuracy was similar to off-set centroid core algorithm.

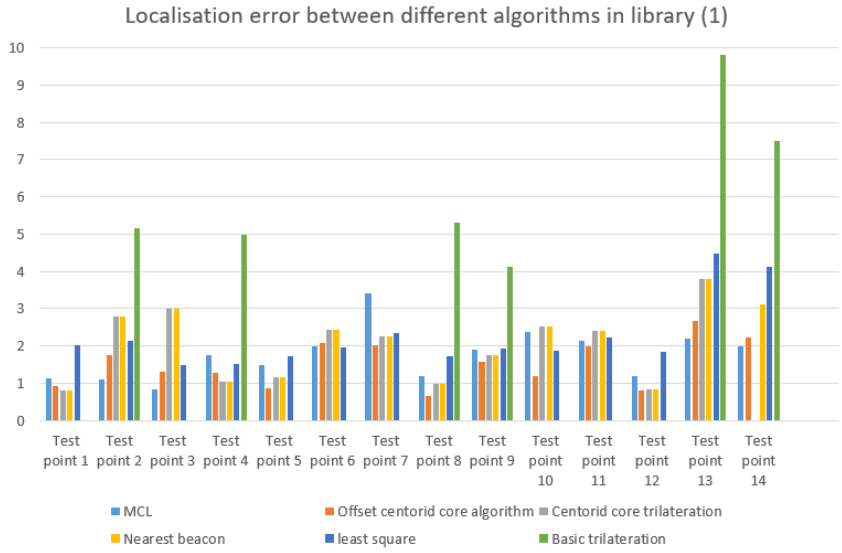

Figure 6. 38 Localisation error between algorithms in library (1)

Experiment 3 in library (2)

The second set of tests in the library were tested in the book area. A total of 5 BLE beacons were used. The number of test points was 9. The following figures show the results of the four test points at test points 1, 3, 5, and 8.

Figure 6. 39 Experimental result of test point 1

Figure 6. 40 Experimental result of test point 3

Figure 6. 41Experimental result of test point 5

Figure 6. 42 Experimental result of test point 8

Note that the result of test point 8 is located at test point 5. After numerical analysis of the RSSI of beacon 3, it was found that the RSSI value of beacon 3 was very high when the user was at test point 8 (approximately 70dBm). This was also the main reason that test point 8 was located at test point 5.

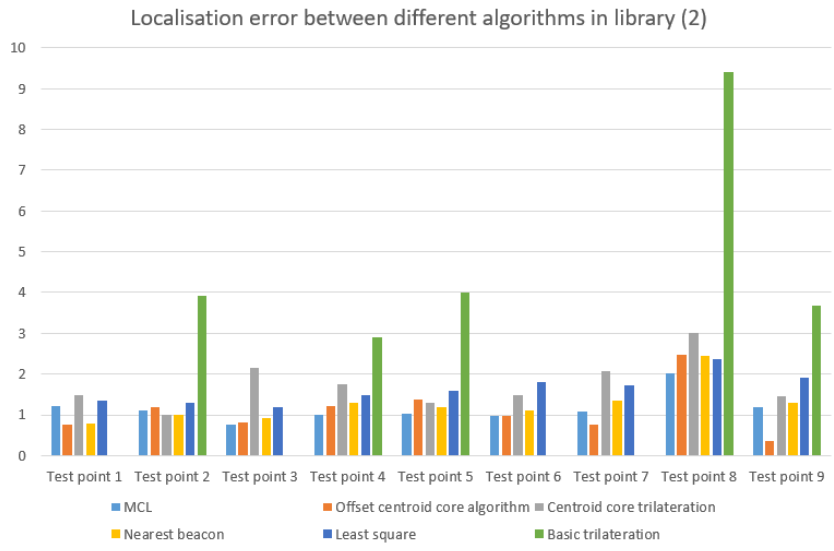

Figure 6. 43 Localisation error between algorithms in library (2)

The figure above shows the positioning accuracy of each test point for different algorithms in this test environment. It can be seen that, in addition to basic triangulation, nearest beacon algorithm error is relatively related to the distance between test points and their nearest beacons. In fact, most algorithms exclude basic trilateration algorithm calculate positioning accuracy of 1-3 metres because the beacon deployment density is significantly large. This also shows that the main determinant of positioning accuracy is the accuracy of the distance calculated from the RSSI value.

Experiment 4 in supermarket

The last set of tests was conducted in the supermarket environment. Two kinds of beacon deployment method were used. The first group of test signal deployment density was smaller than the second group of test signals. The aim of these sets of experiments was to measure the performance of MCL in a very complex Non-LOS environment.

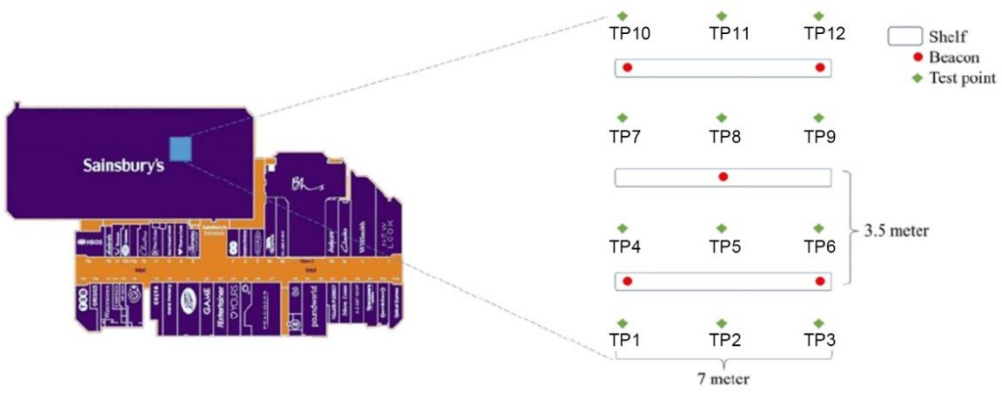

Figure 6. 44 Set up of the experimental environment in supermarket (1)

A total of five BLE beacons were deployed in the first set of tests in three double-sided goods shelves. In this set of experiments, a total of 12 test points were tested separately. The examples of test points 1, 3, 5, and 12 are shown below.

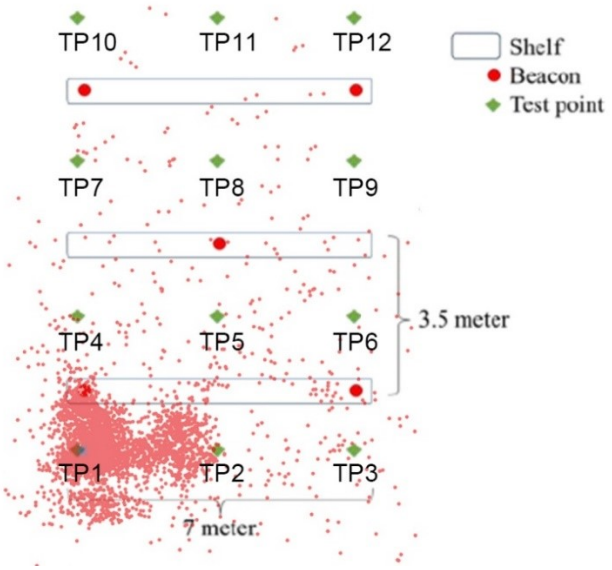

Figure 6. 45 Experimental result of test point 1

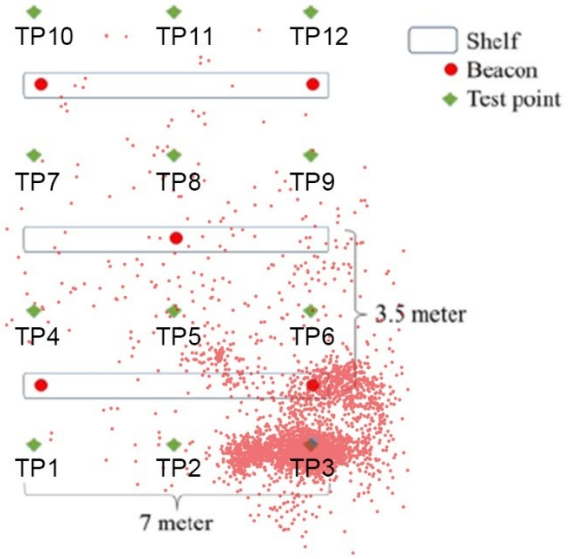

Figure 6. 46 Experimental result of test point 3

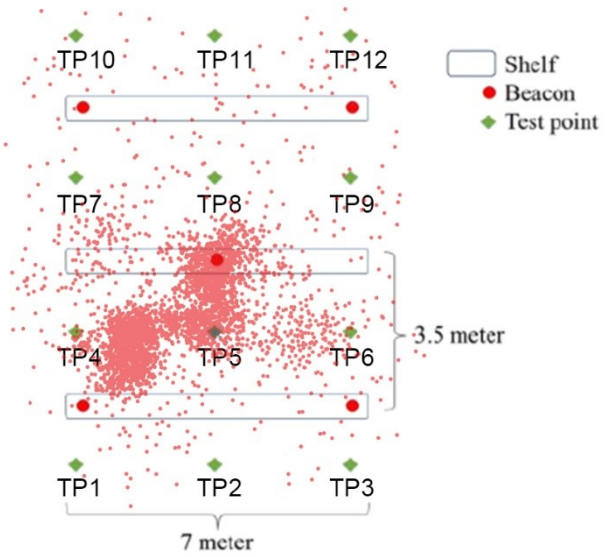

Figure 6. 47 Experimental result of test point 5

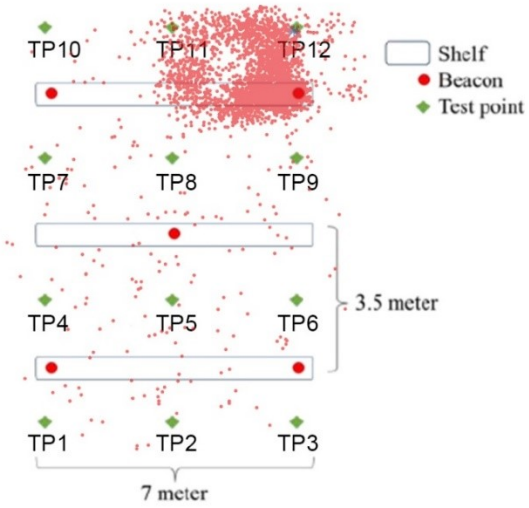

Figure 6. 48 Experimental result of test point 12

The figure below shows the localisation error using different positioning algorithms. The positioning results provided by basic triangulation are effectively incorrect. Most of the errors of these results were generally above 5 metres. At some test points, the RSSI value was less than -100 dBm at some time points, resulting in a measurement distance exceeding 50 metres. It is worth mentioning that the

proposed off-set central core positioning algorithm showed a slightly more accurate positioning result at test point 1 and 4 than that of MCL. However, because of the limitations of the effective positioning error mentioned previously, the localisation error of the proposed algorithm in chapter 5 were significantly greater than MCL such as test point 2 an test point 11.

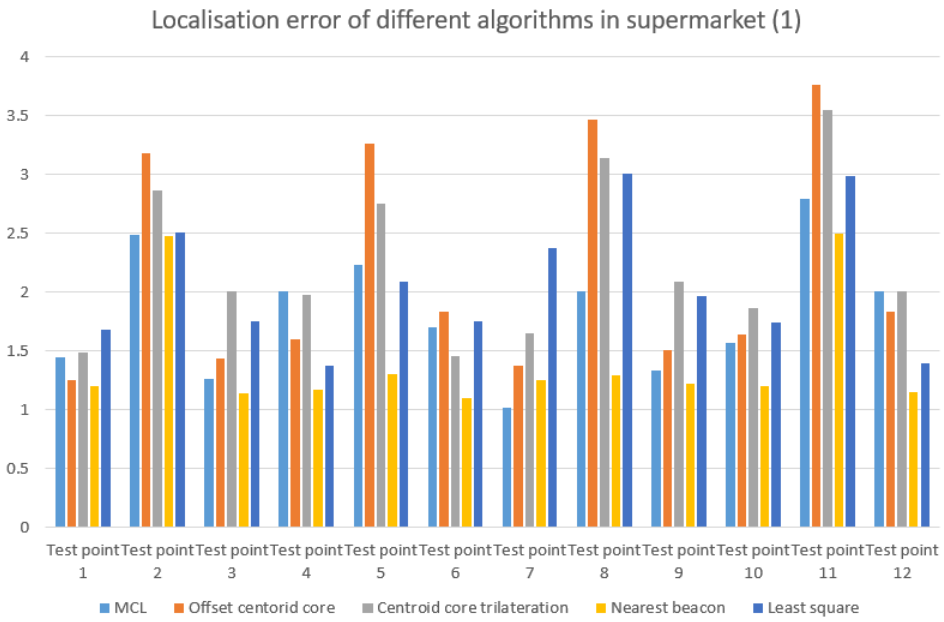

Figure 6. 49 Localisation error between algorithms in supermarket (1)

Experiment 5 in supermarket

The last set of tests used six beacon tests in the same area. All beacons were deployed in two rows of double-sided shelves. This test employed a total of nine test points. The example of test point 2 and test point 5 are detailed in the figure below:

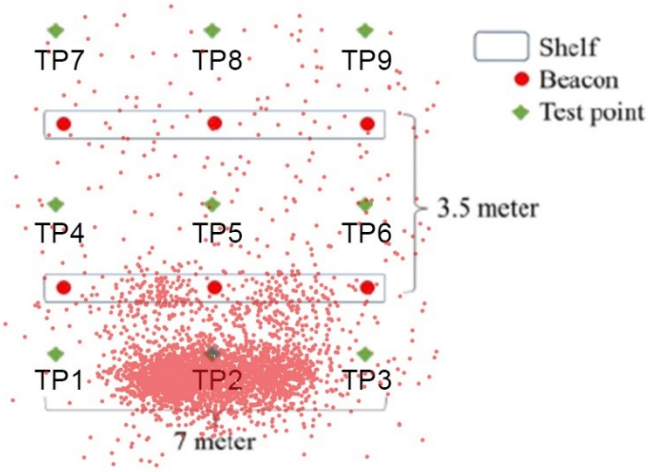

Figure 6. 50 Experimental result of test point 2

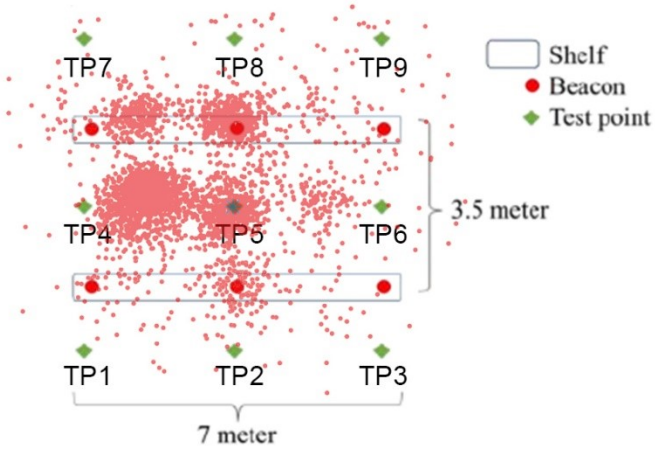

Figure 6. 51 Experimental result of test point 5

As can be seen from the above two examples, increasing the beacon deployment density did not significantly increase the positioning accuracy, but may result in the dispersion of weights due to too much received information. It can be observed that test point 2's signal cover density was less than test point 5. However, the former test point's error was a little bit smaller than the latter.

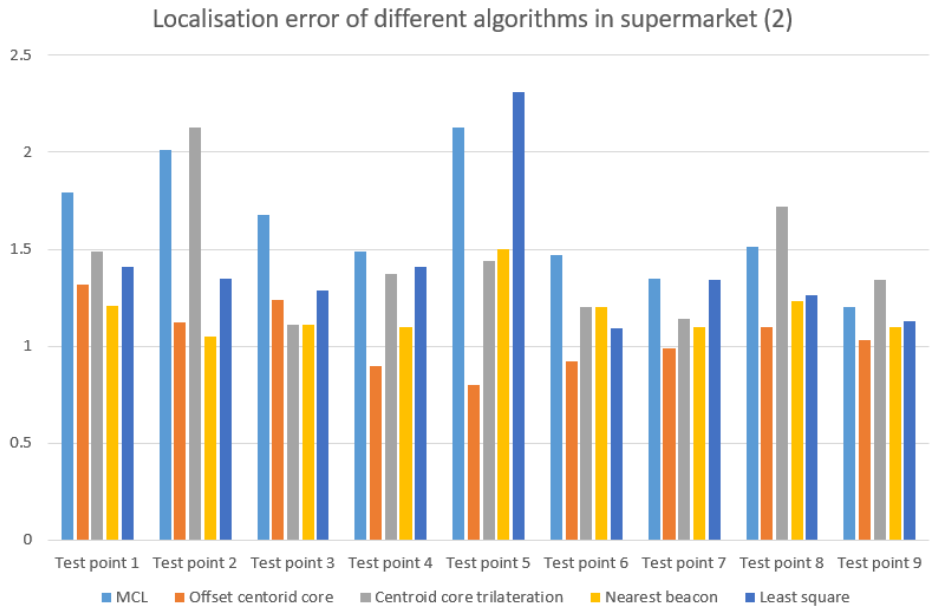

Figure 6. 52 Localisation error between algorithms in supermarket (2)

Figure 6.54 above shows the positioning accuracy of different algorithms in each test point. As can be seen, increasing signal cover density can significantly increase the accuracy of nearest beacon positioning. Basic triangulation still cannot provide more reliable positioning results. The accuracy of the Least square algorithm is slightly higher than that of the previous algorithm, which proves that the least square algorithm is also limited by the quantity and quality of received location information. The localisation accuracy of the proposed algorithm in chapter 5 is not significantly different from the error of the central core trilateration algorithm. This also shows that the minimum localisation error of these two algorithms is limited by the algorithm themselves. The localisation accuracy of Nearest beacon is between 1-2 metre, this is because the beacon deployment density is very high: all of these test points are located close to at least one

beacon(less than 2 metre distance. However, the beacon deployment density under this test cannot be utilised in most of practical applications.

6.5 Conclusion

In this chapter, MCL based on the particle filter was introduced with the Hidden Markov Mode. The entire MCL was divided into two parts, the first part was an estimation update, the other part being an observation update. Within these two parts, methods of how to use an accelerometer and compass to provide estimation update, and use of the RSSI value provided by BLE beacons as an observation update was presented in detail. Three sets of tests were run to select the optimal parameters of MCL. After testing, 3000 particles with a 30% re-deployment ratio was chosen. The assumption of MCL is Gaussian distribution. The MCLs were then tested separately in three different test environments: the ‘cabin office’ (a LOS environment), the Kings Building Library (a complex Non-LOS environment) and the supermarket (a very complex Non-LOS environment with lots of moving people) The test results were compared with the off-set centroid core positioning algorithm and the other positioning algorithms proposed. The results show that MCL's positioning accuracy and adaptability to complex environments are better than other algorithms, and does not require very high signal cover density. Meanwhile, the demand for beacon's deployment density is also not high.

Chapter 7 : Conclusion

7.1 Thesis Summary

This paper provides two indoor positioning algorithms with adaptive and self-correcting systems, which are designed to provide an indoor positioning system that can operate in complex environments with an average accuracy of 1-3 metres. Initially, this paper investigates the development of the current indoor positioning system and its use of the algorithms. In this context，the following aspects have been discussed while implementing the indoor positioning system: power consumption, accuracy, costs, and deployment conditions. First of all, due to the popularity of smart phones, BLE-based indoor positioning is currently more likely to be achieved because most of today's smart phones are integrated with BLE 4.0 features. At the same time, BLE beacons are cheaper and smaller in size than Wi-Fi routers, so using a BLE beacon as a feature source for indoor positioning systems can provide higher signal deployment density and higher signal coverage area than a similarly expensive system which employs Wi-Fi routers, which can provide a higher localization accuracy. In addition, BLE's low-power features can significantly reduce the overall power consumption of the system. Based on the analysis of the above problems in this paper, an RSSI-based BLE network is used as the main carrier of the indoor positioning system. And two different filters are used to reduce the noise in the RSSI sequence.

With regards to the choice of algorithm, two different systems were built based on the two different algorithms, and then compared. First, a self-adaptive trilateration-based indoor positioning algorithm was proposed. A weighted framework was applied to increase the localization accuracy. Conversely, an MCL algorithm using Bluetooth as the observed information provider was also designed. An accelerometer and compass were also selected to be used to provide estimation updates.

The remainder of this chapter summarises the research covered in this thesis, and concludes and evaluates the achievements of the thesis and their impact on the field. Finally, it discusses and highlights the key areas that require improvements alongside the possibility for future research related to the work covered in this thesis.

The main contributions of this thesis are presented chapters 3, 4, 5, and 6, while chapters 1 and 2 give an introduction and overview of relevant work. In chapter 2, an introduction of indoor positioning systems is provided to introduce the basics of indoor positioning in terms of system design, carrier selection, and algorithm selection. First of all, the advantages and disadvantages of the different hardware platforms utilised by indoor positioning systems were introduced and analysed. Following this, special or general-purpose indoor positioning algorithms based on different platforms, such as TDOA, Fingerprint, and Trilateration, were introduced and compared. This chapter also reviewed the relevant research that has a direct relation with the work presented in this thesis.

In the third chapter, BLE signals were introduced. In the ideal case of an indoor transmission model, the free space transmission mode, which is the basic theory

of the path loss model. In this thesis, the path loss model was used to calculate the relationship between RSSI and distance. Because the size of the indoor space is limited, the biggest factor in the stability of the signal is due to small scale fading caused. This leads to the fact that the RSSI sequence suffers from violent fluctuations in the case where the distance between the user and BLE beacon is constant, which significantly reduces the accuracy of indoor positioning. A smoothing filter was used to de-noise the signal strength in order to reduce the signal fluctuation caused by small scale fading. First, the theory of this smoothing filter was introduced. Then, different parameters in the implementation phase, such as window width, and the stage of multi-pass smoothing filters were tested and compared. Finally, this chapter also compared the performance of the smoothing filter in dealing with RSSI sequences that pass through different materials (such as brick, plywood).

In Chapter 4, another filter: the wavelet filter, was chosen to reduce the degradation in positioning accuracy caused by small scale fading. First, the theory behind the wavelet filter was introduced. The wavelet filter is also a filter based on frequency domain analysis. As a comparison, the Fourier transform based filter was first introduced. The Fourier change based filter’s biggest drawback is that it cannot get high accuracy in both time domain and frequency domain. The wavelet filter is different, it inherited and developed the idea of short-time Fourier transform localization, while overcoming the window size does not vary with frequency and other shortcomings, it can provide a frequency change with the "time - frequency" window. The wavelet filter is scaled by dynamically transforming wavelet scale in order to scale or extend the mother wavelet to obtain a higher accuracy in time domain in the high frequency region and get high accuracy in time domain in the

low frequency region at the same time. In this way, the wavelet filter shows better performance in reducing the noise of the RSSI sequence. This is due to the fact that the RSSI sequence is not a stable signal in the time domain, or that the process is not a stationary stochastic process. Following this, in the implementation section, a set of experiments were used to test the performance of different parameters of the wavelet. Ultimately, the performance of the wavelet and the performance of the smoothing filter were compared and accompanied by an analysis of two different principles of the advantages and disadvantages of the filter.

The Trilateration algorithm is one of the main algorithms for indoor positioning, and is widely used in various positioning systems. In the fifth chapter, first, the basic trilateration algorithm was described in detail. The methodology, advantages, and disadvantages of the algorithm were thoroughly discussed. The main advantage was easy to highlight, the calculation is low. Shortcomings were evident when the three circles generated by three BLE beacons do not have common points between each circle. In this scenario, the algorithm cannot calculate the positioning results accurately. As a solution, some other trilateration-based localisation algorithms, such as the least square algorithm, were proposed in order to deal with this disadvantage. However, creating a sub-algorithm in each particular case increases the complexity and uncertainty of the positioning system. In this paper, improvements to the traditional trilateration algorithm were proposed in the form of an off-set trilateration (triangulation) algorithm. The algorithm is referred to as the ‘Centroid Core Triangulation Algorithm’ [reference]. It uses the centroid of the triangle as a reference point and the distance ratio as the offset reference source. The algorithm can be applied to both trilateration and

triangulation positioning systems. At the same time, a weight framework was proposed to dynamically select the optimal BLE beacon as the provider of distance information when more than three BLE beacon signals were received. Specifically, the algorithm uses a three-level weight framework, the best signal provider can be selected along with the most appropriate BLE beacon group for indoor positioning calculation. In the implementation section, the appropriate formula was used to integrate the three-level framework to one equation, without losing positioning accuracy. This resulted in a significant reduction of the complexity and computation required in the weighted framework. In the experimental stage, the algorithm was tested in different environments. The results showed that the positioning was accurate to 1m in the LOS indoor environment, and the positioning error was not more than 4 meters in a complex indoor environment.

The indoor positioning algorithm proposed in Chapter 5 was a single information source based indoor positioning system. BLE's RSSI was used as the only information source for location information. In Chapter 6, a multi-information source indoor localization system was proposed to further enhance the localization accuracy of BLE-based indoor positioning systems. First, the method of Bayes was introduced, which was the fundamental theory of the Monte Carlo filter which is also known as particle filter. Whether Bayes filter, particle filter, or Markov filter, are belongs to the probabilistic based filter. The Monte Carlo Localisation algorithm is based on the principle of the particle filter. In the Methodology section, MCL's mathematical principles were introduced. In this proposed positioning system, BLE was applied to provide observational updates of computing users' positions using BLE RSSI values. Additionally, an

accelerometer and compass were applied to provide estimated update information. In the implementation section, the specific implementation of the system was detailed. The description of how to use the compass and accelerometer information was given, as well as effective methods regarding updating the location of the particle, and how to establish a calibration system to increase the indoor positioning system's accuracy in the event of an unknown error situation of self-correction. As in Chapter 5, the MCL algorithm was tested several times in three different sets of environments to verify its positioning accuracy. Concurrently, various other algorithms were also simulated, the results were used and compared with MCL.

7.2 Future Work

Several aspects of the work presented in this thesis can be further investigated or improved upon. Some possibilities are listed below:

- **Using a wider variety of filter types**: In theory, smoothing filters and wavelet filters are used to reduce interference due to small scale fading. The effect shows a significant increase in the stability of the system. However, a wider variety of different filters, such as fast smoothing and differentiation filters, can also be used to attempt to de-noise the RSSI sequence. In the meantime, the research on the wavelet filter in this paper can be studied further, for example, discussing the use of mother wavelet with different shapes. The problem of how to build a composite filtering system using different filters to increase the stability of the RSSI sequence without losing effective information is still a challenging issue.

  The standard deviation of the RSSI sequence can be used to detect if the current transmission path is LOS environment or not [104]. Specifically, under the LOS environment, the standard deviation of the RSSI is higher than the value of the non-LOS environment. Furthermore, non-LOS transmission medium circumstances involving brick, plywood and other materials have differing standard deviations. If a dynamic algorithm to analyse the standard deviation of the RSSI value can be established to determine the current transmission environment, the analysis results used to adjust the filter parameters can greatly improve positioning accuracy.

- **Algorithm Optimisation**: In Chapter 5, we proposed a weighted off-set trilateration algorithm for locating complex situations. The algorithm's

weighted framework can still be further optimized, with regards to beacon selection. More varied environmental tests could be conducted to further test the performance of the algorithm in complex environments, these test results could potentially be used to further optimize the algorithm.

- **Investigate different re-deployment algorithms**: In this research, the BLE beacons are deployment and re-deployment manually, which are decided by the shape of indoor environments and the possible deployment density with reasonable costs. It is regretted that most of the behaviour mentioned above are depending on the operator's experience. In such case, developing an automatic BLE beacon deployment and re deployment system using different types of algorithms could decrease the workload of setting up the BLE network and increase the effective deployment density with lower numbers of beacons.

- **MCL Optimisation**: In Chapter 6, an MCL-based indoor positioning system using BLE, compass, and accelerometer was designed for indoor positioning in complex environments. First, Gaussian distribution was employed to make an assumption of error while making an estimation update. In practice, the introduction of Gaussian distribution for each particle's estimated update produces a large computation. In this case, weighted even distribution could be used instead of Gaussian distribution to derive an assumption of error, which has the potential to greatly reduce overall computational complexity.

  When using the RSSI information provided by BLE to provide observation updates, the total number of particles and the number of particles selected

each time are fixed. In different environments, because environmental interference and overall BLE beacon deployment conditions are not identical, the use of particle numbers and their selection should also be dynamically changing with the environment. By employing deep learning to build an algorithm, the dynamic adjustment of the number of particles used can greatly reduce the computation of the system. The introduction of deep learning to dynamically adjust the weighted parameters can also greatly improve positioning accuracy.

- **Greater sources of information**: In this article, a BLE beacon system was used as the primary reference provider for positioning systems due to its low power consumption, strong anti-jamming capability, and low cost. The Wi-Fi signal Centre frequency and that of BLE is nearly identical (2.45GHz). The entire system from the filter, single source localization algorithm, to MCL algorithm, has strong compatibility with Wi-Fi. As mentioned above, due to the shortcomings of Wi-Fi, it is not suitable as a primary location information provider. However, if Wi-Fi can be successfully integrated into the indoor positioning systems proposed in this paper, indoor positioning accuracy can be significantly improved. As Wi-Fi routers are already heavily deployed in public places, using Wi-Fi as a reference source of positioning information does not significantly increase the cost of the entire positioning system.

  Geomagnetic fields use the KNN fingerprint algorithm to record the magnetic field value of each reference point in the environment during the training phase to serve as a database and then compare this with the magnetic field value collected by the user during the locating phase [105].

The biggest benefit of this system is that it does not require additional elements to collect geomagnetic field data for cell phone users. Therefore, this system has a strong compatibility with mobile-based indoor positioning systems. The Geomagnetic field-based positioning system can also be integrated into the MCL positioning system proposed in chapter 7 as an auxiliary observation update source to correct any inaccuracies in positioning results, thereby further increasing the accuracy and stability of the positioning system.

Reference

[1] F. Seco, C. Plagemann, A. R. Jiménez, and W. Burgard, "Improving RFID-based indoor positioning accuracy using Gaussian processes," in *Indoor Positioning and Indoor Navigation (IPIN), 2010 International Conference on*, 2010, pp. 1-8.

[2] I. Sharp and K. Yu, "Enhanced least-squares positioning algorithm for indoor positioning," *IEEE Transactions on Mobile Computing,* vol. 12, pp. 1640-1650, 2013.

[3] S. Viswanathan and S. Srinivasan, "Improved path loss prediction model for short range indoor positioning using bluetooth low energy," in *SENSORS, 2015 IEEE*, 2015, pp. 1-4.

[4] H. Steendam, T. Q. Wang, and J. Armstrong, "Cramer-Rao bound for indoor visible light positioning using an aperture-based angular-diversity receiver," in *Communications (ICC), 2016 IEEE International Conference on*, 2016, pp. 1-6.

[5] H. Liu, H. Darabi, P. Banerjee, and J. Liu, "Survey of wireless indoor positioning techniques and systems," *IEEE Transactions on Systems, Man, and Cybernetics, Part C (Applications and Reviews),* vol. 37, pp. 1067-1080, 2007.

[6] R. Faragher and R. Harle, "Location fingerprinting with bluetooth low energy beacons," *IEEE journal on Selected Areas in Communications,* vol. 33, pp. 2418-2428, 2015.

[7] (12/30). *comparison of different technology for server-based indoor positioning*. Available: https://www.infsoft.com/indoor-positioning

[8] B. Kim, W. Bong, and Y. C. Kim, "Indoor localization for Wi-Fi devices by cross-monitoring AP and weighted triangulation," in *Consumer Communications and Networking Conference (CCNC), 2011 IEEE*, 2011, pp. 933-936.

[9] R. Di Taranto, S. Muppirisetty, R. Raulefs, D. Slock, T. Svensson, and H. Wymeersch, "Location-aware communications for 5G networks: How location information can improve scalability, latency, and robustness of 5G," *IEEE Signal Processing Magazine,* vol. 31, pp. 102-112, 2014.

[10] L.-C. Wang and S. Rangapillai, "A survey on green 5G cellular networks," in *Signal Processing and Communications (SPCOM), 2012 International Conference on*, 2012, pp. 1-5.

[11] T. Gigl, G. J. Janssen, V. Dizdarevic, K. Witrisal, and Z. Irahhauten, "Analysis of a UWB indoor positioning system based on received signal strength," in *Positioning, Navigation and Communication, 2007. WPNC'07. 4th Workshop on*, 2007, pp. 97-101.

[12] B. Alavi and K. Pahlavan, "Modeling of the TOA-based distance measurement error using UWB indoor radio measurements," *IEEE communications letters,* vol. 10, pp. 275-277, 2006.

[13] T.-N. Lin and P.-C. Lin, "Performance comparison of indoor positioning techniques based on location fingerprinting in wireless networks," in *Wireless Networks, Communications and Mobile Computing, 2005 International Conference on*, 2005, pp. 1569-1574.

[14] C. Yang and H.-R. Shao, "WiFi-based indoor positioning," *IEEE Communications Magazine,* vol. 53, pp. 150-157, 2015.

[15] N. Le Dortz, F. Gain, and P. Zetterberg, "WiFi fingerprint indoor positioning system using probability distribution comparison," in *Acoustics, Speech and Signal Processing (ICASSP), 2012 IEEE International Conference on*, 2012, pp. 2301-2304.

[16] C.-H. Lim, Y. Wan, B.-P. Ng, and C.-M. S. See, "A real-time indoor WiFi localization system utilizing smart antennas," *IEEE Transactions on Consumer Electronics,* vol. 53, 2007.

[17] C. Rizos, A. G. Dempster, B. Li, and J. Salter, "Indoor positioning techniques based on wireless LAN," 2007.

[18] J. Na, "The blind interactive guide system using RFID-based indoor positioning system," *Computers Helping People with Special Needs,* pp. 1298-1305, 2006.

[19] Y.-H. Wei, Q. Leng, S. Han, A. K. Mok, W. Zhang, and M. Tomizuka, "RT-WiFi: Real-time high-speed communication protocol for wireless cyber-physical control applications," in *Real-Time Systems Symposium (RTSS), 2013 IEEE 34th*, 2013, pp. 140-149.

[20] D. Camps-Mur, A. Garcia-Saavedra, and P. Serrano, "Device-to-device communications with Wi-Fi Direct: overview and experimentation," *IEEE wireless communications,* vol. 20, pp. 96-104, 2013.

[21] (12/30). *Example of Wi-Fi based indoor positioning system*. Available: https://www.pinterest.com.au/explore/indoor-positioning-system/

[22] S. Ingram, D. Harmer, and M. Quinlan, "Ultrawideband indoor positioning systems and their use in emergencies," in *Position Location and Navigation Symposium, 2004. PLANS 2004*, 2004, pp. 706-715.

[23] J. Xu, M. Ma, and C. L. Law, "Position estimation using UWB TDOA measurements," in *Ultra-wideband, the 2006 IEEE 2006 International Conference on*, 2006, pp. 605-610.

[24] D. P. Young, C. M. Keller, D. W. Bliss, and K. W. Forsythe, "Ultra-wideband (UWB) transmitter location using time difference of arrival (TDOA) techniques," in *Signals, Systems and Computers, 2004. Conference Record of the Thirty-Seventh Asilomar Conference on*, 2003, pp. 1225-1229.

[25] R. Fujiwara, K. Mizugaki, T. Nakagawa, D. Maeda, and M. Miyazaki, "TOA/TDOA hybrid relative positioning system using UWB-IR," in *Radio and Wireless Symposium, 2009. RWS'09. IEEE*, 2009, pp. 679-682.

[26] (12/30). *NICT, Fujitsu develop indoor guidance technology for the blind using ultra wide band positioning, smartphones*. Available: https://phys.org/news/2012-07-nict-fujitsu-indoor-guidance-technology.html

[27] H. Zou, H. Wang, L. Xie, and Q.-S. Jia, "An RFID indoor positioning system by using weighted path loss and extreme learning machine," in *Cyber-Physical Systems, Networks, and Applications (CPSNA), 2013 IEEE 1st International Conference on*, 2013, pp. 66-71.

[28] A. Bekkali, H. Sanson, and M. Matsumoto, "RFID indoor positioning based on probabilistic RFID map and Kalman filtering," in *Wireless and Mobile Computing, Networking and Communications, 2007. WiMOB 2007. Third IEEE International Conference on*, 2007, pp. 21-21.

[29] L. M. Ni, Y. Liu, Y. C. Lau, and A. P. Patil, "LANDMARC: indoor location sensing using active RFID," *Wireless networks,* vol. 10, pp. 701-710, 2004.

[30] C. Gomez, J. Oller, and J. Paradells, "Overview and evaluation of bluetooth low energy: An emerging low-power wireless technology," *Sensors,* vol. 12, pp. 11734-11753, 2012.

[31] E. Ferro and F. Potorti, "Bluetooth and Wi-Fi wireless protocols: a survey and a comparison," *IEEE Wireless Communications,* vol. 12, pp. 12-26, 2005.

[32] M. Siekkinen, M. Hiienkari, J. K. Nurminen, and J. Nieminen, "How low energy is bluetooth low energy? comparative measurements with zigbee/802.15. 4," in *Wireless Communications and Networking Conference Workshops (WCNCW), 2012 IEEE*, 2012, pp. 232-237.

[33] J. Padgette, "Guide to bluetooth security," *NIST Special Publication,* vol. 800, p. 121, 2017.

[34] J. Lansford, A. Stephens, and R. Nevo, "Wi-Fi (802.11 b) and Bluetooth: enabling coexistence," *IEEE network,* vol. 15, pp. 20-27, 2001.

[35] (12/30). *How iBeacons Can Help You Keep Your Office High Productive*. Available: https://itechcraft.com/ibeacon-and-enterprises/

[36] P. Kułakowski, J. Vales-Alonso, E. Egea-López, W. Ludwin, and J. García-Haro, "Angle-of-arrival localization based on antenna arrays for wireless sensor networks," *Computers & Electrical Engineering,* vol. 36, pp. 1181-1186, 2010.

[37] D.-H. Shin and T.-K. Sung, "Comparisons of error characteristics between TOA and TDOA positioning," *IEEE Transactions on Aerospace and Electronic Systems,* vol. 38, pp. 307-311, 2002.

[38] G. Shen, R. Zetik, and R. S. Thoma, "Performance comparison of TOA and TDOA based location estimation algorithms in LOS environment," in *Positioning, Navigation and Communication, 2008. WPNC 2008. 5th Workshop on*, 2008, pp. 71-78.

[39] (12/30). *TOF VS TDOA*. Available: https://pixie-technology.com/tof-vs-dtoa/

[40] C. Park, D. Park, J. Park, Y. Lee, and Y. An, "Localization algorithm design and implementation to utilization RSSI and AOA of Zigbee," in *Future Information Technology (FutureTech), 2010 5th International Conference on*, 2010, pp. 1-4.

[41] (12/30). *Angle-of-Arrival*. Available: https://www.ese.wustl.edu/~nehorai/josh/students.cec.wustl.edu/_jly1/doa.html

[42] K. Kaemarungsi and P. Krishnamurthy, "Modeling of indoor positioning systems based on location fingerprinting," in *INFOCOM 2004. Twenty-third AnnualJoint Conference of the IEEE Computer and Communications Societies*, 2004, pp. 1012-1022.

[43] K. Kaemarungsi, "Design of indoor positioning systems based on location fingerprinting technique," University of Pittsburgh, 2005.

[44] X. Liang, X. Gou, and Y. Liu, "Fingerprint-based location positoning using improved KNN," in *Network Infrastructure and Digital Content (IC-NIDC), 2012 3rd IEEE International Conference on*, 2012, pp. 57-61.

[45] J. Ma, X. Li, X. Tao, and J. Lu, "Cluster filtered KNN: A WLAN-based indoor positioning scheme," in *World of Wireless, Mobile and Multimedia Networks, 2008. WoWMoM 2008. 2008 International Symposium on a*, 2008, pp. 1-8.

[46] M. Youssef and A. Agrawala, "The Horus WLAN location determination system," in Proceedings of the 3rd international conference on Mobile systems, applications, and services, 2005, pp. 205-218.

[47] W. Leung, S. Leung, W. Lau, and A. Luk, "Fingerprint recognition using neural network," in *Neural Networks for Signal Processing [1991]., Proceedings of the 1991 IEEE Workshop*, 1991, pp. 226-235.

[48] O. M. Badawy and M. A. B. Hasan, "Decision tree approach to estimate user location in WLAN based on location fingerprinting," in *Radio Science Conference, 2007. NRSC 2007. National*, 2007, pp. 1-10.

[49] J. Niu, B. Wang, L. Cheng, and J. J. Rodrigues, "WicLoc: An indoor localization system based on WiFi fingerprints and crowdsourcing," in *Communications (ICC), 2015 IEEE International Conference on*, 2015, pp. 3008-3013.

[50] B. Wang, Q. Chen, L. T. Yang, and H.-C. Chao, "Indoor smartphone localization via fingerprint crowdsourcing: Challenges and approaches," *IEEE Wireless Communications,* vol. 23, pp. 82-89, 2016.

[51] (12/30). *Fusing Bluetooth Beacon Data with Wi-Fi Radiomaps for Improved I ndoor Localization*. Available: https://www.researchgate.net/figure/315839931_Figure-2-Combined-BLE-and-Wi-Fi-fingerprint-based-indoor-positioning

[52] V. Filonenko, C. Cullen, and J. D. Carswell, "Indoor positioning for smartphones using asynchronous ultrasound trilateration," *ISPRS International Journal of Geo-Information,* vol. 2, pp. 598-620, 2013.

[53] N. A. Mahiddin, N. Safie, E. Nadia, S. Safei, and E. Fadzli, "Indoor position detection using WiFi and trilateration technique," in *The International Conference on Informatics and Applications (ICIA2012)*, 2012, pp. 362-366.

[54] V. Filonenko, C. Cullen, and J. Carswell, "Asynchronous ultrasonic trilateration for indoor positioning of mobile phones," *Web and Wireless Geographical Information Systems,* pp. 33-46, 2012.

[55] Z.-A. Deng, Y. Hu, J. Yu, and Z. Na, "Extended kalman filter for real time indoor localization by fusing WiFi and smartphone inertial sensors," Micromachines, vol. 6, pp. 523-543, 2015.

[56] W. Wang and Q. Zhu, "RSS-based Monte Carlo localisation for mobile sensor networks," *IET communications,* vol. 2, pp. 673-681, 2008.

[57] J. C. Krumm and K. P. Hinckley, "Proximity detection using wireless signal strengths," ed: Google Patents, 2009.

[58] V. Zeimpekis, G. M. Giaglis, and G. Lekakos, "A taxonomy of indoor and outdoor positioning techniques for mobile location services," *ACM SIGecom Exchanges,* vol. 3, pp. 19-27, 2002.

[59] D. M. Pozar, *Microwave engineering*: John Wiley & Sons, 2009.

[60] H. T. Friis, "The free space transmission equation," *Proc. IRE,* vol. 34, p. 254, 1946.

[61] S. Karp, R. M. Gagliardi, S. E. Moran, and L. B. Stotts, "Introduction," in *Optical Channels*, ed: Springer, 1988, pp. 1-27.

[62] K. Benkic, M. Malajner, P. Planinsic, and Z. Cucej, "Using RSSI value for distance estimation in wireless sensor networks based on ZigBee," in *Systems, signals and image processing, 2008. IWSSIP 2008. 15th international conference on*, 2008, pp. 303-306.

[63] K. Kaemarungsi and P. Krishnamurthy, "Properties of indoor received signal strength for WLAN location fingerprinting," in *Mobile and Ubiquitous Systems: Networking and Services, 2004. MOBIQUITOUS 2004. The First Annual International Conference on*, 2004, pp. 14-23.

[64] K. Laasonen, "Radio propagation modeling," *University of Helsinki, Tech. Rep,* 2003.

[65] Z. Xiang, S. Song, J. Chen, H. Wang, J. Huang, and X. Gao, "A wireless LAN-based indoor positioning technology," *IBM Journal of research and development,* vol. 48, pp. 617-626, 2004.

[66] C. Perez-Vega and J. L. G. Garcia, "A simple approach to a statistical path loss model for indoor communications," in *Microwave Conference, 1997. 27th European*, 1997, pp. 617-623.

[67] (12/30). *Path loss.* Available: https://www.utdallas.edu/~torlak/courses/ee4367/lectures/lectureradio.pdf

[68] S. Y. Seidel and T. S. Rappaport, "914 MHz path loss prediction models for indoor wireless communications in multifloored buildings," *IEEE transactions on Antennas and Propagation,* vol. 40, pp. 207-217, 1992.

[69] G. D. Durgin and T. S. Rappaport, "Theory of multipath shape factors for small-scale fading wireless channels," *IEEE Transactions on Antennas and Propagation,* vol. 48, pp. 682-693, 2000.

[70] A. A. Saleh and R. Valenzuela, "A statistical model for indoor multipath propagation," *IEEE Journal on selected areas in communications,* vol. 5, pp. 128-137, 1987.

[71] T. O'Haver, "A Pragmatic introduction to signal processing," ed, 1997.

[72] (12/30). *CC2540 beacon*. Available: http://www.ti.com/product/CC2540?keyMatch=CC2540

[73] A. Graps, "An introduction to wavelets," *IEEE computational science and engineering,* vol. 2, pp. 50-61, 1995.

[74] G. Kaiser, *A friendly guide to wavelets*: Springer Science & Business Media, 2010.

[75] R. Polikar, "The wavelet tutorial," 1996.

[76] P. Vaidyanathan, "Quadrature mirror filter banks, M-band extensions and pe rfect-reconstruction techniques," *IEEE Assp Magazine,* vol. 4, pp. 4-20, 1987.

[77] E. Hewitt and R. E. Hewitt, "The Gibbs-Wilbraham phenomenon: an episode in Fourier analysis," *Archive for history of Exact Sciences,* vol. 21, pp. 129-160, 1979.

[78] (12/30). *Gibbs Phenomenon*. Available: https://archive.lib.msu.edu/crcmath/math/math/g/g164.htm

[79] S. Chan and G. Sohn, "Indoor localization using Wi-Fi based fingerprinting and trilateration techiques for LBS applications," *International Archives of the Photogrammetry, Remote Sensing and Spatial Information Sciences,* vol. 38, p. C26, 2012.

[80] J. Li and M. Wu, "The improvement of positioning accuracy with weighted least square based on SNR," in *Wireless Communications, Networking and Mobile Computing, 2009. WiCom'09. 5th International Conference on*, 2009, pp. 1-4.

[81] (12/30). *Scottish Microelectronics Centre*. Available: https://www.eng.ed.ac.uk/research/facilities-and-resources/resources/scottish-microelectronics-centre

[82] (12/30). *Noreen and Kenneth Murray Library*. Available: https://www.ed.ac.uk/information-services/computing/desktop-personal/open-access/locations/kings-buildings/kb-library

[83] (12/30). *Cameron toll*. Available: http://www.camerontoll.co.uk/

[84] G. Kitagawa, "Monte Carlo filter and smoother for non-Gaussian nonlinear state space models," *Journal of computational and graphical statistics,* vol. 5, pp. 1-25, 1996.

[85] J. M. Hammersley and K. W. Morton, "Poor man's monte carlo," *Journal of the Royal Statistical Society. Series B (Methodological),* pp. 23-38, 1954.

[86] J. Hammersley and K. Morton, "A new Monte Carlo technique: antithetic variates," in *Mathematical proceedings of the Cambridge philosophical society*, 1956, pp. 449-475.

[87] N. J. Gordon, D. J. Salmond, and A. F. Smith, "Novel approach to nonlinear/non-Gaussian Bayesian state estimation," in *IEE Proceedings F (Radar and Signal Processing)*, 1993, pp. 107-113.

[88] R. E. Kalman, "A new approach to linear filtering and prediction problems," *Journal of basic Engineering,* vol. 82, pp. 35-45, 1960.

[89] S. Thrun, D. Fox, W. Burgard, and F. Dellaert, "Robust Monte Carlo localization for mobile robots," *Artificial intelligence,* vol. 128, pp. 99-141, 2001.

[90] L. Turner and C. Sherlock, "An introduction to particle filtering," *Technical Report,* 2013.

[91] N. Gordon, B. Ristic, and S. Arulampalam, "Beyond the kalman filter: Particle filters for tracking applications," *Artech House, London,* vol. 830, 2004.

[92] M. S. Arulampalam, S. Maskell, N. Gordon, and T. Clapp, "A tutorial on particle filters for online nonlinear/non-Gaussian Bayesian tracking," *IEEE Transactions on signal processing,* vol. 50, pp. 174-188, 2002.

[93] A. Doucet, S. Godsill, and C. Andrieu, "On sequential Monte Carlo sampling methods for Bayesian filtering," *Statistics and computing,* vol. 10, pp. 197-208, 2000.

[94] M. Pollock, "Introduction to particle filtering: Discussion," *Technical Report,* 2010.

[95] A. Doucet and A. M. Johansen, "A tutorial on particle filtering and smoothing: Fifteen years later," *Handbook of nonlinear filtering,* vol. 12, p. 3, 2009.

[96] V. Fox, J. Hightower, L. Liao, D. Schulz, and G. Borriello, "Bayesian filtering for location estimation," *IEEE pervasive computing,* vol. 2, pp. 24-33, 2003.

[97] L. Rabiner and B. Juang, "An introduction to hidden Markov models," *ieee assp magazine,* vol. 3, pp. 4-16, 1986.

[98] L. E. Baum and T. Petrie, "Statistical inference for probabilistic functions of finite state Markov chains," *The annals of mathematical statistics,* vol. 37, pp. 1554-1563, 1966.

[99] C. Andrieu, A. Doucet, and R. Holenstein, "Particle markov chain monte carlo methods," *Journal of the Royal Statistical Society: Series B (Statistical Methodology),* vol. 72, pp. 269-342, 2010.

[100] D. Fox, W. Burgard, and S. Thrun, "Markov localization for mobile robots in dynamic environments," *Journal of Artificial Intelligence Research,* vol. 11, pp. 391-427, 1999.

[101] (12/30). *Accelerometer information*. Available: http://www.globalspec.com/learnmore/sensors_transducers_detectors/acceleration_vibration_sensing/accelerometers

[102] H. Shi, "A new weighted centroid localization algorithm based on RSSI," in *Information and Automation (ICIA), 2012 International Conference on*, 2012, pp. 137-141.

[103] P. Dickinson, G. Cielniak, O. Szymanezyk, and M. Mannion, "Indoor positioning of shoppers using a network of Bluetooth Low Energy beacons," in *Indoor Positioning and Indoor Navigation (IPIN), 2016 International Conference on*, 2016, pp. 1-8.

[104] A. A. Juri, T. Arslan, and F. Wang, "Obstruction-aware Bluetooth Low Energy Indoor Positioning," in *29th International Technical Meeting of The Satellite Division of the Institute of Navigation (ION GNSS+ 2016)*, Portland, Oregon, 2016, pp. 2254-2261.

[105] Y. Du, T. Arslan, and A. Juri, "Camera-aided region-based magnetic field indoor positioning " in *Indoor Positioning and Indoor Navigation (IPIN), 2016 International Conference on*, 2016, pp. 1-7.